AD-A115 514 AIR FORCE INST OF TECH WRIGHT-PATTERSON AFB OH SCHOO--ETC F/G 18/3
A TWO STEP METHOD TO TREAT VARIABLE WINDS IN FALLOUT SMEARING C--ETC(U)
MAR 82 A T HOPKINS

UNCLASSIFIED AFIT/GNE/PH/82M-10 NL

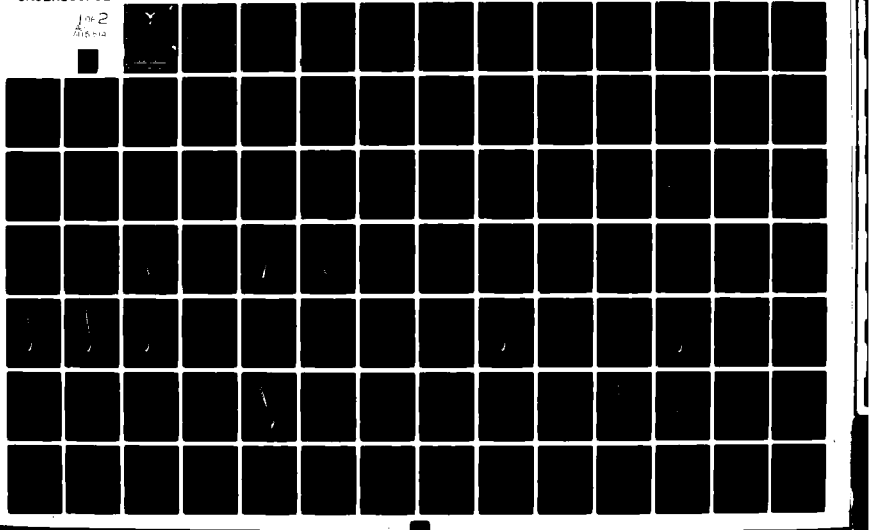

DEPARTMENT OF THE AIR FORCE
AIR UNIVERSITY (ATC)

AIR FORCE INSTITUTE OF TECHNOLOGY

Wright-Patterson Air Force Base, Ohio

AFIT/GNE/PH/82M-10

A TWO STEP METHOD TO TREAT VARIABLE WINDS IN FALLOUT SMEARING CODES

THESIS

Arthur T. Hopkins
AFIT/GNE/PH/82M-10 Capt USAF

Approved for Public Release; Distribution Unlimited

AFIT/GNE/PH/82M-10

A TWO STEP METHOD TO TREAT VARIABLE WINDS IN FALLOUT SMEARING CODES

THESIS

Presented to the Faculty of the School of Engineering
of the Air Force Institute of Technology
Air University
in Partial Fulfillment of the
Requirements for the Degree of
Master of Science

by
Arthur T. Hopkins, B.S.E., M.S.E.
Capt USAF
Graduate Nuclear Engineering

March 1982

Preface

The purpose of this study was to develop a method for predicting realistically curved fallout contours with variable winds in smearing codes. The method requires two steps: (1) location of the curved hotline, and (2) calculation of off-axis dose rates. A curved hotline locator model was developed from correlated DELFIC wafer height data and a real wind particle translation scheme. The model was tested by comparing results to DELFIC output and to Castle-Bravo fallout footprints. The two-dimensional dose rate integral was solved analytically, enabling the calculation of off-axis dose rates.

This two-step method can be adapted to existing smearing codes by incorporating the hotline locator model and the dose-rate equation.

I thank Dr. C.J. Bridgman for his patience and guidance during this thesis study. In addition, I thank Major W.S. Bigelow for providing the microfiche DELFIC data that I used for the stabilized cloud fits, and the Defense Nuclear Agency for providing Castle-Bravo documentation and movies. Finally, thank you, Jeannie.

A.T. Hopkins

Contents

List of Figures

List of Figures

(continued)

List of Figures

(continued)

List of Tables

Abstract

A method was developed to treat non-constant winds in fallout smearing codes. The method consists of two steps:

(1) location of the curved hotline

(2) determination of the off-hotline activity.

To locate the curved hotline, the method begins with an initial cloud of 20 discretely-sized pancake clouds, located at altitudes determined by weapon yield. Next, the particles are tracked through a 300 layer atmosphere, translating with different winds in each layer. The connection of the 20 particles' impact points is the fallout hotline. The hotline location was found to be independent of the assumed particle size distribution in the stabilized cloud. The off-hotline activity distribution is represented as a two-dimensional gaussian function, centered on the curved hotline. Hotline locator model results were compared to numerical calculations of a hypothetical 100 kt burst and to the actual hotline produced by the Castle-Bravo 15 Mt nuclear test.

A TWO STEP METHOD TO TREAT VARIABLE WINDS IN FALLOUT SMEARING CODES

I. Introduction

Background

An atmospheric nuclear burst produces a cloud of radioactive particles which translate with the winds as they fall. Military and civilian studies (Refs 1 through 4) use both numerical and analytic fallout prediction models to compute fallout activity levels as a function of location. Analytic models (Refs 1 and 2) are used for most studies, primarily because they are economical. Economy is achieved, in part, by using a constant wind vector (speed and direction) to smear radioactivity along the ground. However, the constant wind assumption is a severe restriction on the smearing model which is universally recognized (Ref 1). The smearing code's ground trace is symmetric about the downwind axis, or hotline, the locus of peak activity levels. These hotlines are always straight because the wind is assumed constant at all altitudes beneath the falling cloud. Figure 1 shows fallout contours obtained from constant vs variable winds in a smearing calculation.

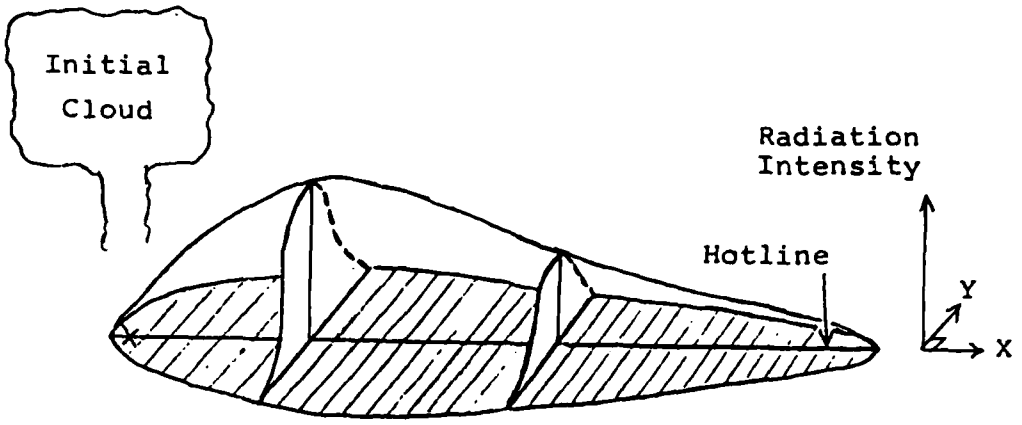

Fallout From Constant Vector Wind
(Ground Footprint Shaded)

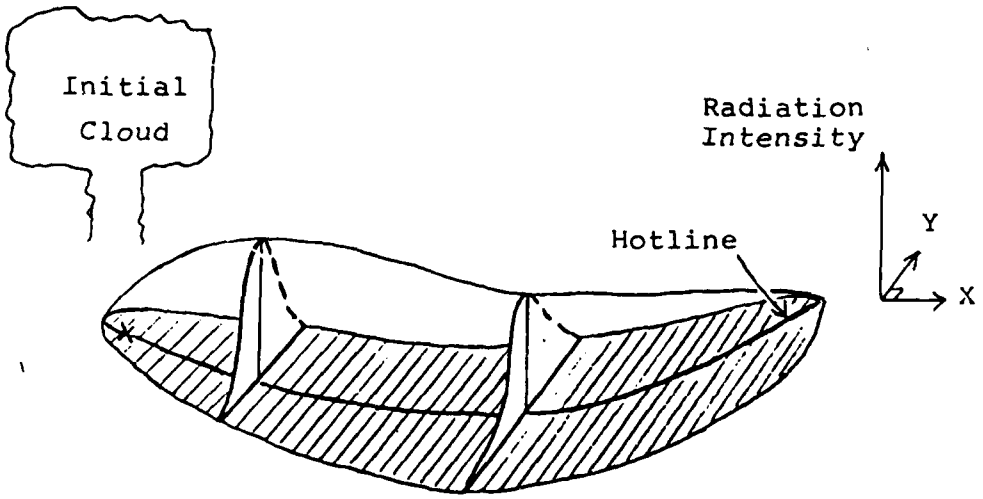

Fallout From Variable Winds
(Ground Footprint Shaded)

Figure 1. Fallout Contours

Problem Statement

Fallout smearing codes need to account for spatially and temporally varying winds. Specifically, smearing codes need techniques to locate curved hotlines and to compute off-axis dose rates.

Approach

Two steps are taken to model variable winds in fallout smearing codes. First, the hotline is located. Second, the off-hotline dose is predicted.

To locate the hotline, a model was developed to compute trajectories of 20 different particle sizes. The particles start from altitudes computed with empirical fits to numerical code data, and fall through a discretely-layered atmosphere. Each atmosphere layer is 100 meters thick and the model has 300 layers. The Davies-McDonald method was used to compute terminal velocities in model layers. The horizontal motion of each particle is computed and summed from starting altitude to the ground. The fallout hotline is the connection of the 20 particles' landing points.

To predict dose rates, the two-dimensional dose rate integral was solved analytically. The solution will enable the smearing codes to calculate dose rates as a function of two-dimensional winds.

Organization

Section II briefly describes the two principal types of fallout codes. Sections III through VII discuss the first step: hotline location. Section III quantifies the working hypothesis of a stabilized cloud with particle sizes that have been gravity-sorted in altitude. Section IV describes the hotline locator model with altitude-varying winds. Sections V and VI contain results of case studies in which computed hotlines are compared to numerical model results and an actual nuclear test hotline. Section VII describes a method to account for temporal variations in winds.

Section VIII presents the second step: the analytic solution of the two-dimensional dose rate integral.

The Appendices contain detailed descriptions of the atmosphere equations and the hotline locator model.

II. Current Fallout Prediction Models

This section briefly describes the two principal types of fallout codes: disc tosser and smearing.

Disc Tosser (DELFIC)

The Department of Defense Land Fallout Interpretive Code (DELFIC) is the standard numerical fallout code for military studies (Ref 1). DELFIC is a multi-dimensional model which describes the motions of fallout particles contained in discrete pancake wafers of discrete particle size groups. The DELFIC data (Ref 5) used in this study represented the particle clouds with one hundred discrete particle size groups (3 μm to 4.6 mm) and at least twenty wafers per size group. Wafer motion is modeled in DELFIC as the fireball rises, cools and expands and as the stabilized cloud falls through real winds. As a research tool, DELFIC provided valuable data for empirical fits of stabilized wafer heights and for benchmark comparisons of curved hotlines. However, DELFIC is too costly and detailed to use when large numbers of hypothetical fallout cases must be analyzed. Fast-running, economical analytic codes (Refs 1 and 2) have been developed to support parametric studies.

Smearing Codes (AFIT and WSEG)

The AFIT (Air Force Institute of Technology) and WSEG (Army Weapon Systems Evaluation Group) codes (Refs 1 and 2) are examples of fallout smearing prediction models. Both AFIT and WSEG models simulate particle transport and deposition by smearing the falling radioactive cloud along the ground, as a constant wind vector translates airborne particles downwind. The radioactive fallout is symmetrically distributed on the ground, normal to the downwind axis (hot-line) of the fallout footprint. Smearing codes can only predict unidirectional hotlines because they assume a constant wind vector for particle transport. The fundamental equation for computing ground dose rate by smearing the descending cloud is: (Ref 1)

$$\dot{D}(x,y) = KY_k \int_0^\infty f(x,y,t')g(t')dt' \qquad \text{(II-1)}$$

$\dot{D}$ = Dose rate at ground coordinates (x,y) $\frac{\text{Roentgens}}{\text{hour}}$

K = Source normalization constant

(typically, $2350 \frac{\text{Roentgens}}{\text{hour}} \frac{\text{miles}^2}{\text{kilotons}}$)

Y_k = Yield (kilotons, kt)

$f(x,y,t')$ = normalized cloud spatial distribution (miles^{-2})

$g(t)$ = time-dependent arrival rate of radioactivity on the ground ($hour^{-1}$)

x = distance downwind (mi)

y = distance crosswind (mi)

The normalized spatial distribution function describes the lateral (crosswind and downwind) extent of the radioactive ground trace. Assuming gaussian distributions for the x and y dependence of $f(x,y,t')$, the activity function is:

$$f(x,y,t') = \frac{1}{\sqrt{2\pi}\sigma_X\ (t')}\ \text{EXP}\left[-\tfrac{1}{2}\left(\frac{x-v_x t'}{\sigma_x}\right)\right]^2 \cdot \frac{1}{\sqrt{2\pi}\sigma_Y\ (t')}\ \text{EXP}\left[-\tfrac{1}{2}\left(\frac{y-v_y t'}{\sigma_Y}\right)\right]^2 \qquad \text{(II-2)}$$

σ_X = standard deviation in x-direction (mi)

σ_Y = standard deviation in y-direction (mi)

v_x = wind velocity in x-direction (mi/hr)

v_y = wind velocity in y-direction (mi/hr)

Both smearing codes solve the dose rate integral by assuming an "effective" constant wind (Ref 8) which is actually a particle residence time-weighted average of a vertical wind profile. Essentially, the x-direction is defined as downwind

and v_y is zero. The dose rate integral then contains a single time-dependent exponential term and is solved analytically:

$$\dot{D} = \frac{KY_k \, g(t_a)}{\sqrt{2\pi} \, v_x \sigma_Y \, (t_a)} \; e^{-\frac{1}{2}\left(\frac{y}{\sigma_Y}\right)^2} \qquad \text{(II-3)}$$

Equation (II-3) is the working equation for dose rate in both the WSEG and AFIT smearing codes (Refs 1 and 2).

III. The Initial Stabilized Cloud

Description

A surface nuclear burst produces a fireball which rises, expands and cools, entraining air and surface debris. The buoyant cloud contains vaporized, radioactive particles which eventually recondense on microscopic nuclei or on the surfaces of other particles. When the gravitational force on a particle exceeds the force induced by updraft in the rising cloud, the particle falls from the cloud. Therefore, larger, heavier particles should begin to fall from the rising cloud sooner than small particles. However, sorting by terminal velocity is not perfect because particles have different shapes and densities, and because the flow inside the rising cloud is not a simple updraft. Toroidal flow and temperature-dependent changes in the air properties help to mix the particles during cloud rise to stabilization.

Pancake Cloud

The smearing codes (Refs 1 and 2) assume that all fallout particles fall from altitudes related to the stabilized cloud center height. The WSEG model assumes that radioactivity is normally distributed about a fallout cloud altitude given by: (Ref 2)

$$HC = 44.0+6.1 \cdot \ell nY-.205(\ell nY+2.42)|\ell nY+2.42| \qquad \text{(III-1)}$$

HC = Cloud Height (kilofeet)

Y = Weapon Yield (megatons, Mt)

Bridgman (Ref 1) showed that the vertical cloud distribution can be reduced to a pancake cloud at HC. In fact, Reference 1 demonstrates that the pancake cloud is a convenient, accurate simplification of the nuclear fallout cloud if the vertical distribution of activity is symmetric about HC. However, when particles start from pancake clouds and fall through real, variable winds, they impact in a nearly straight line. Therefore, the AFIT simplification of a pancake initial cloud cannot be used to predict curved hotlines with real winds.

Distributed Cloud

DELFIC data (Ref 5) showed that the particles in stabilized clouds are gravity sorted, with large particles generally lower in altitude than small particles. To quantify the distributed initial cloud, the DELFIC data (Ref 5) was used to generate a generalized initial condition.

DELFIC's Advective Transport Module divides an assumed particle size distribution into 100 discrete groups and distributes each group vertically into approximately 20 wafers. Each wafer has finite dimensions. A total of 2348 wafer top and bottom heights were used for this study. For each yield (15 Mt, 1 Mt, 100 kt, 10 kt, 1 kt) and particle size, wafer

height was taken to be the middle of each wafer top and wafer bottom height. Figure 2 shows a typical range of wafer heights for particles in a stabilized cloud.

Linear Regressions of Wafer Center Heights

To obtain a single-valued function of particle diameter vs height for use in the smearing codes, the spatial center height for each size wafer set was computed as the average of the wafer center heights for each particle diameter. Plots of the spatial center heights vs particle diameters for each yield showed that a linear fit accurately represented the vertical distribution. If the average wafer height of each size represents the maximum radioactivity for that size, then the locus of points along the ground, where the peak of each size falls, would be the fallout hotline. To test the "peak radioactivity height" hypothesis, this thesis study includes a direct comparison with the DELFIC hotline for a 100 kt surface burst. The hotlines match very well, suggesting that size-dependent radioactivity peaks can be modeled at spatial average wafer heights in the stabilized cloud. The case study is described in Section V. The five DELFIC output listings (1 kt, 10 kt, 100 kt, 1 Mt, 15 Mt) provided data to derive five linear fits. Particle diameters were correlated with spatial central wafer heights; the data and lines are shown in Figure 3. Higher yields generate larger vertical "spreads," steeper curves and higher clouds.

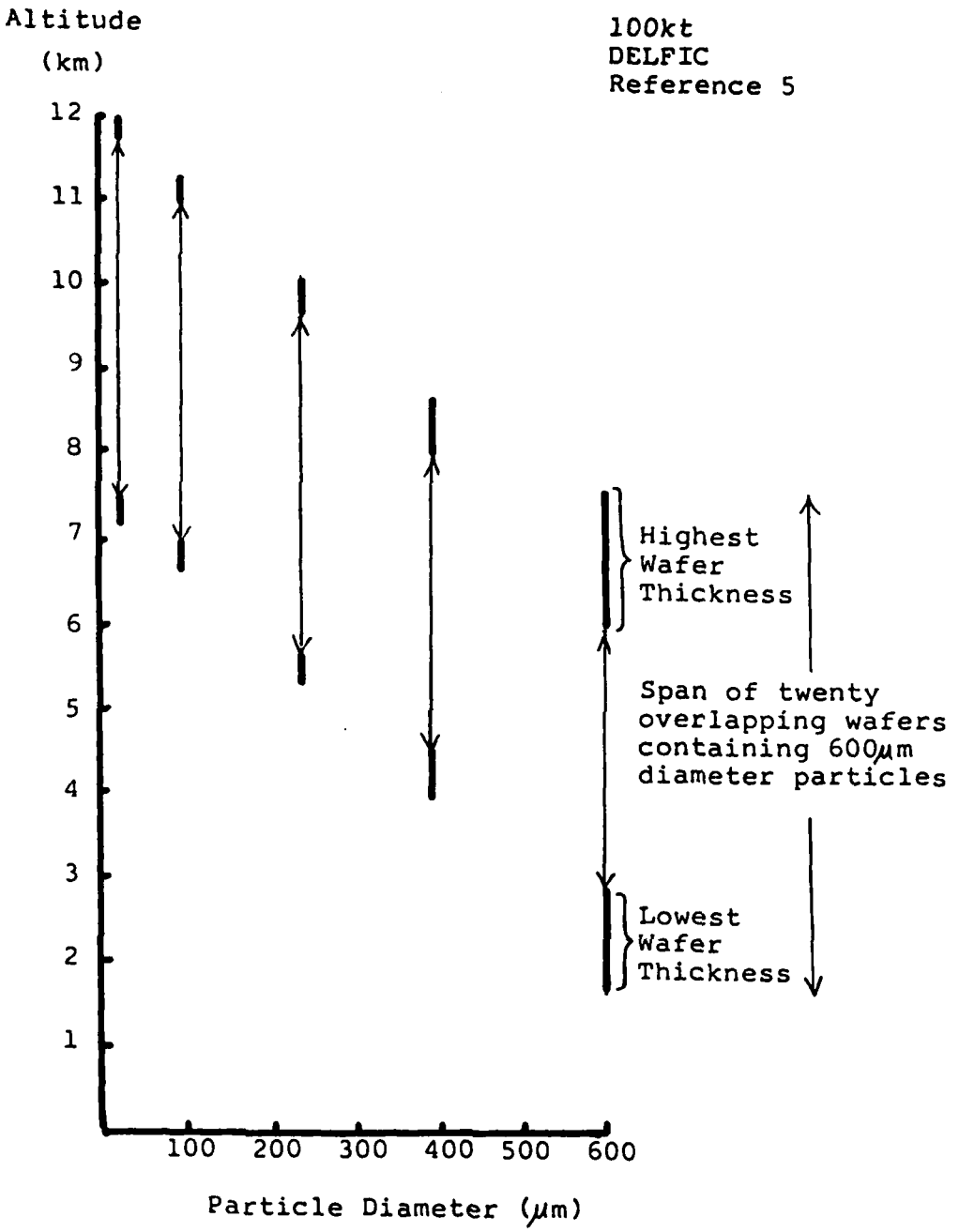

Figure 2. Typical Range of DELFIC Wafer Heights in a Stabilized Cloud

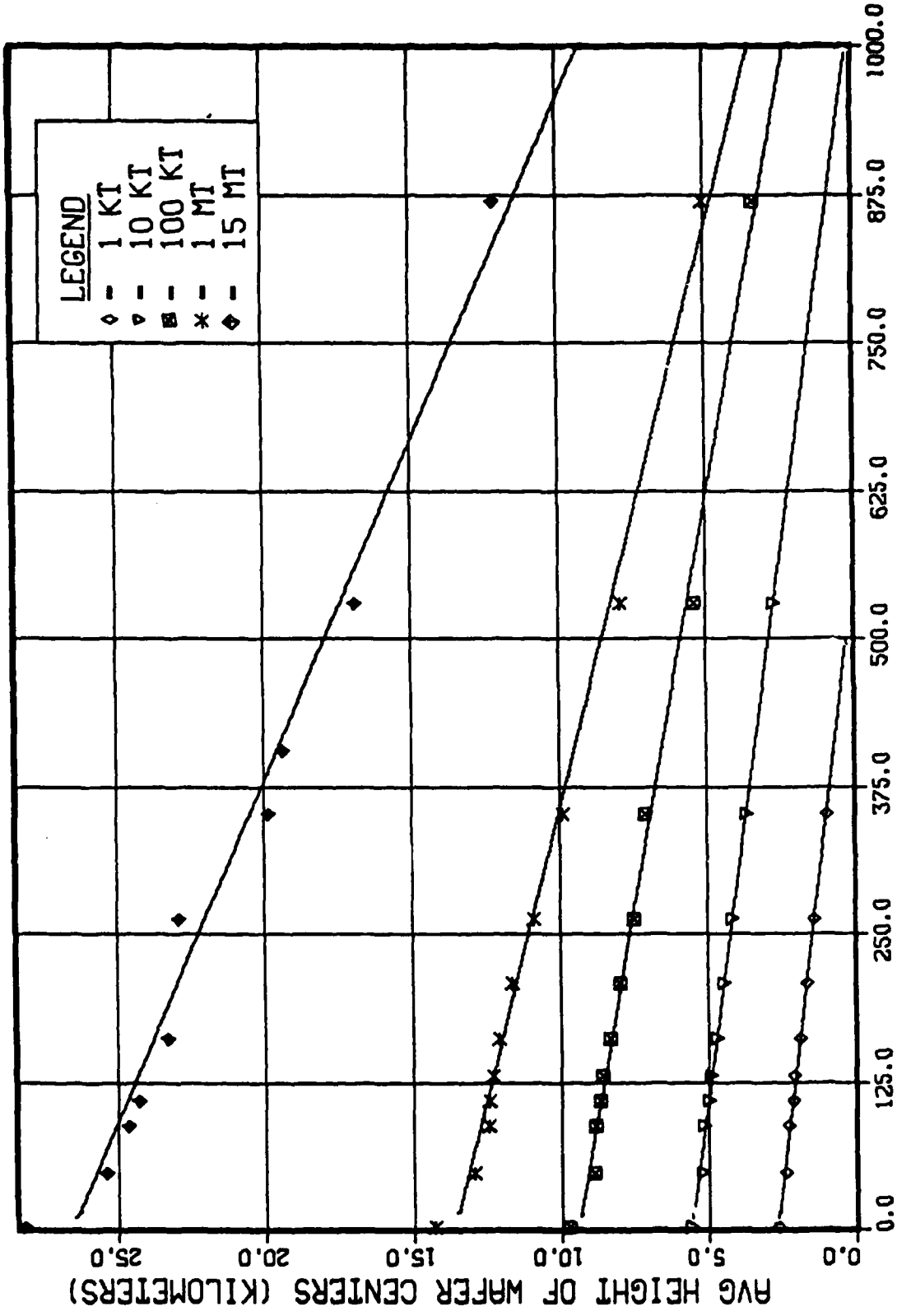

Figure 3. Average Wafer Height vs Particle Size in a Stabilized Cloud

Following are the equations developed from linear regressions:

$$H_c = (SLOPE)(D_p) + INTERCEPT \qquad (III.2)$$

H_c = Average height of wafer centers in stabilized cloud (m)

D_p = Particle diameter (micrometers)

SLOPE = (meters/micrometer)

INTERCEPT = Altitude of $D_p = 0$ on a Linear Fit (m)

Y	SLOPE	INTERCEPT
1 kt	-4.82	2670 (m)
10 kt	-5.44	5581
100 kt	-7.22	9496
1 Mt	-10.2	13677
15 Mt	-17.4	26643

Polynomial Least Squares Fits

To obtain similar relations for other yields, the slopes and intercepts were correlated, using a polynomial least-squares program (Ref 12). The following fits were obtained:

$$SLOPE = -EXP(1.574-.01197\ell nY+.03636(\ell nY)^2 - .0041(\ell nY)^3+.0001965(\ell nY)^4) \quad \text{(III-3)}$$

$$INTERCEPT = EXP(7.889+.34\ell nY+.001226(\ell nY)^2 - .005227(\ell nY)^3+.000417(\ell nY)^4) \quad \text{(III-4)}$$

Y = weapon yield (kilotons, kt)

Figure 4 shows the variations in slopes (absolute values) and intercepts with weapon yield. Given a weapon yield, the polynomial fits are used to generate values of slopes and intercepts, defining the linear equation for vertical distribution in a stabilized cloud. So, in a stabilized cloud, the central wafer height of a particle with diameter, d(m) , is given by (III-2). Figure 5 shows the parametric variation of central wafer height with weapon yield for thirteen particle sizes. As expected, larger yields raise wafers higher in the atmosphere.

Summary

The assumption of a single pancake initial cloud used in the AFIT model has been replaced with a vertical array of pancake clouds, one for each particle size. Particle size vs height in the initial cloud is computed from an empirical fit to DELFIC data.

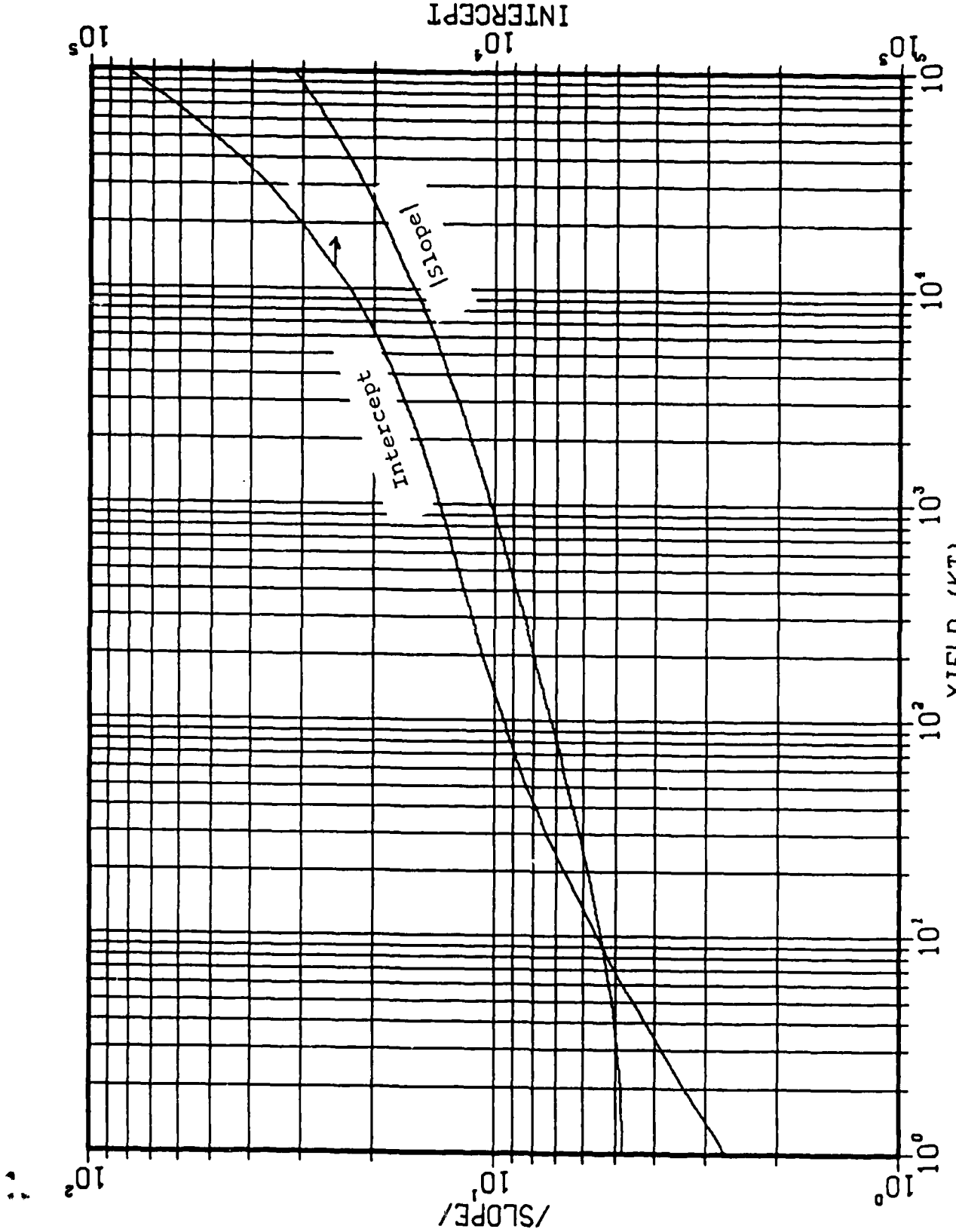

Figure 4. |Slope| and Intercept vs Yield

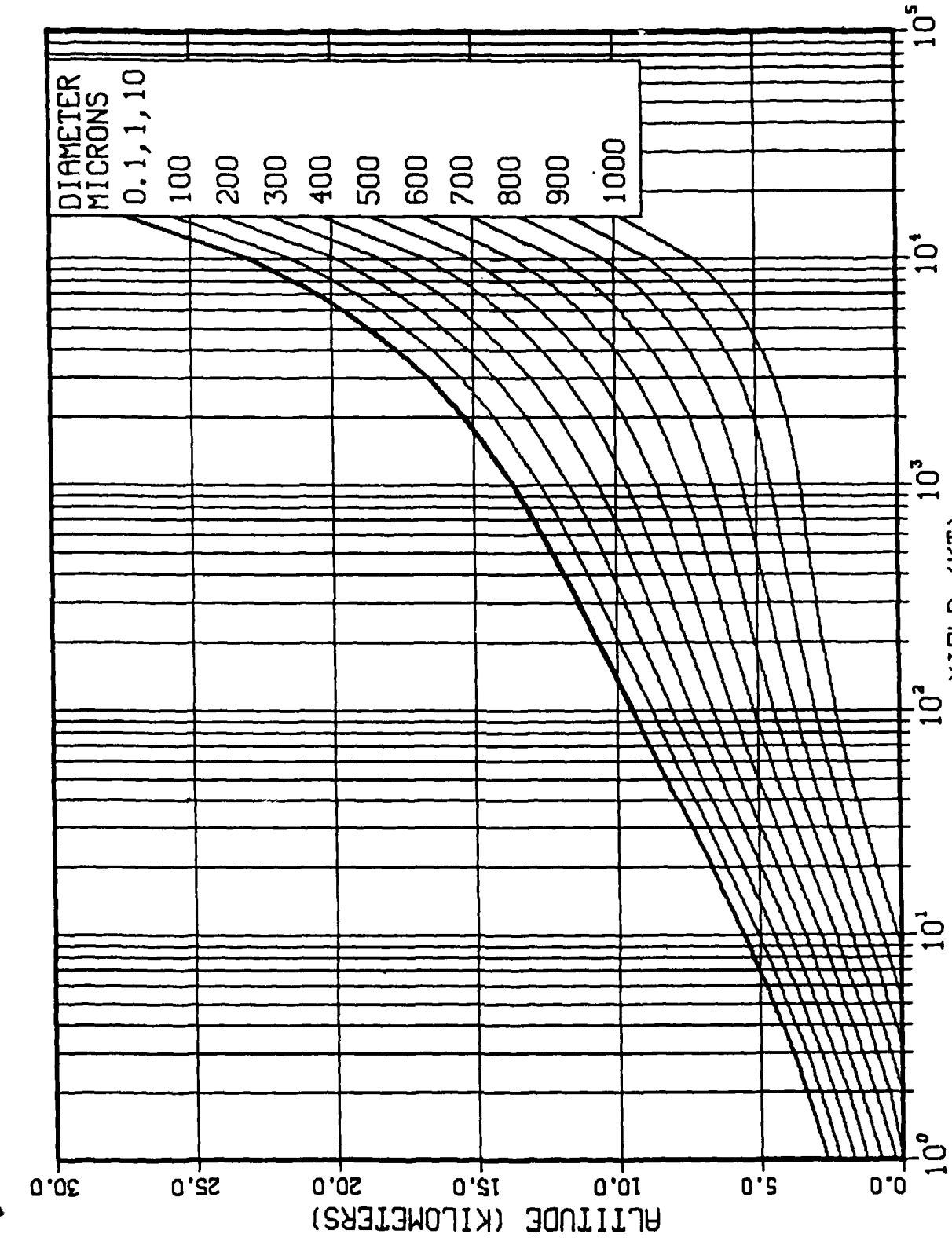

Figure 5. Average Height of Wafer Centers vs Yield

IV. Hotline Locator Model

Fallout hotlines curve realistically in DELFIC calculations because DELFIC traces the motions of wafers containing single-size particles through real wind profiles. The smearing codes compute uni-directional fallout contours with a constant "effective" wind described in References 2 and 8. However, real winds can vary both (spatially) throughout the altitudes where particles fall and (temporally) during the time that the cloud resides in the atmosphere. This section describes the computer model which predicts hotline locations with spatial wind variations beneath the stabilized cloud. Section VII describes a technique to simulate the combined effects of spatial and temporal variations.

Description

The hotline locator model computes and summarizes the motion of the initial cloud described in Section III. The model contains an atmosphere which is divided into three-hundred 100-meter-thick layers, with state properties computed as described in Appendix A. Figure 6 shows the model structure. With a real wind profile as input, the wind velocity and direction are linearly interpolated between data points, and a two-component wind vector (East: positive x, North: positive y) is generated for each atmospheric layer. Twenty particles, representing a fallout size

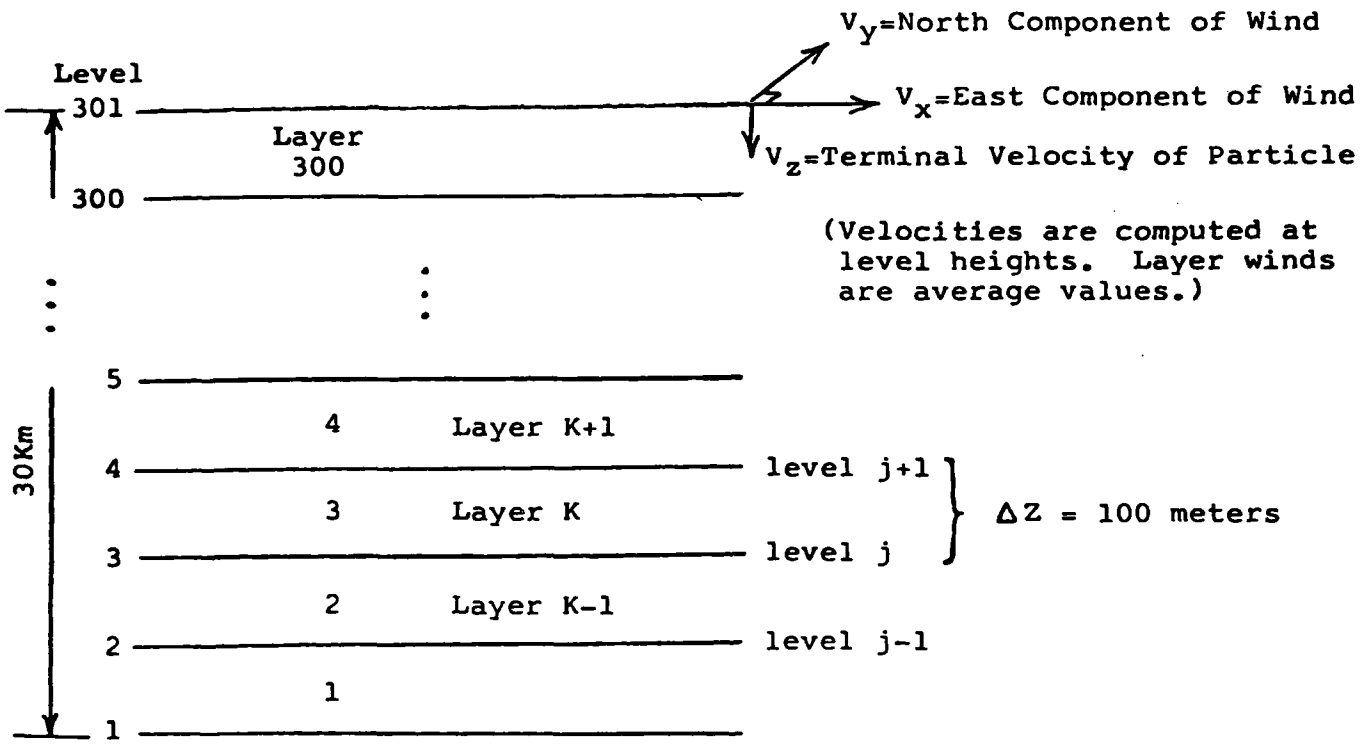

Figure 6. Hotline Locator Model Structure

spectrum, fall from the initial altitudes. Altitudes are computed for a gravity-sorted stabilized cloud using polynomial fits and linear height functions. Particle sizes were selected to represent the fallout population and to give a downrange spread (hotline length) comparable with published data (Refs 5 and 14). Twenty particle diameters are specified and their impact points (x,y) and arrival times are determined by winds, atmospheric state variables and particle residence times in each model layer.

Davies-McDonald Method

Particle-layer residence times were computed from terminal velocities which were calculated with the Davies McDonald method (Refs 6 and 7). Davies showed that Reynolds number, Re , of a moving sphere is related to the product of drag coefficient, C_D , and Re^2 , and the functional dependences were published in Reference 7:

If $C_D Re^2 < 140$ or $Re < 4$

$$Re = C_D Re^2 - 2.3363 \times 10^{-4} (C_D Re^2)^2 + 2.0154 \times 10^{-6} (C_D Re^2)^3 - 6.9104 \times 10^{-9} (C_D Re^2)^4 \quad \text{(IV-1)}$$

If $100 < C_D Re^2 < 4.5 \times 10^7$ or $3 < Re < 1000$

$$\text{Log}_{10} Re = -1.29536 + .986(\log_{10} C_D Re^2) - .046677 \cdot (\log_{10} C_D Re^2)^2 + .0011235(\log_{10} C_D Re^2)^3 \quad . \qquad \text{(IV-2)}$$

McDonald (Ref 6) showed that $C_D Re^2$ can be obtained explicitly for a given particle size and density at an altitude with known kinematic viscosity and density:

$$C_D Re^2 = 8W/\pi\rho\nu^2 \quad , \qquad \text{(IV-3)}$$

where

C_D = drag coefficient

Re = Reynolds number = $\frac{V_z d}{\nu}$

ρ = density of air (g/cm^3)

V_z = terminal velocity of particle (cm/sec)

d = particle diameter (cm)

ν = kinematic viscosity of air (cm^2/sec)

W = weight of particle = $\frac{4}{3}\pi(\frac{d}{2})^3 \rho_s g \ (\frac{gcm}{sec^2})$

ρ_s = density of solid particle (g/sec^2)

g = gravitational constant (cm/sec^2)

Centimeter-gram-second (cgs) units were used to facilitate comparisons with data published in References 6 and 7. Terminal velocity of a particle at a specified altitude is obtained by (a) computing $C_D Re^2$, (b) using Davies' equations to obtain Re, and (c) from the definition of Re:

$$V_z = \frac{Re\nu}{d}$$

The residence time, τ (sec), of a particle in a model layer of thickness ΔZ was computed from the average velocity of the particle in the layer.

$$\tau_{ik} = \left[\frac{\Delta Z}{\frac{(V_z)_j + (V_z)_{j+1}}{2}}\right] \qquad \text{(IV-4)}$$

where

τ_{ik} = residence time of i^{th} particle in layer k (sec)

ΔZ = thickness of layer (cm)

$(V_z)_j$ = terminal velocity of particle at bottom height of layer, level j (cm/sec)

$(V_z)_{j+1}$ = terminal velocity of particle at top height of layer, level j+1 (cm/sec)

(layer k is bounded by heights j and j+1) .

Knowing the residence time, particle translation in each layer was computed from the layer's mean wind components. Hotline coordinates (x,y, on the ground) were obtained by summing translations in all layers.

$$x = \sum_{H_p}^{H_g} V_{xk}\, \tau_{ik} \quad , \qquad y = \sum_{H_p}^{H_g} V_{yk}\, \tau_{ik}$$

where

x = ground coordinate in x (east) direction (m)

y = ground coordinate in y (north) direction (m)

V_{xk} = x component of wind velocity in layer k (m/sec)

V_{yk} = y component of wind velocity in layer k (m/sec)

τ_{ik} = residence time of i^{th} particle size in layer k (sec)

H_g = height of ground, MSL (m)

H_p = height of particle in stabilized cloud (m)

Summary

The model computes the total horizontal movement of 20 particles as they fall from an initial, vertically-distributed cloud. Real wind data is interpolated into each model layer. Particle fall speeds are determined by

the Davies-McDonald method. The hotline is the connection of the particles' ground impact points. Appendix B describes the computational algorithm and includes a code listing.

V. Case Study 1: Washington DC, 3 Oct 68, 100 kt Hypothetical

In Reference 4, Norment compared the fallout contours generated by DELFIC, WSEG and SEER in real winds using a set of hypothetical and real atmospheric nuclear detonations. To compare hotline locations generated in this thesis study with DELFIC results, the Washington DC, 3 Oct 68, 100 kt case was selected, primarily because the DELFIC hotline exhibited curvature. The wind profile is shown in Figure 7.

DELFIC Hotline and Size Distribution Independence

Dose rate contours from DELFIC (Ref 4) are shown in Figure 8. The double hotline was confirmed by analyzing the DELFIC numerical output for this case provided in Reference 5. Two peaks in dose rate were observed at downrange distances greater than ∿35 km. Figure 9 is a plot of two sets of DELFIC hotline coordinates, generated by two different particle size distributions (PSD). As shown in Table I, the default PSD contains an average particle diameter of .407 μm, and the large PSD contains a 24.0 μm average diameter. In the region of the double hotline, the bottom line has higher dose rates, suggesting that the hotline is curving downward as the cloud translates downwind. The two DELFIC calculations were analyzed to identify downrange locations of peak dose rate, thereby defining

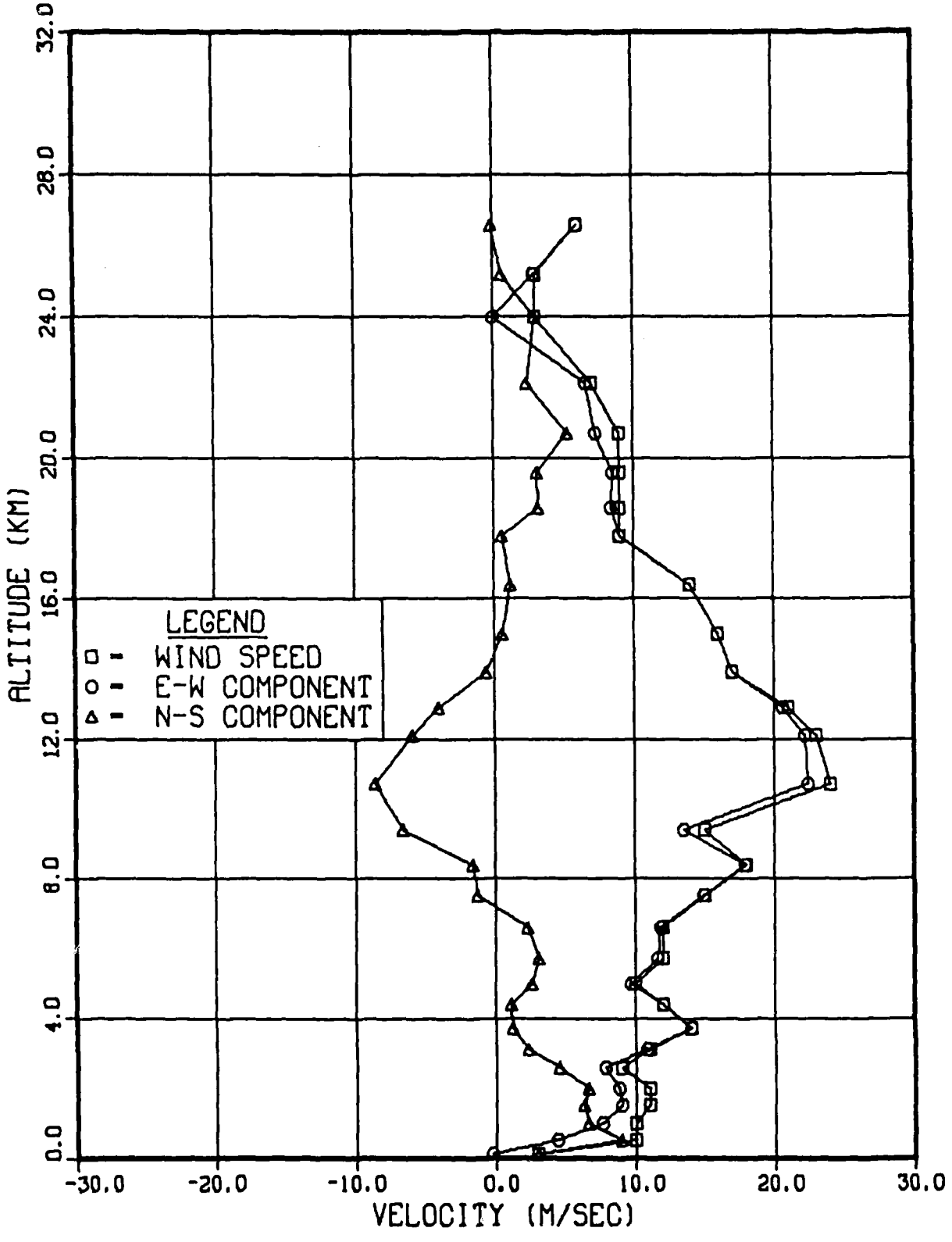

Figure 7. Wind Profile, Washington, D.C., 3 Oct 68

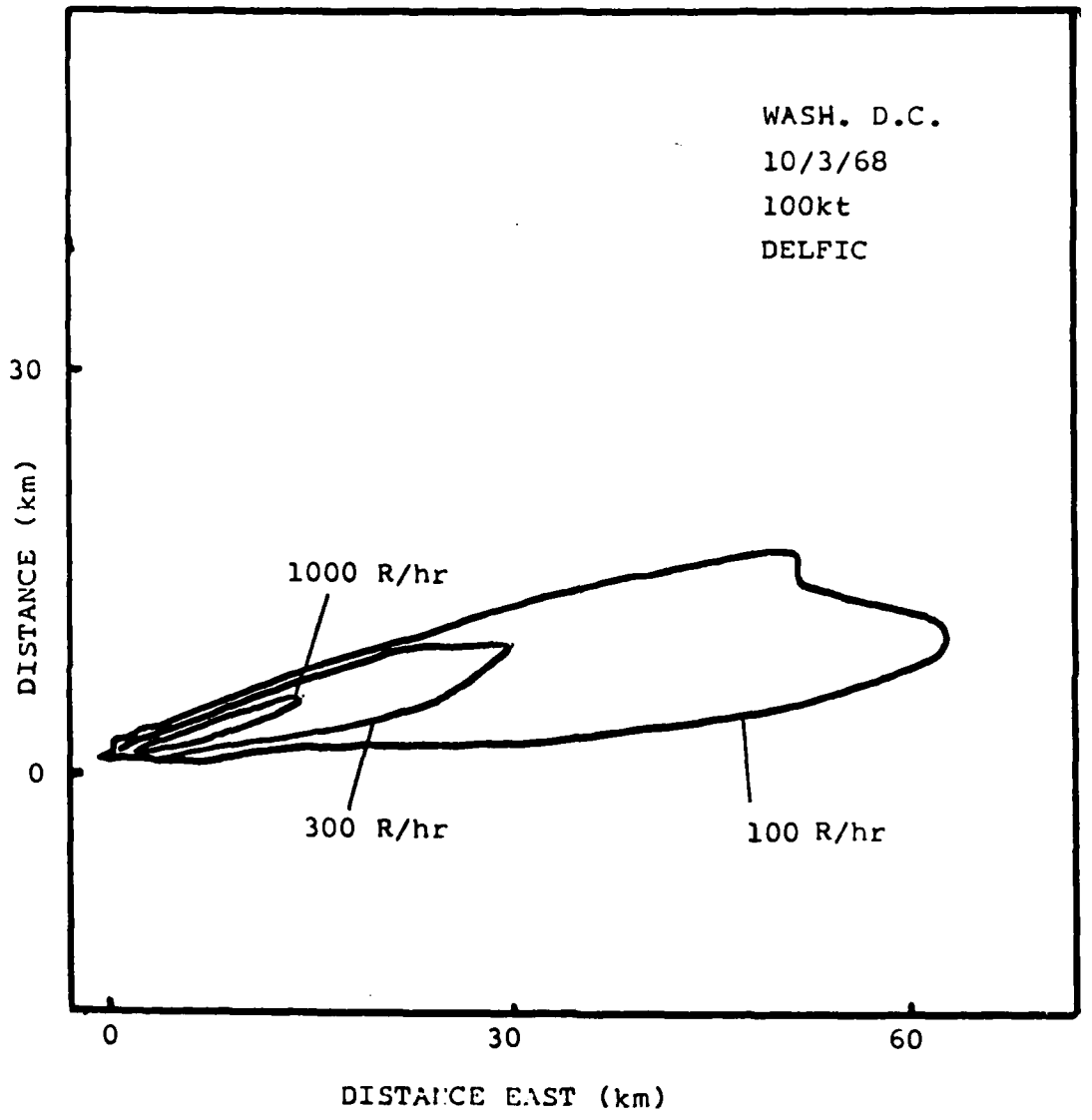

Figure 8. DELFIC Dose Rate Contours for Wash., D.C., 3 Oct 68, 100kt Case (Norment)

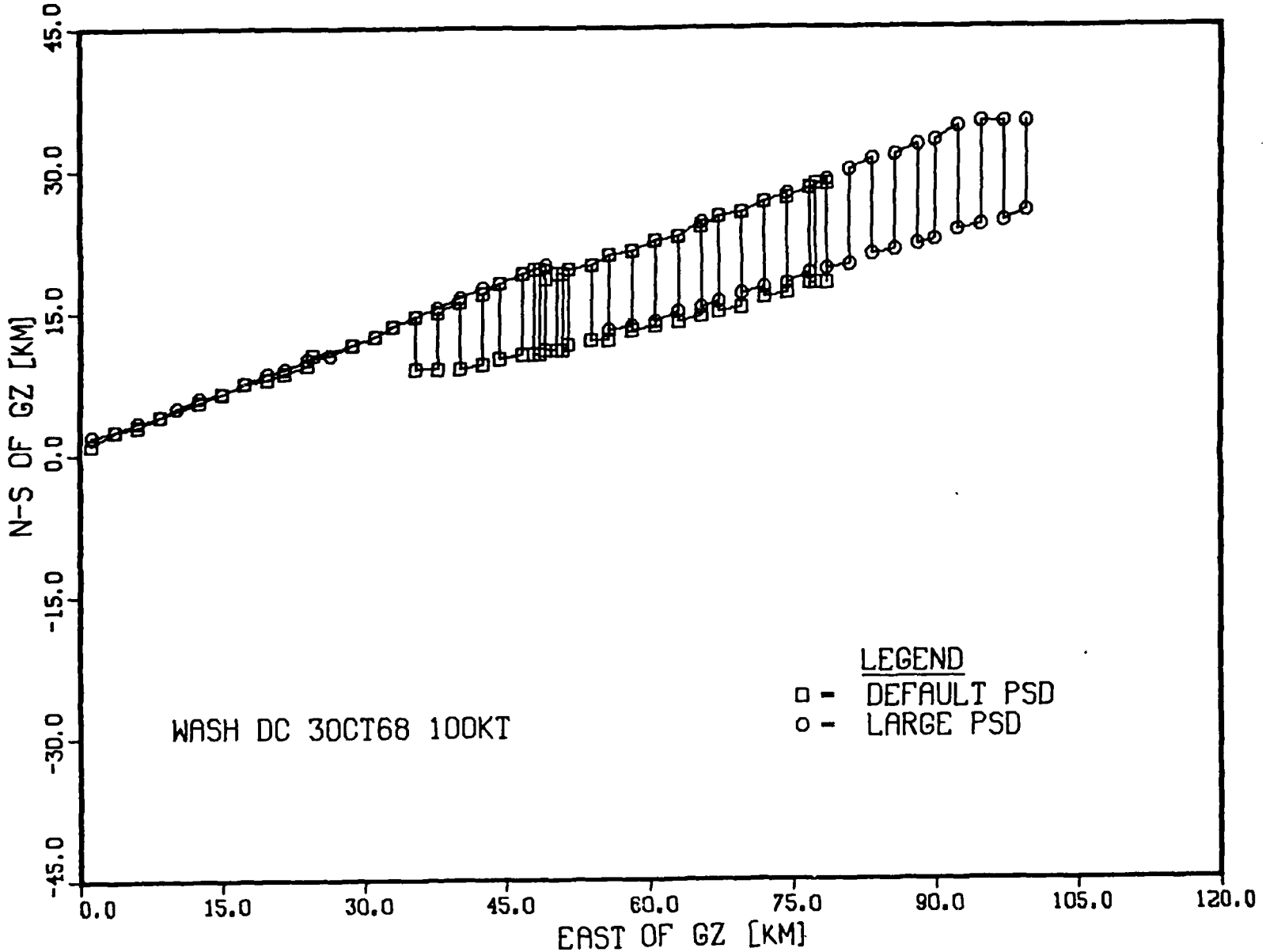

Figure 9. Hotlines (DELFIC) Washington, D.C., 3 Oct 68, 100kt

the hotline. Figure 9 also shows the hotline provided by the larger distribution. The DELFIC hotline locations are identical, independent of the two different particle size distributions assumed for the calculations. For a given yield, DELFIC raises wafers of fixed particle size to the same heights in the stabilized cloud. Since the two size distributions overlap, DELFIC predicted the same hotlines. In the region where the distributions do not overlap, the hotlines are continuous. So, given a yield and a wind profile, DELFIC will predict constant hotline locations. Therefore, a hotline locator model should predict the same hotline locations with different assumed particle size distributions. In fact, the hotline locator model contains an array of particle sizes, selected only to resolve hotline coordinates.

Hotline Comparisons

The hotline locator model, described in Section IV, was used to predict the Washington DC 100 kt hotline. Particle sizes selected for the calculations are shown in Table I. Particle sizes were selected from the DELFIC calculation to represent (approximately) intervals of 5% in cloud activity. The wind profile from Figure 7 was used as input.

Table I

Particle Size Distributions

$$N(d) = \frac{1}{\sqrt{2\pi}\ \ell n(r)d} \quad EXP\text{-}\tfrac{1}{2}\left[\frac{\ell n(d) - \ell n(\bar{d})}{\ell n\sigma}\right]^2$$

N(d) = Number per micrometer size range

d = Particle diameter (m)

	Median Diameter $\bar{d}$, μm	Deviation σ, μm
Default PSD	0.407	24.0
Large PSD	4.0	2.0

Table II

Particle Size Array (diameter, cm)

.0605	.0089
.0290	.0081
.0218	.0074
.0184	.0067
.0160	.0050
.0144	.0054
.0129	.0048
.0117	.0042
.0106	.0035
.0097	.0026

Figure 10 shows two predictions from the hotline locator model and the DELFIC hotline. The pancake cloud hotline was generated by starting all particles at 9.2 km altitude, computed with Eq (III-1). The wafer centers hotline (labeled "wafer ctrs") was produced by starting the particles from altitudes computed from linear size-height relations described in Section III. All computations used real wind profiles beneath the stabilized cloud.

The pancake cloud hotline is nearly unidirectional. Computations performed for this thesis study indicate that the pancake cloud assumption severely restricts hotline curvature. If all particles fall from the same altitude, hotline curvature must be caused by different fall velocities (residence times) in wind layers. From a pancake cloud, the differences are not large enough to produce significant curvature in the particles' ground traces. The pancake cloud hotline deviated (crossrange) from the DELFIC hotline by approximately 10 km at 50 km downrange. At long distance (> 200 km) the pancake and "wafer ctrs" hotlines agree within 5 km.

The "wafer ctrs" hotline is on the DELFIC hotline at ranges less than 40 km, where it properly curves toward the more intense part of DELFIC's dual ground trace. The agreement between the "wafer ctrs" hotline and DELFIC is expected because the "wafer ctrs" inputs are DELFIC wafer heights. However, since a single height was used for each

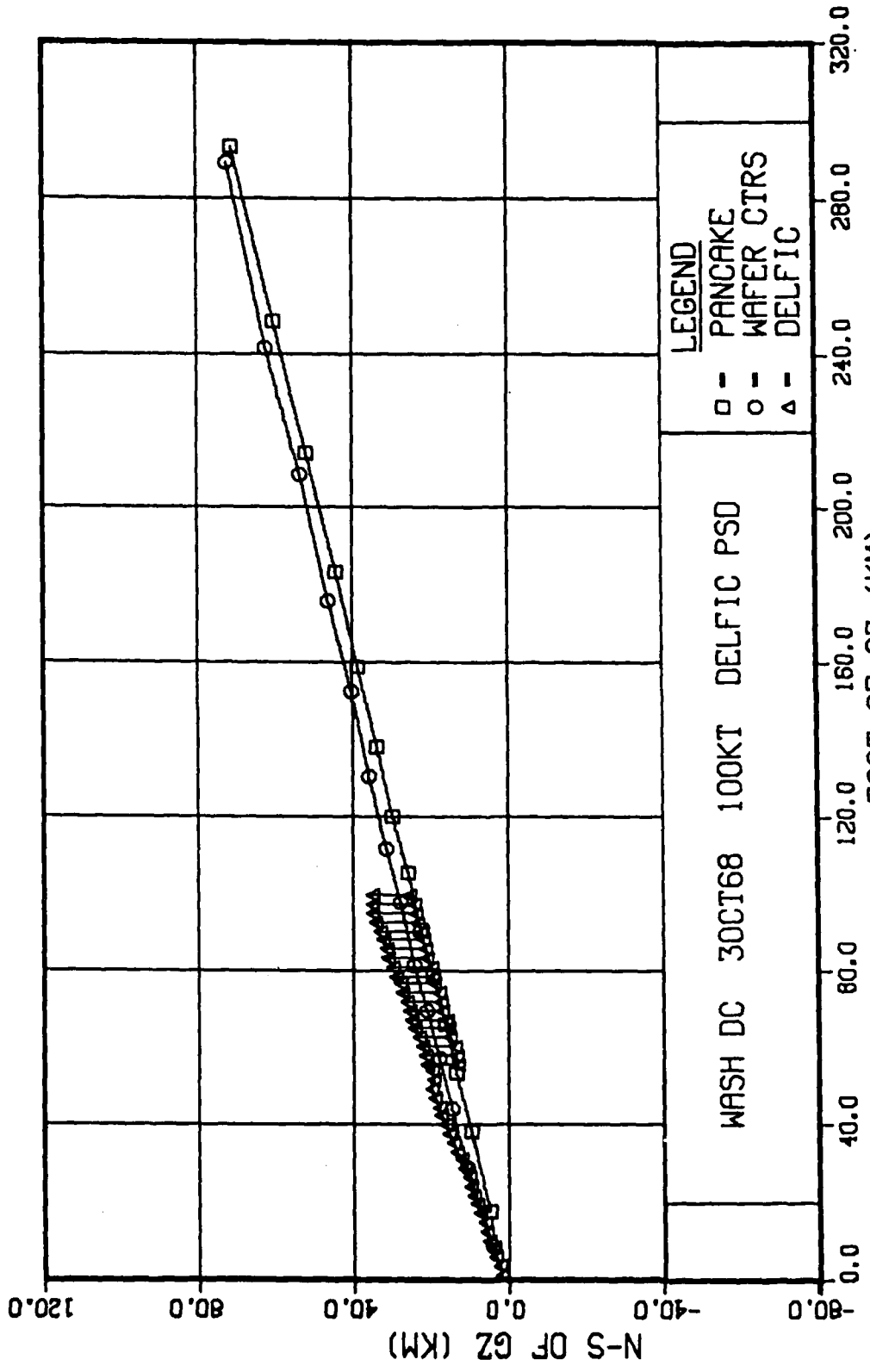

Figure 10. Hotline, Washington, D.C., 3 Oct 68, 100kt

particle size in the hotline locator model, this case study showed that the hotline location can be computed from a stabilized cloud modeled with a linear relationship between particle size and height. Furthermore, since the hotline represents the locus of peak activity on the ground, it can be inferred that the wafer central heights represent maxima in vertical activity distributions for corresponding particle sizes in the initial stabilized cloud.

Sensitivities

For 100 kt, Eqs (III-3) and (III-4) give 7.228 $\frac{m}{\mu m}$ and 9496 m for slope and intercept of the particle size vs height array in stabilized clouds. To evaluate the sensitivity of hotline location to consistent variations in the vertical array, additional calculations were performed with yield varying by ± 10% and ± 20%. Sensitivity of stabilized cloud height is shown in Figure 11, in terms of variations in the mean wafer center heights. A variation of ± 20% in weapon yield produced about ± 5% variation in height over the entire range of particle sizes. Hotline location was relatively insensitive to variations (uncertainties) in weapon yield. Figure 12 shows the maximum hotline excursion, obtained for Yield = 80 kt.

In summary, the Washington DC case study supports the following conclusions:

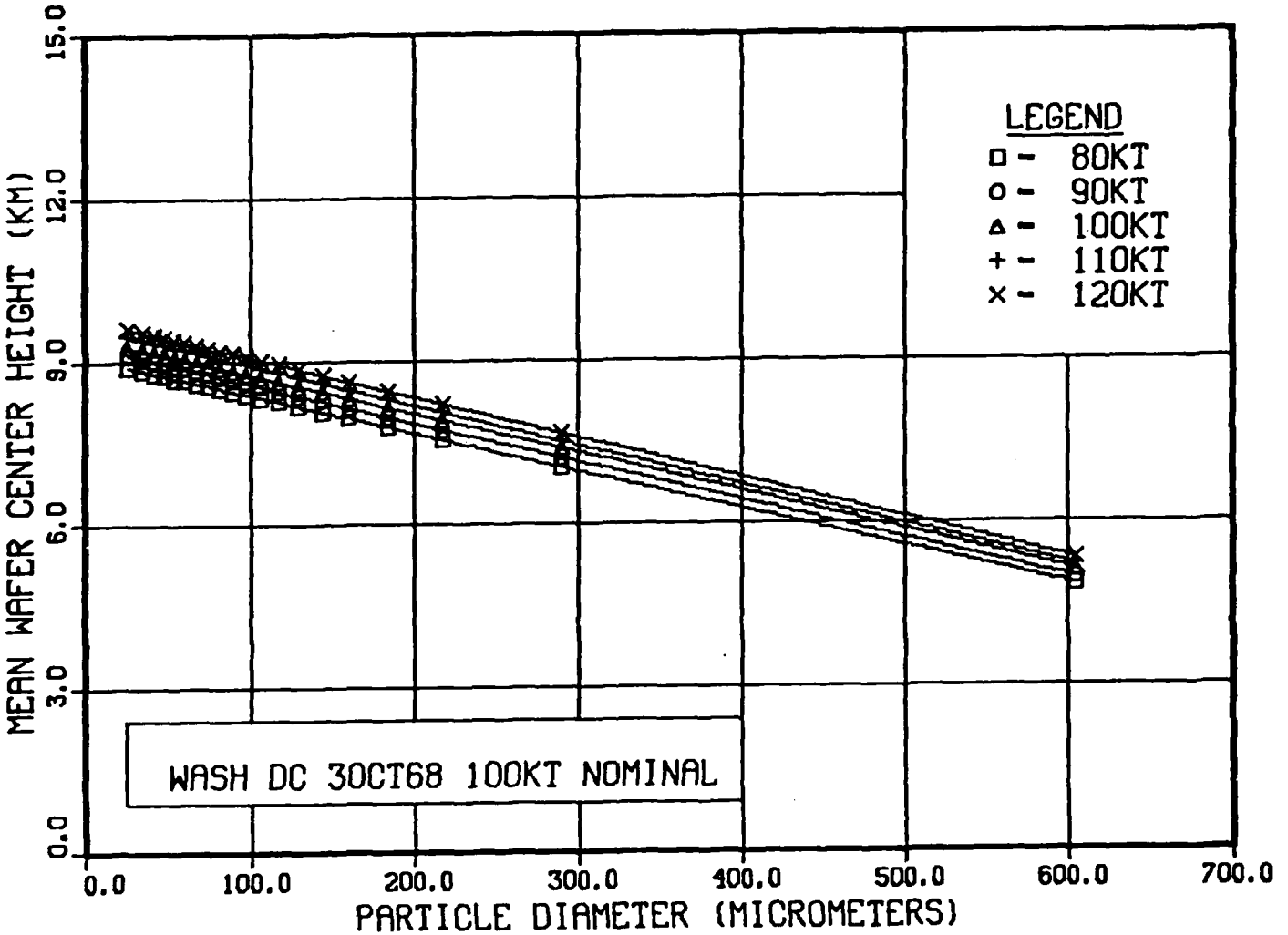

Figure 11. Yield Sensitivity of the Stabilized Cloud

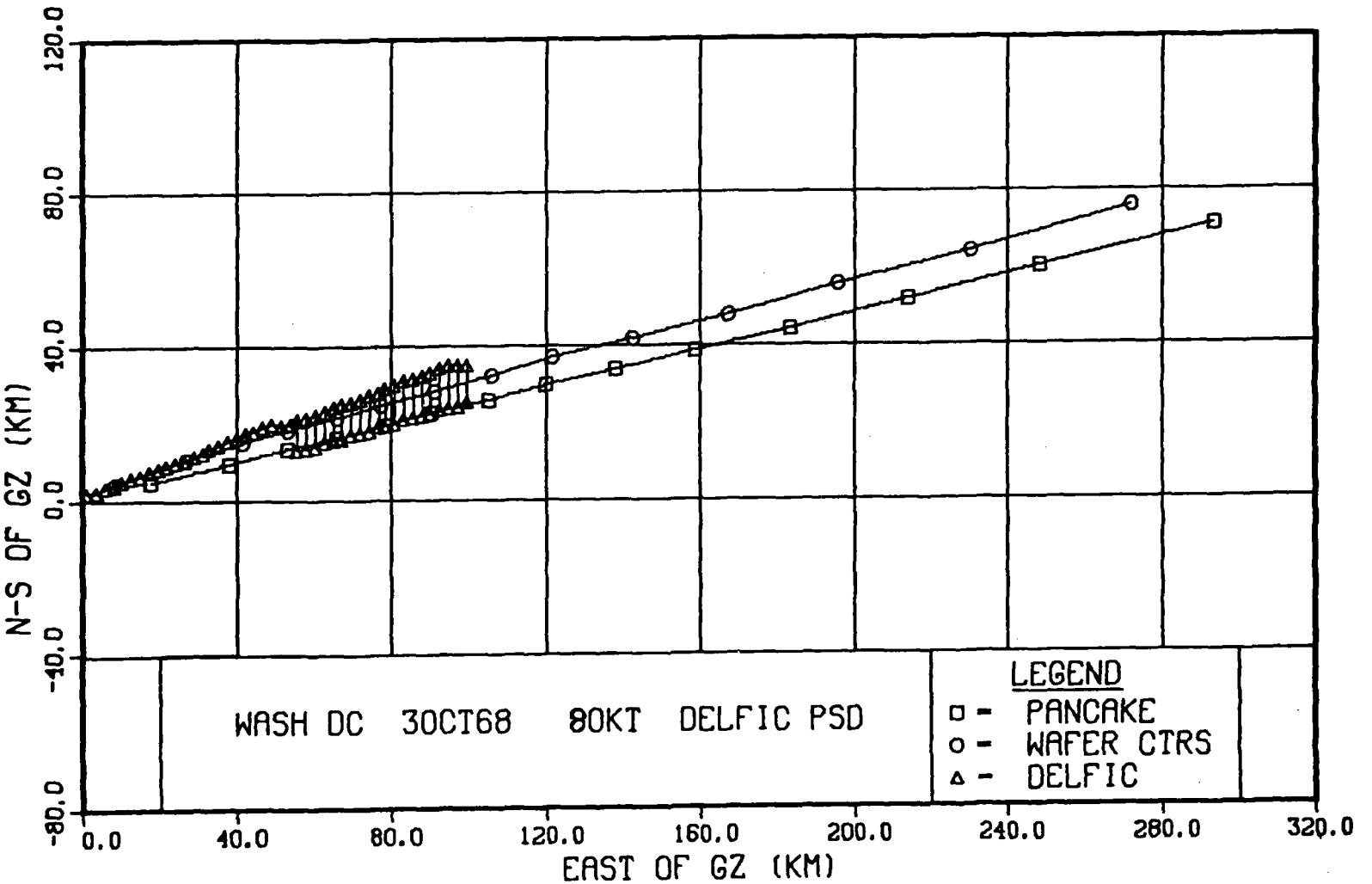

Figure 12. Hotlines, 80kt Sensitivity

1. DELFIC hotline location is independent of the assumed particle size distribution;
2. The hotline location can be computed from a linear relation between particle size and height in the initial stabilized cloud.

VI. Case Study 2: Castle-Bravo
4 Mar 54, 15 Mt, Pacific Test

The hotline locator model was used to compute the hotline coordinates of the Castle-Bravo nuclear cloud. Castle-Bravo was also predicted by DELFIC, so this case study was an opportunity to compare the hotline locator results to both DELFIC and actual fallout contours. When it was learned that the models agreed, but neither predicted the actual hotline, a new technique was developed to back calculate initial particle heights in the cloud. These back calculations provided a new interpretation of the stabilized cloud produced by the high yield Pacific test.

AFSWP Fallout Contours

The Castle-Bravo nuclear weapon test was detonated in the Bikini Atoll on 4 March 1954. The unexpectedly high fission yield and changes in the wind structure caused significant fallout to reach populated islands (Ref 13). The Armed Forces Special Weapons Project (AFSWP) collected air and ground fallout samples and constructed the fallout contour map shown in Figure 13 (Ref 14). The fallout hotline dipped southward before tracking to the east and northeast. Figure 13 shows estimates of fallout arrival times at various distances downrange. Wind data

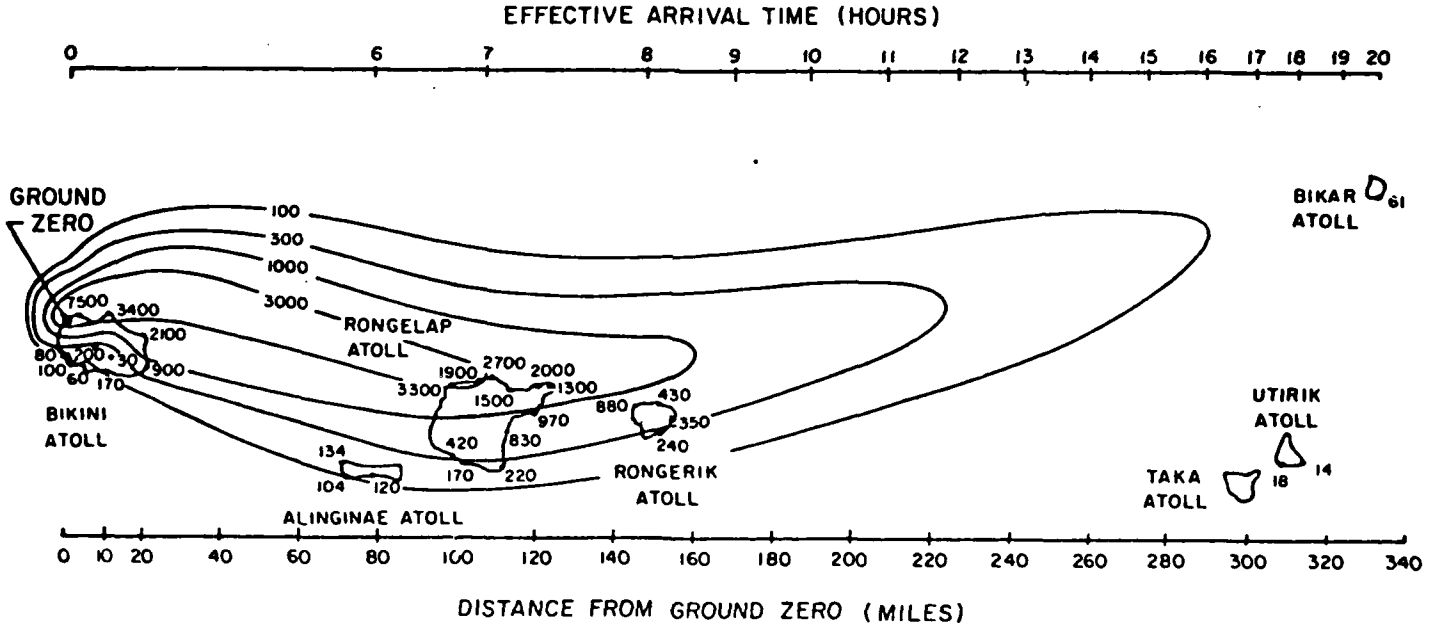

Figure 13. Castle-Bravo Fallout Contours (Glasstone)

was obtained from Enewetok, Kwajalein and Rongerik Islands, as well as the U.S. Navy ship S.S. Curtis. The best fallout predictions were calculated with a wind profile developed from data reported by Dean and Olmstead (Ref 4), and plotted in Figure 14.

Back Calculations

In this study, the hotline locator model was used to predict the Bravo hotline. The prediction generally agreed with DELFIC, but did not agree with the experimental (AFSWP) hotline. Figure 15 shows the DELFIC prediction (Ref 4). Figure 16 shows the AFSWP hotline and two predictions with the hotline locator model. "Wafer ctrs" refer to calculations with the particle starting heights computed from polynomial correlations of linear fit parameters. The pancake hotline was produced by a single pancake cloud located at 16.9 km (computed with Eq (III-1). Dean and Olmstead winds were used to translate the particles.

To help explain the Bravo fallout motion, this study used real winds in a "vertical stack" diagnostic technique to back calculate the initial heights in the stabilized cloud from which particles had to fall in order to have landed on the AFSWP hotline. The "vertical stack" technique computes ground traces of continuous single-size-particle stacks from surface to 30 km altitude. The intersections of vertical stack ground traces with the actual hotline

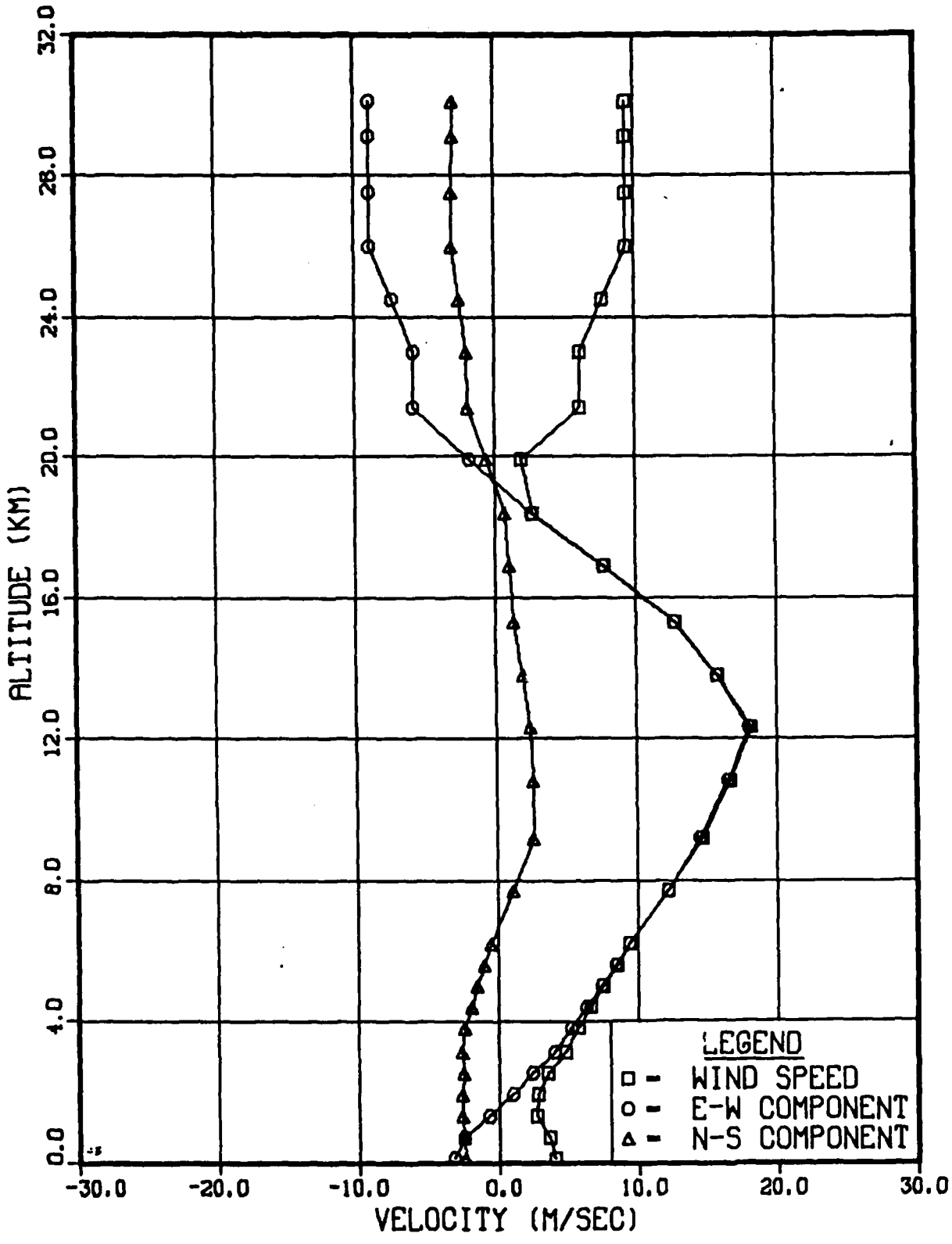

Figure 14. Wind Profile, Castle-Bravo, T-0, Dean and Olmstead Winds

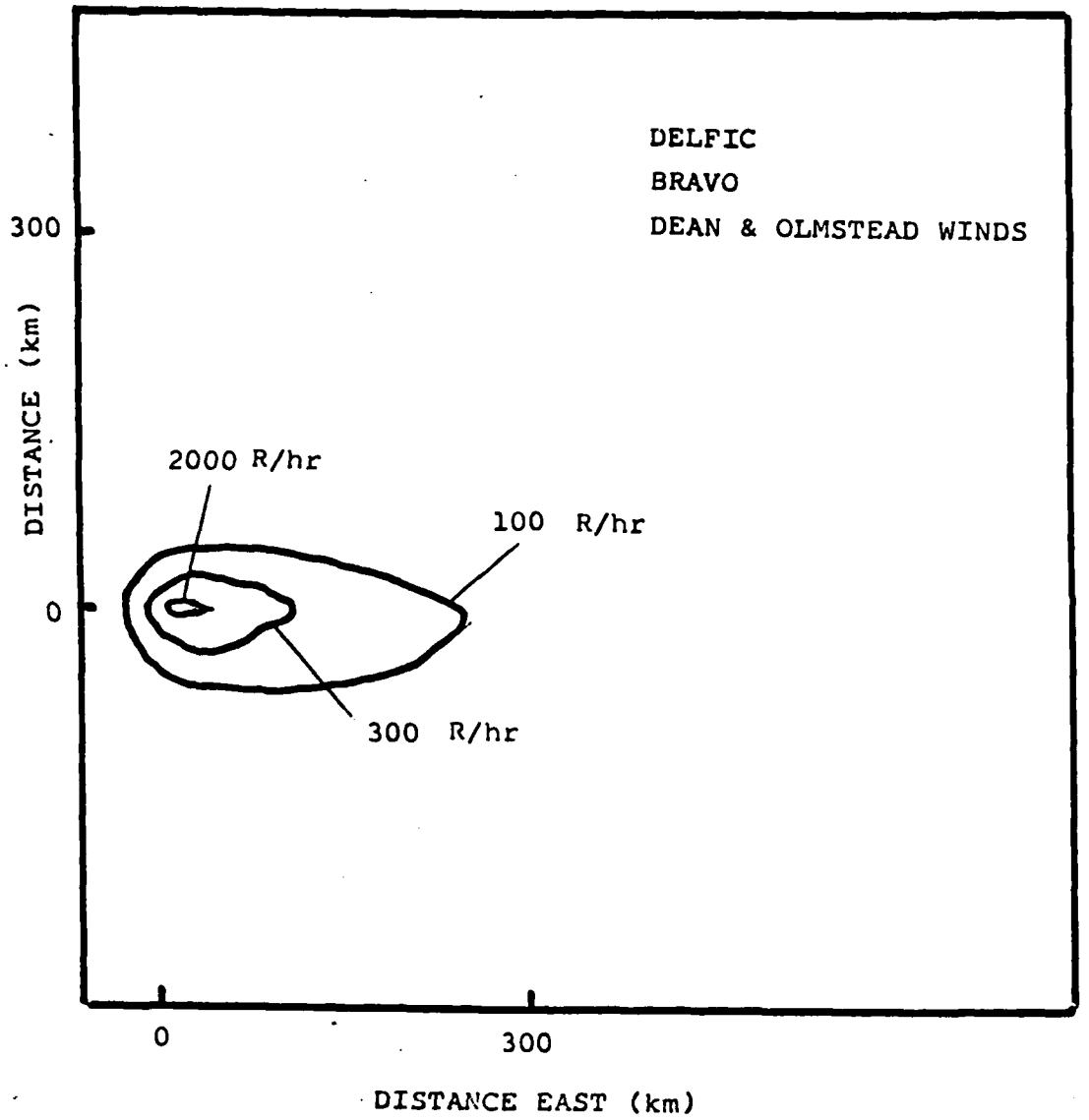

Figure 15. DELFIC Calculation of Castle-Bravo Fallout Contours (Norment)

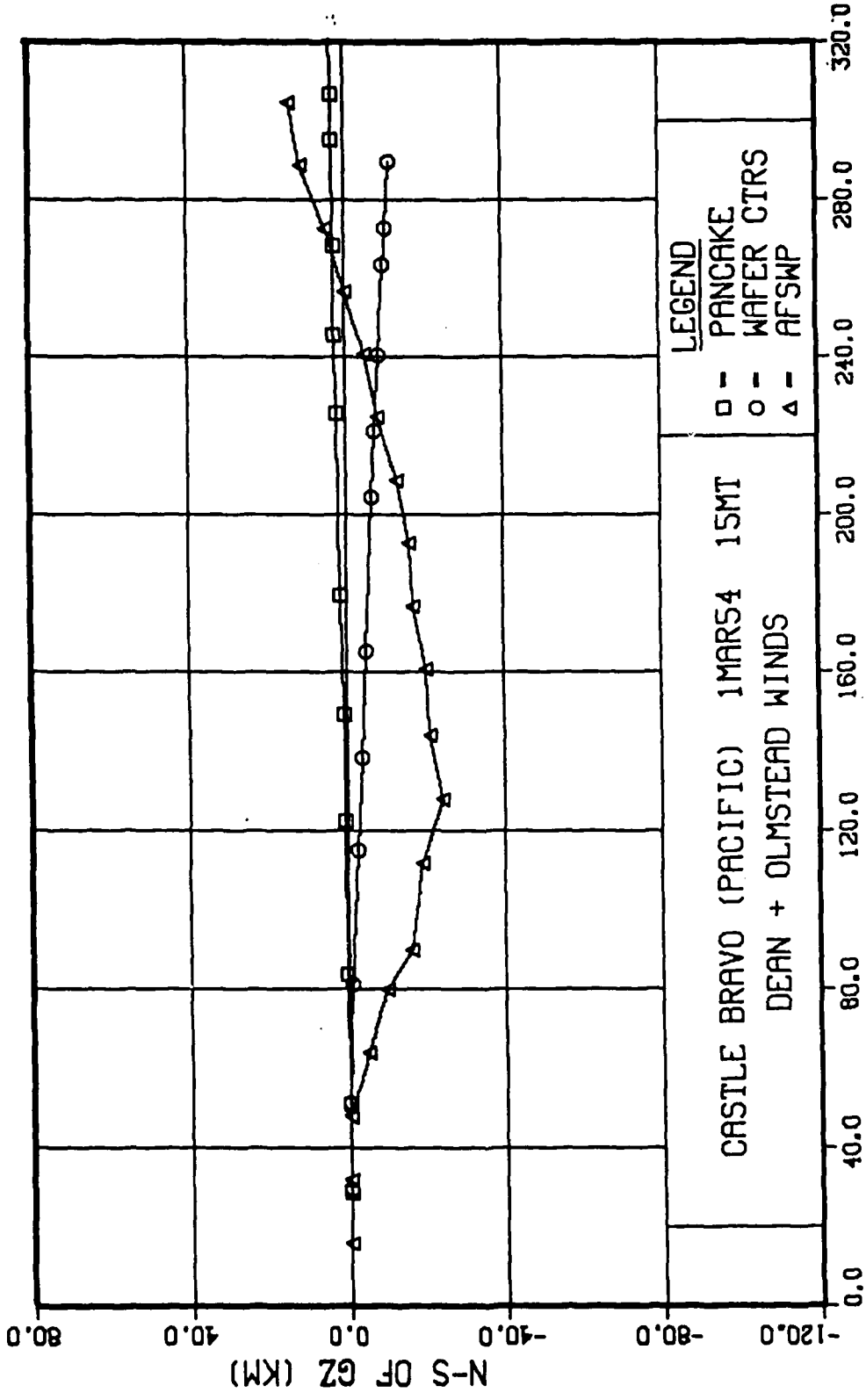

Figure 16. Hotlines, Castle-Bravo (Pacific) 1 Mar 54 15Mt, Dean and Olmstead T-0 Winds

define the starting altitudes of specific particle sizes. Different size particles have different ground traces because of differences in terminal velocities, residence times, and vector translations in wind layers.

Figures 17 and 18 show ground traces of vertical stacks. In Figure 17, the stacks extended up to the lowest wafer bottom height given for each particle size in the corresponding DELFIC calculation (Ref 5). Lowest wafer bottom heights are shown in Table III. The lowest DELFIC wafers landed closest to the AFSWP hotline. Figure 17 shows that DELFIC could not possibly have predicted the AFSWP hotline, since DELFIC's stabilized cloud was too high for wafers to land on the hotline. In Figure 18, the stacks extended up to 30 km, the maximum level height in the hotline locator model. The back calculations clearly display two features which may explain why previous predictions failed to replicate the southward curvature in the Castle-Bravo hotline:

1. Within 130 km of ground zero, particles which landed on the hotline started from altitudes well below stabilized cloud heights predicted by DELFIC and the WSEG empirical equation.
2. Between 130 and 280 km, the hotline is nearly parallel with particle stack ground traces, implying that initial particle sizes did not change much with altitude in the portion of the cloud that landed in that region.

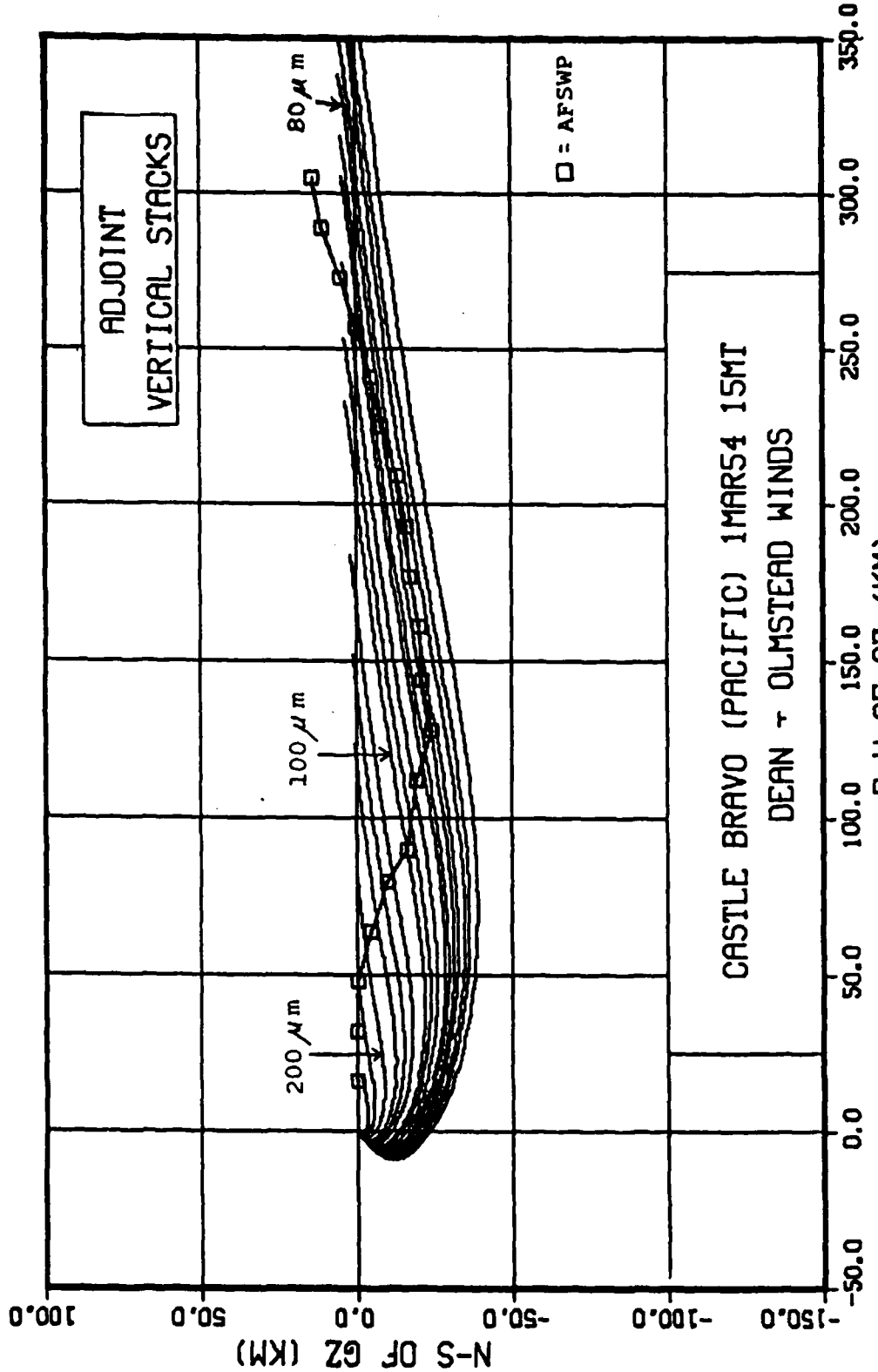

Figure 17. Ground Traces of Single-Size Particle Stacks, up to DELFIC Lowest Wafer Bottom Heights

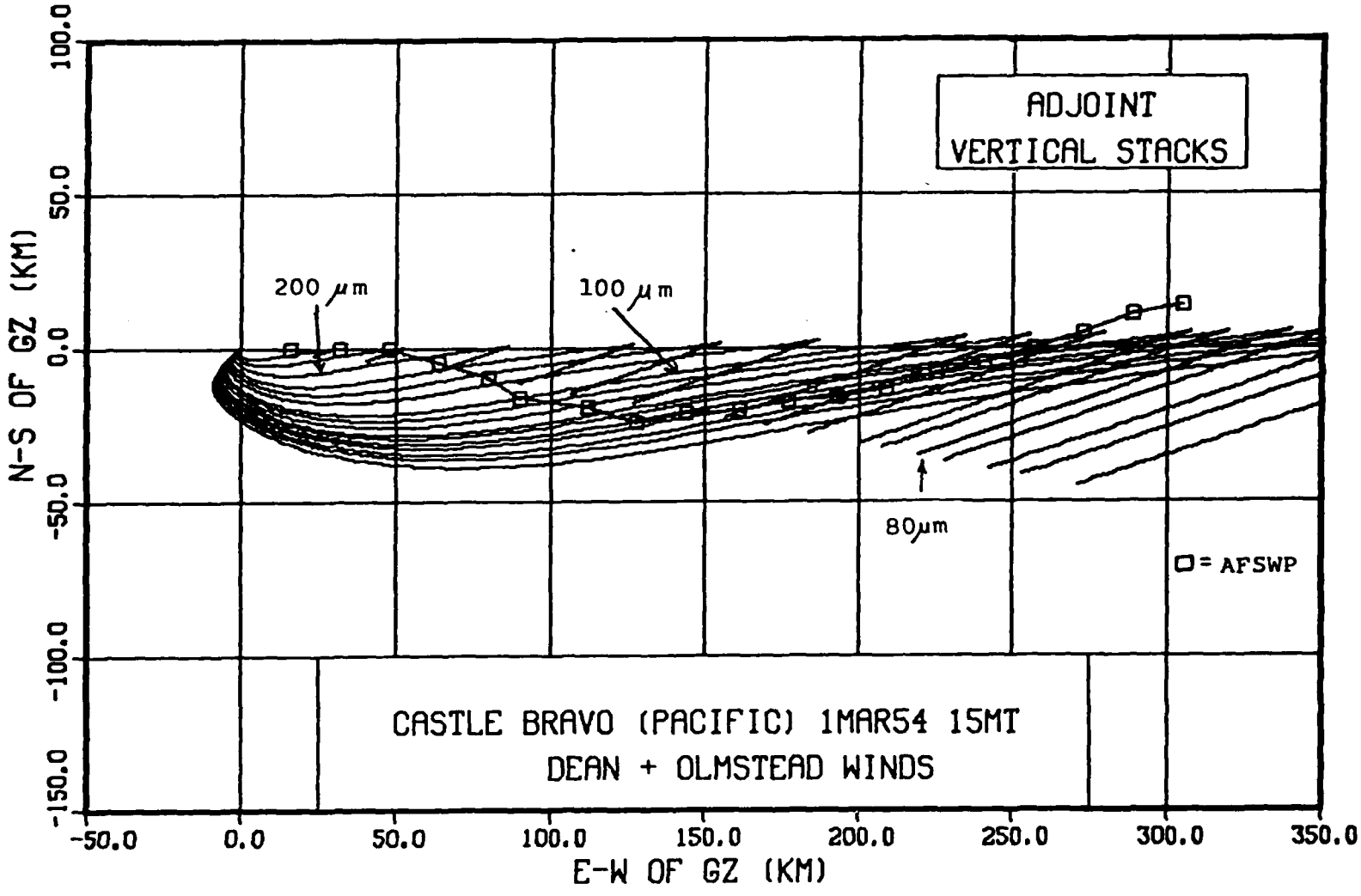

Figure 18. Ground Traces of Single-Size Particle Stacks, up to 30km

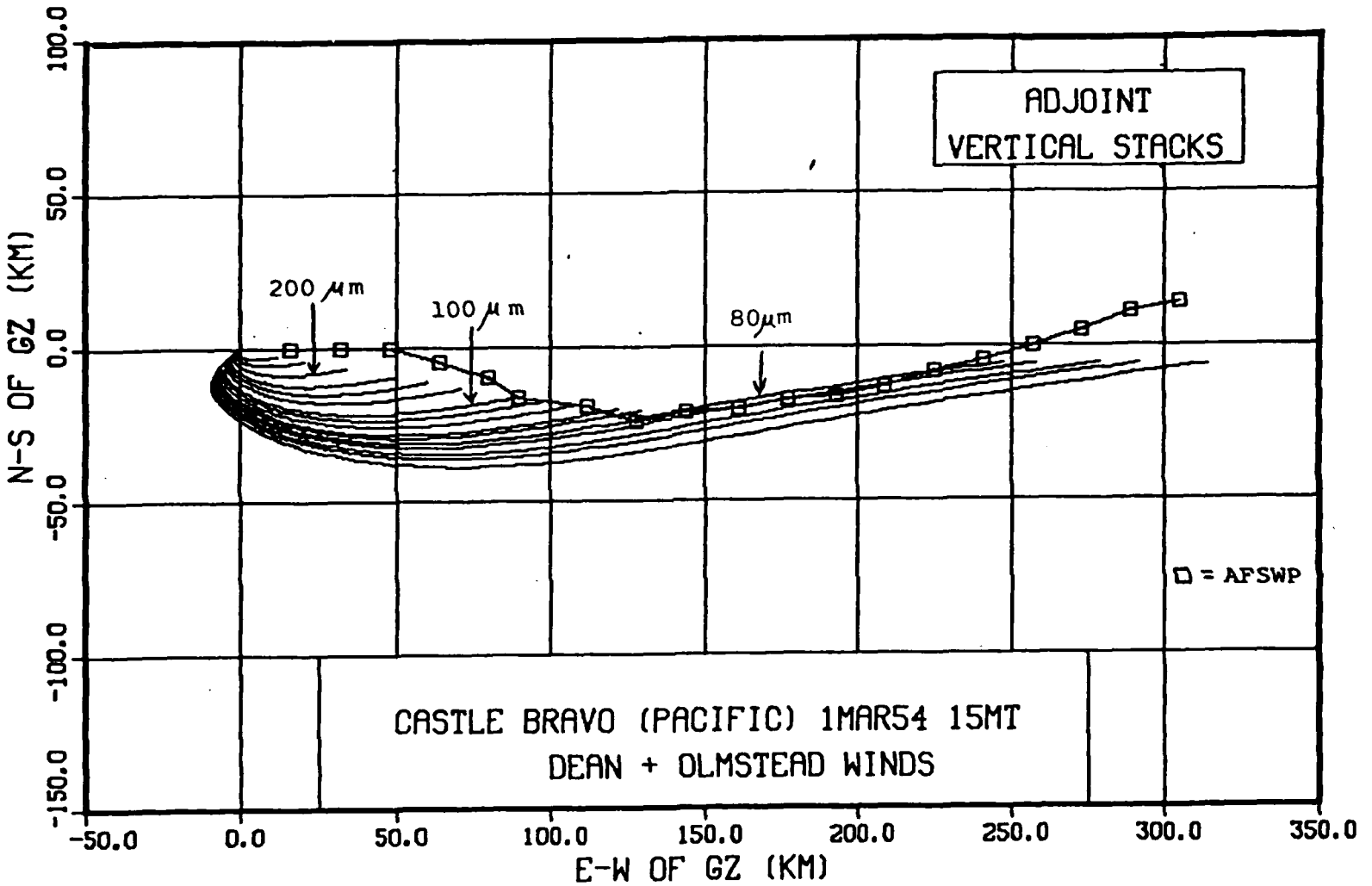

Figure 19. Ground Traces of Single-Size Particle Stacks, up to Adjoint Heights

Table III

DELFIC 15 Mt Calculation
Lowest Wafer Bottom Heights, Hb

Diameter (μm)	Hb (km)
500.	11.5
300.	14.5
200.	16.1
150.	17.0
130.	17.4
115.	17.6
100.	17.9
95.	17.9
90.	18.1
85.	18.1
83.	18.2
80.	18.2
78.	18.3
75.	18.3
73.	18.3
70.	18.4

To define the initial cloud, stack heights were estimated to produce ground traces that intersected the AFSWP hotline. Figure 19 shows ground traces of stacks which extended up to heights given in Table IV. Each ground trace is a

Table IV

Stack Heights for Adjoint Calculation

Particle Diameter (μm)	Stack Height (km)	
500	9.2	Pancake Cloud
300	9.2	
200	9.2	
150	9.2	
130	9.2	
115	9.2	
100	9.2	
95	9.2	
90	9.3	
85	9.4	
83	9.5	
80	9.5	Uniform Size Region
80	10.3	
80	11.3	
80	12.2	
80	13.0	
78	13.0	
75	13.1	
73	13.1	
70	13.1	

connection of N points, where N is the number of layers in a column of fixed diameter particles. The N for each particle size was estimated from the fractional length of the ground trace up to the intersection with the AFSWP hotline. A first estimate for the starting height of a particle is:

$$H = \frac{L_u}{L_T} N \times 100 \text{ meters} .$$

H = height of a particle stack

L_u = length of trace upwind of intersection point

L_T = total length of trace

N = number of points on trace

100 meters = layer thickness

The method is shown schematically on Figure 20. Fine-tuning is done by trial and error, putting new estimates of particle stack heights into the model.

The actual Bravo hotline (AFSWP) can be approximated with three segments:

(1) $x \leq 130$ km

(2) 130 km $\leq x \leq$ 280 km

(3) 280 km $\leq x$.

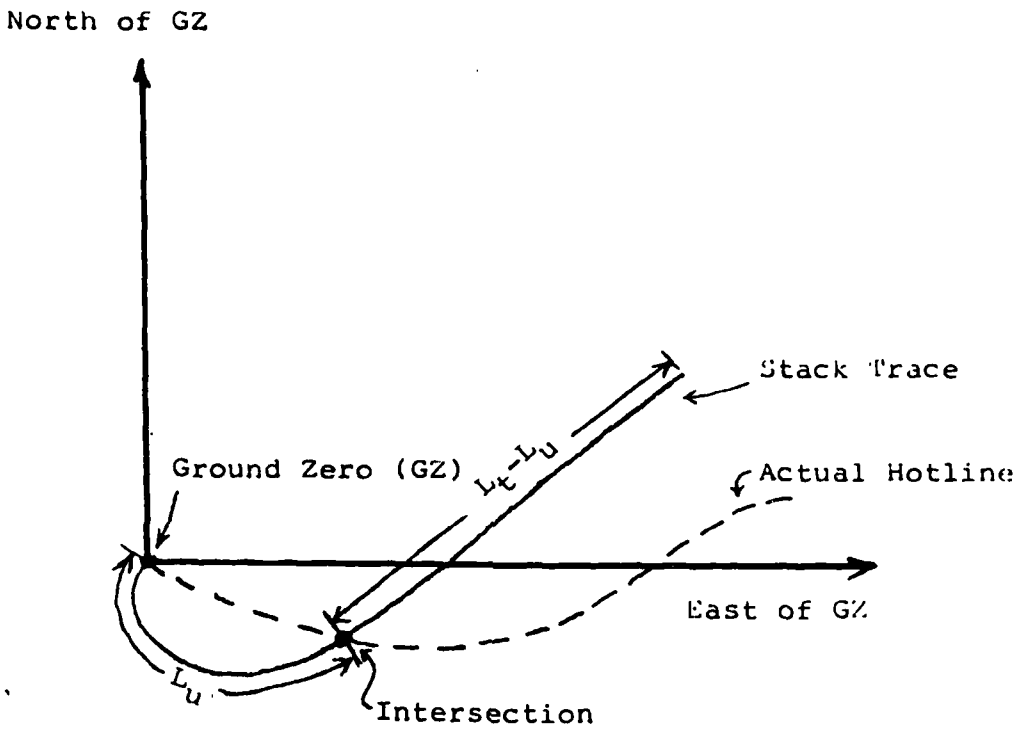

Figure 20. Ground Trace Intersection Method

Back calculations of the first segment showed that particle starting heights were inconsistent with observed fallout arrival times. Furthermore, the back calculated initial cloud was not gravity size sorted. This observation suggested that the early fallout came from a complex distribution of particle sizes at low altitudes (stem). To generate the southeastward trace of the actual hotline, the first segment was approximated with a pancake cloud located at 9.2 km altitude. The stack contours for the pancake are shown in Figure 21, and the pancake hotline is shown in Figure 22. From Figure 17, it was observed that the second segment is nearly identical to the 80 μm diameter particle trace. Therefore, the first two segments of the AFSWP hotline (the curved part) can be located by computing fallout motion from a low altitude pancake cloud beneath a nearly single-sized "mixing region." This information and the fact that some stack traces intersect the hotline twice, imply that the Bravo cloud had at least two distinct vertical distributions of radioactive fallout particles:

1. A low altitude stem distribution that was primarily affected by the wind profile beneath 9.2 km;
2. A well-mixed, almost uniform size region that accounts for the slow change in particle size along segment 2.

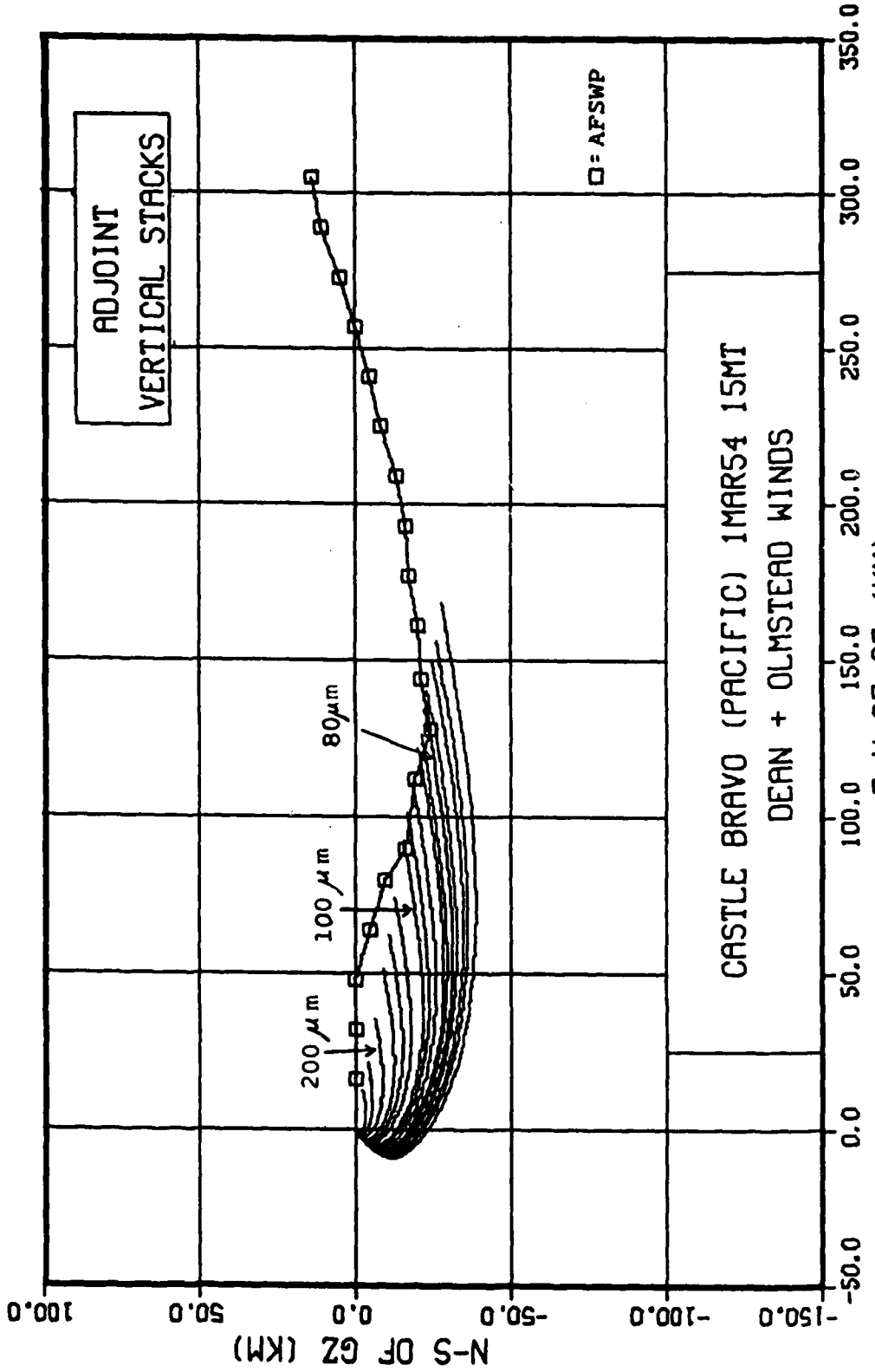

Figure 21. Ground Traces of Single-Size Particle Stacks, Pancake

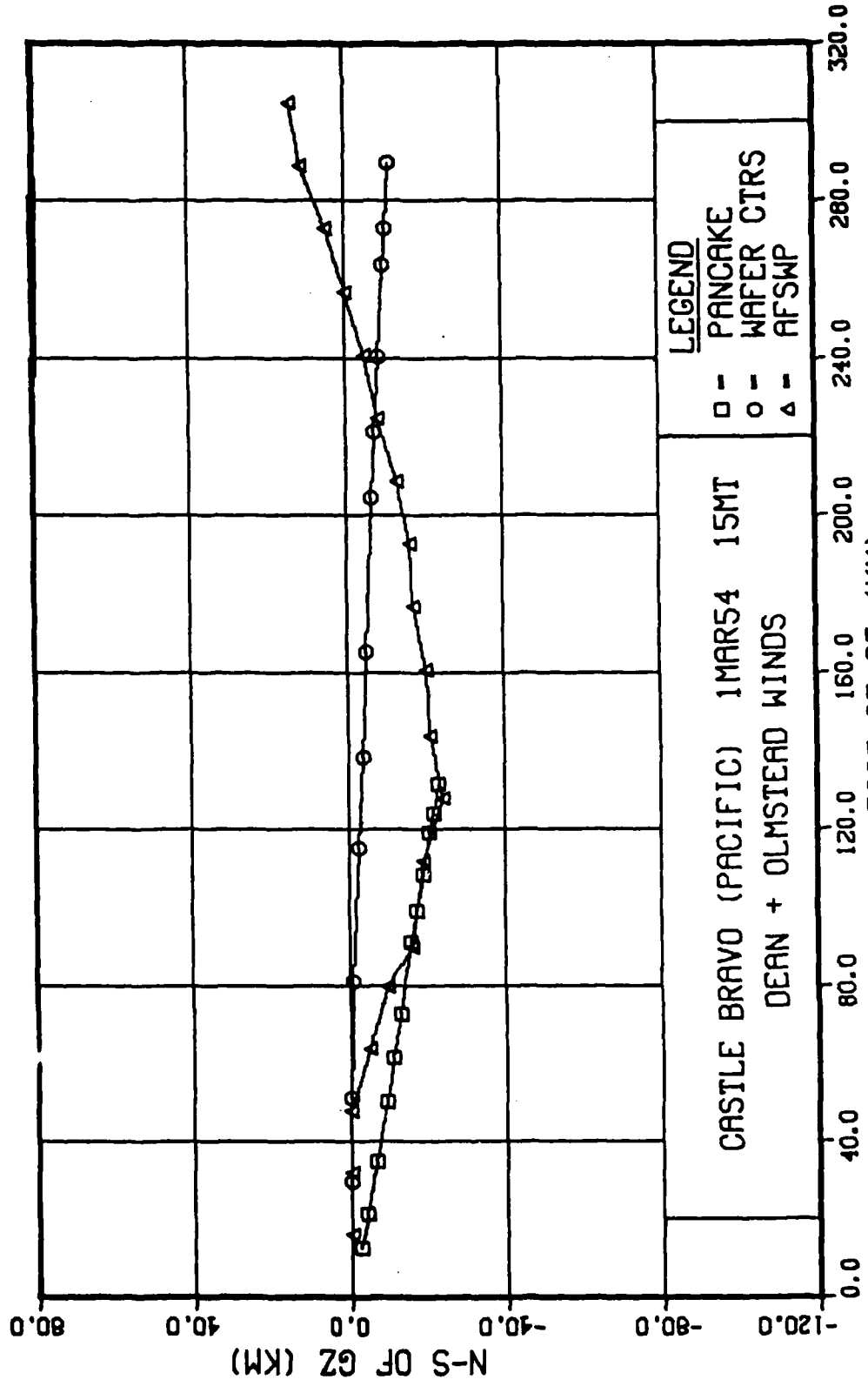

Figure 22. Hotlines, Castle-Bravo, Pancake

Figures 23 and 24 show the adjoint hotline calculation with a pancake cloud to represent the stem and a well-mixed single-size (80 μm) layer between 10 and 16 km altitude.

The need for a special treatment of the Castle-Bravo fallout was recognized by Norment (Ref 4):

> ". . .high yield explosions over coral and ocean water need special treatment. . .Clearly a particle size or size activity distribution that is quite distinct from any used here is required for this shot." (Ref 4:65)

Reference 15 further notes that the WSEG-10 model produces good agreement with the AFSWP contours, "in spite of a stabilized cloud that is half as high as it should be." (Ref 15:65) Table V shows cloud top and bottom heights used in Reference 4:

Table V

Castle-Bravo Cloud Heights

	Observed	DELFIC	WSEG-10
Cloud Base (km)	16.9	20.3	10.7
Cloud Top (km)	34.7	39.7	22.8

On the basis of the back calculations for this study, it can be inferred that the WSEG-10 agreement is coincidental, caused by the existence of a stem distribution which occurred well below the observed stabilized cloud height. A different

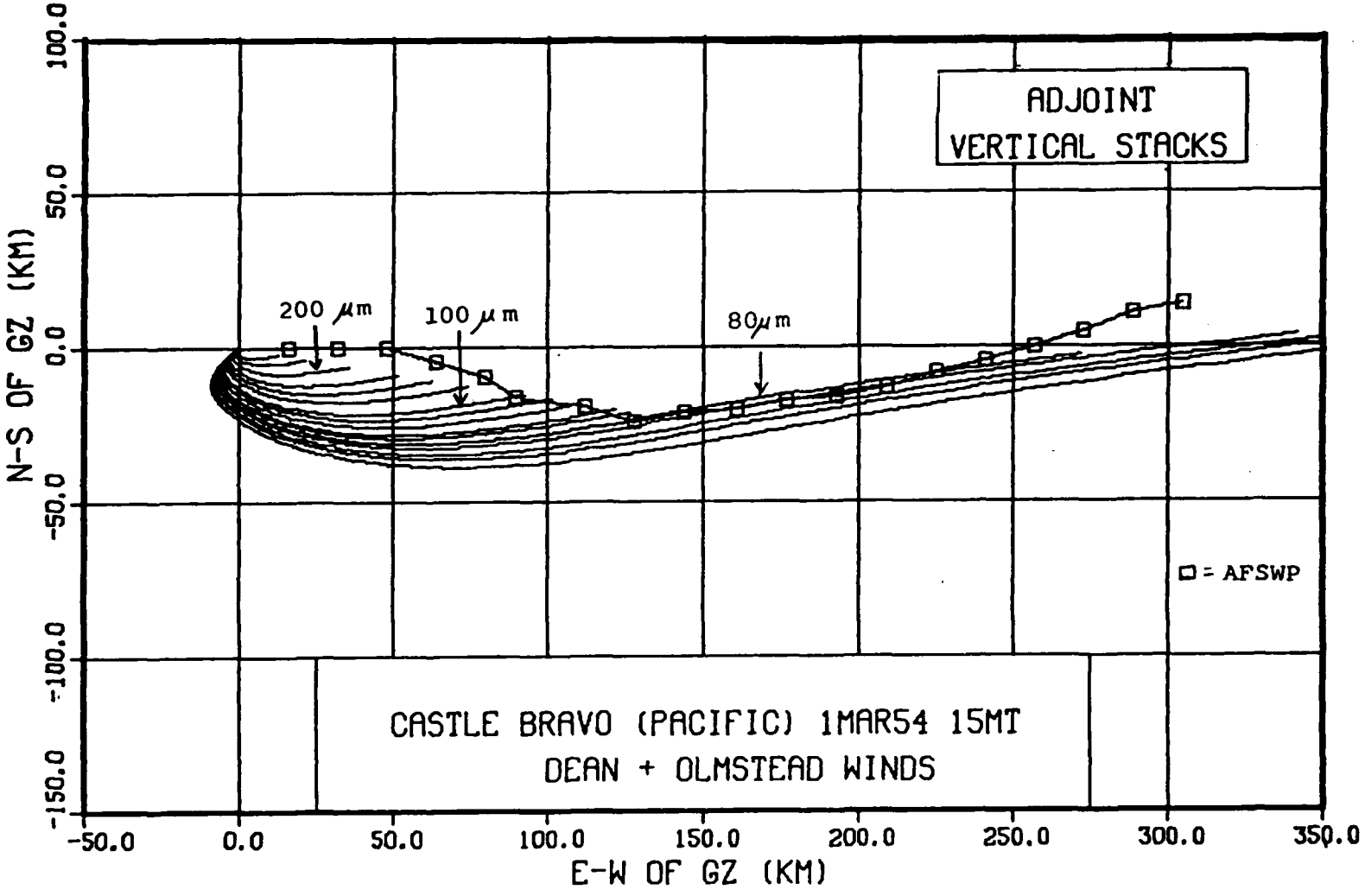

Figure 23. Ground Traces of Single-Size-Particle Stacks, 9.5km Pancake + Single-Size Layer

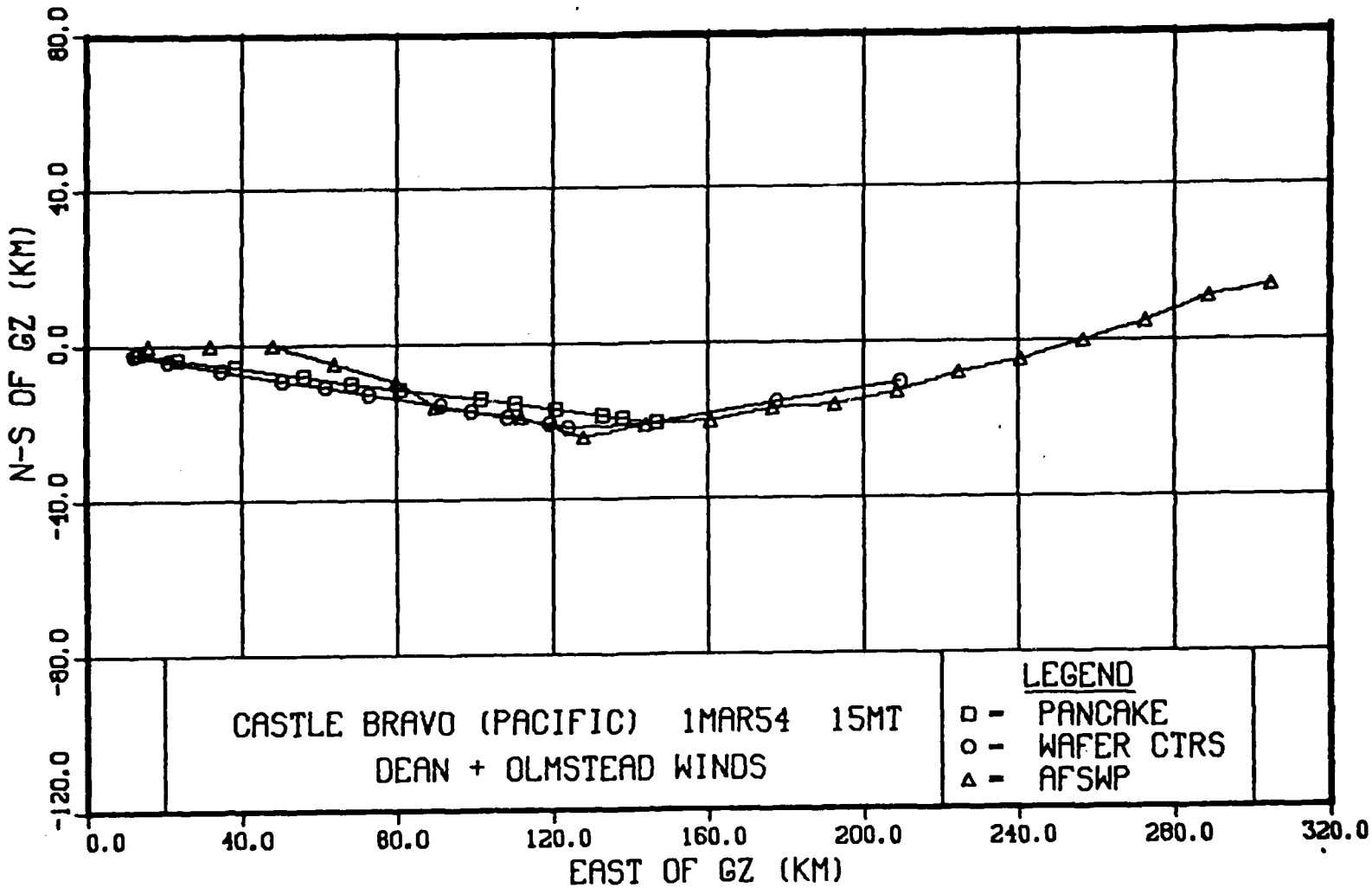

Figure 24. Hotlines, Castle-Bravo, 9.5km Pancake + Single-Size Layer

particle size distribution will not improve code predictions, since the DELFIC hotline location is insensitive to size distribution. Rather, a different (stem + cloud) vertical spatial description of the stabilized cloud is needed to explain the actual location of the fallout hotline.

Beyond 280 km, it is obvious from Figure 18 that the Dean and Olmstead winds at burst time could not have translated particles onto the hotline segment 3. In fact, using shot-time winds to predict fallout locations at 6+ hours after detonation is tacitly assuming no temporal or spatial variations in the wind profile. This assumption will introduce large uncertainties in fallout location predictions, especially when the distances traveled by the fallout particles are on the order of synoptic weather patterns, or 10^4 - 10^6 meters (Ref 15). Over a synoptic scale, fronts and major disturbances can cause large variations in wind velocity and direction. In fact, when the hotline locator model was exercised with the T+1 hr Dean and Olmstead winds, the "wafer ctrs" hotline did move northward. Figure 25 shows the hotline predictions assuming the T+1 hr winds. To correctly represent the wind structure, a model would have to simulate the wind profiles all along the path of a falling particle. Section VII describes a technique to linearly interpolate temporal wind changes in model layers beneath falling particles. The technique was used to predict the segment 3 asymptote with a linear temporal

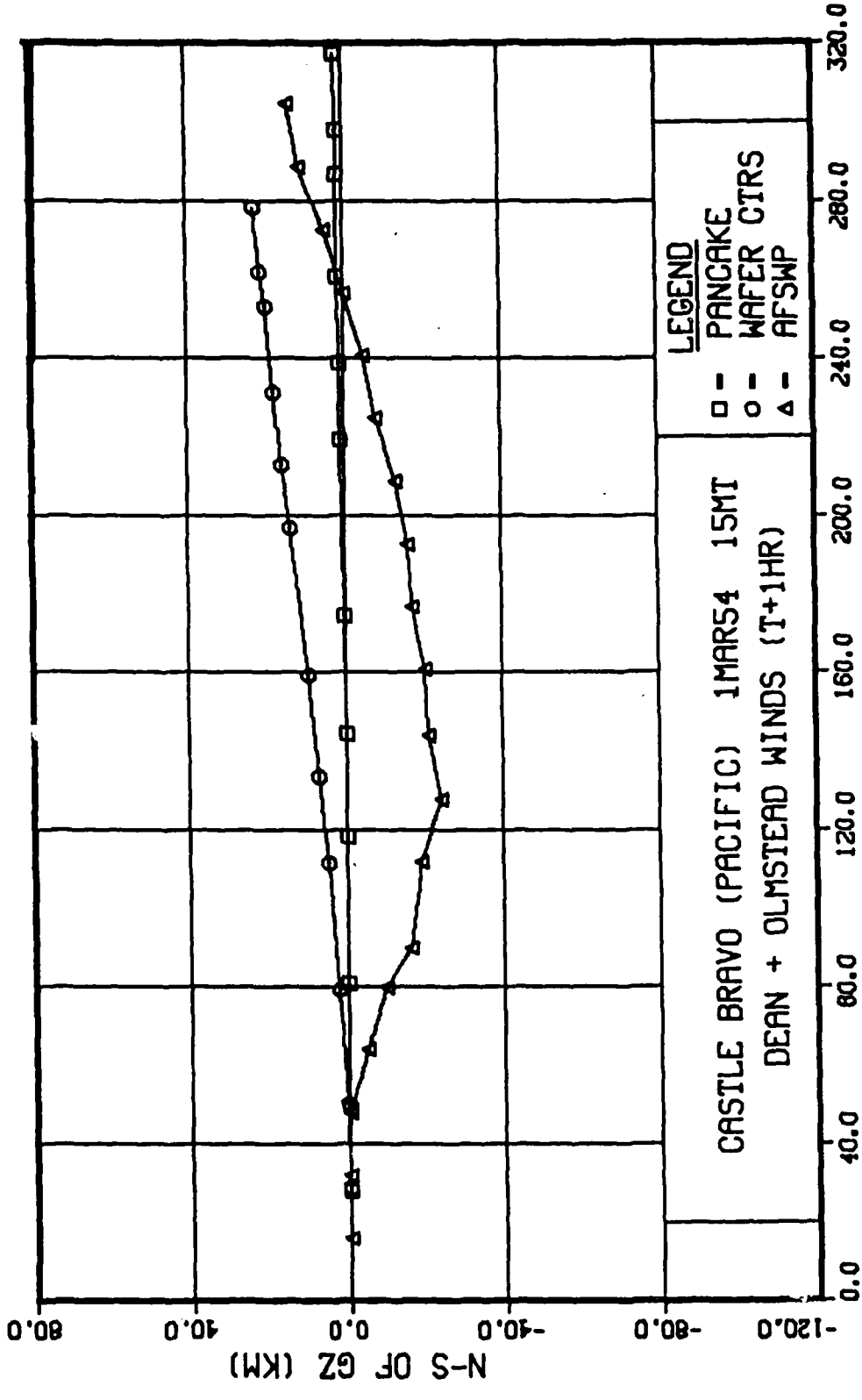

Figure 25. Hotlines, Castle-Bravo, T+1Hr Dean and Olmstead Winds

interpolation of shot-time and T+1 hr wind profiles during particle fall and translation.

Sensitivities

The sensitivity of hotline location was examined for two factors:

1. Pancake cloud altitude
2. Wind profile.

Pancake cloud height variations caused consistent movement of the hotline to directions influenced primarily by the mean "effective" wind beneath the pancake. Figure 26 shows the hotline from a pancake cloud located at 30 km altitude. The agreement with the actual hotline is interesting, but it is unlikely that a 30 km high pancake cloud could have generated the Bravo fallout hotline. A 70 μm particle takes 19.5 hours to fall from 30 km in a tropical atmosphere, whereas Figure 13 indicates that fallout particles arrived in the atolls 4 to 6 hours after detonation (Ref 14).

Hotline location sensitivity to the assumed wind profile was addressed by computing hotlines and stack traces with different winds. Figures 27 and 28 show that hotline predictions would change dramatically if the particles were translated in the original Three Point Average winds vs the Dean and Olmstead winds. Three point average winds and components are plotted in Figure 29.

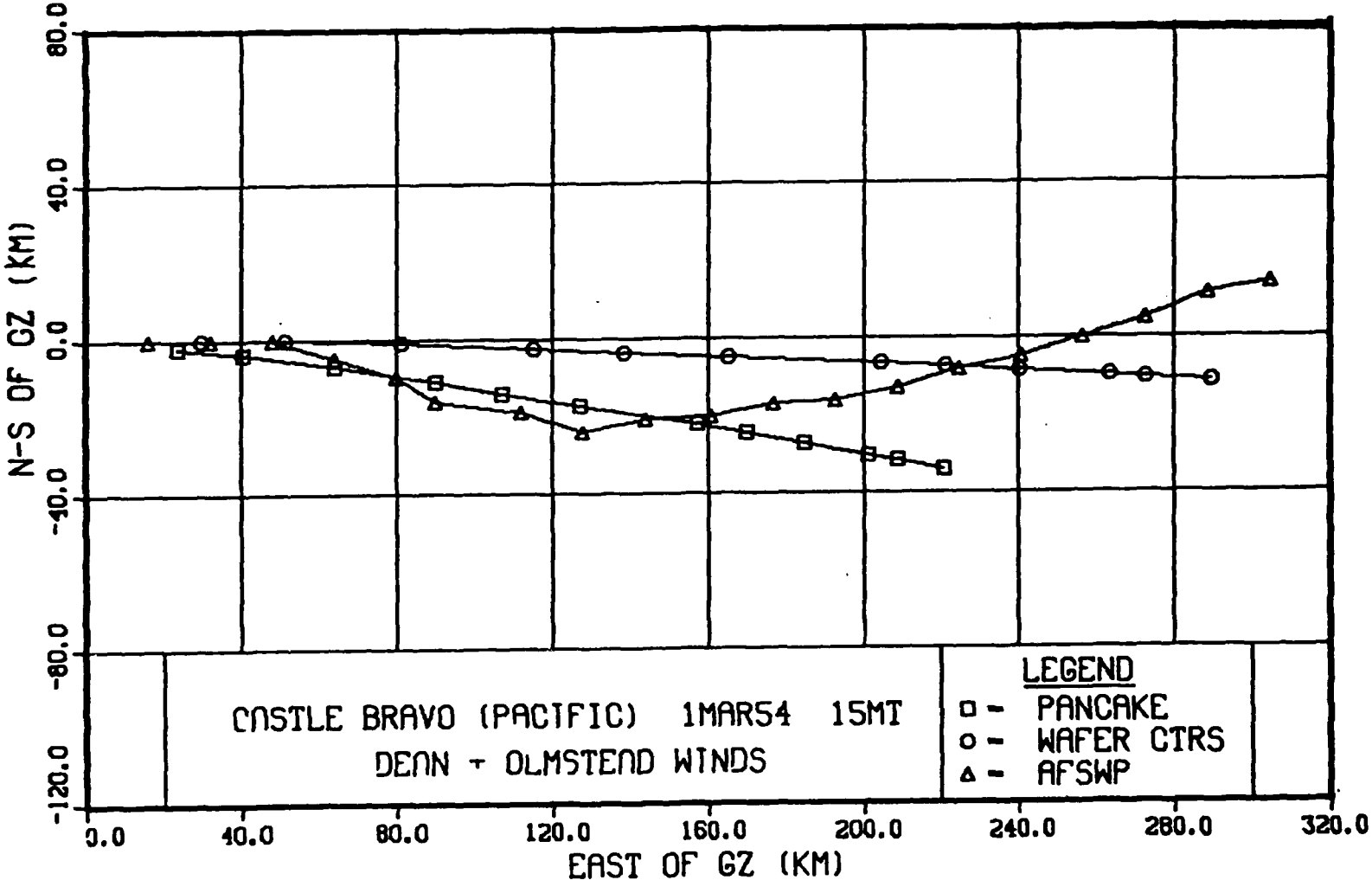

Figure 26. Hotlines, Castle-Bravo, 30km Pancake Cloud

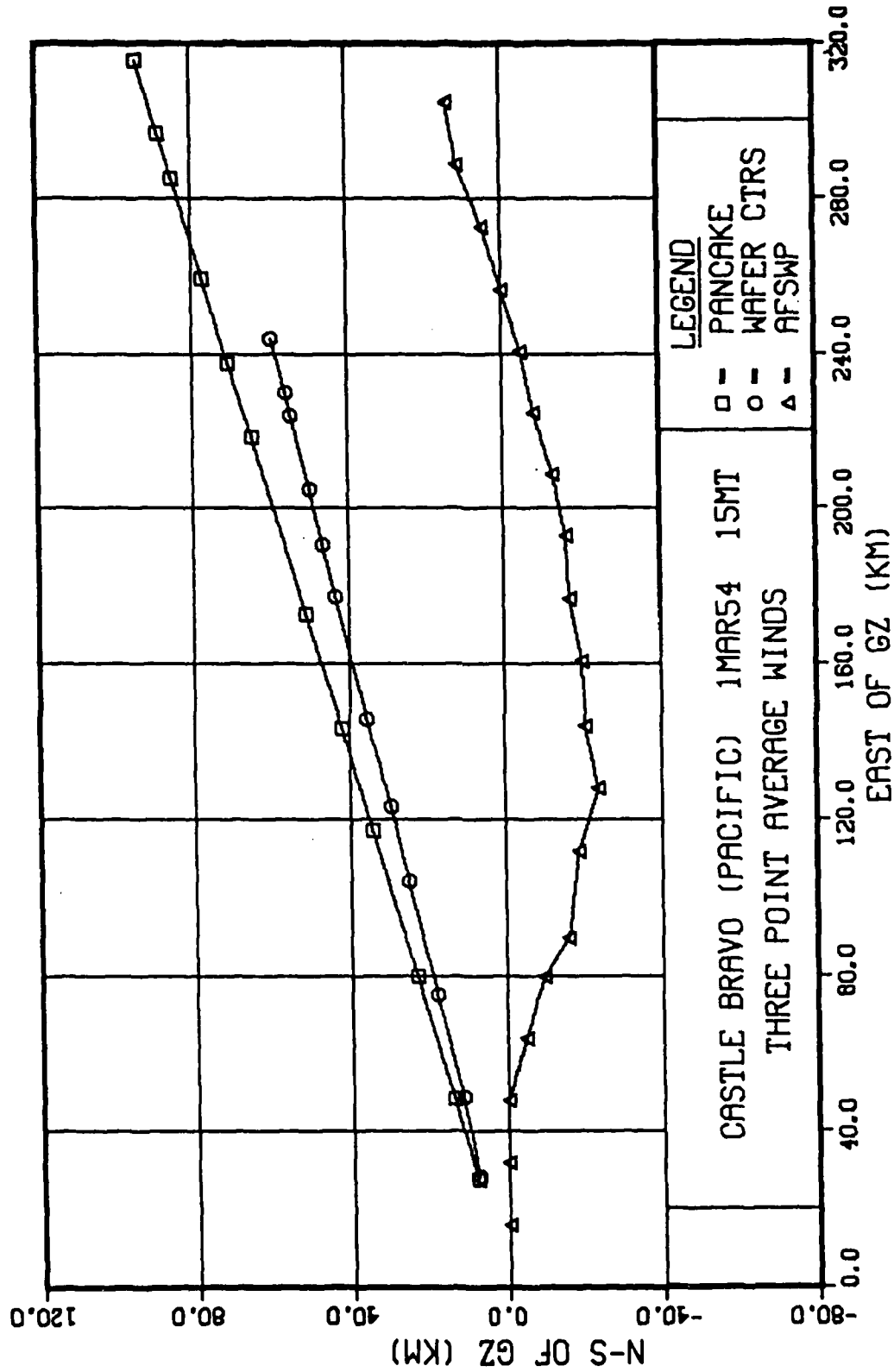

Figure 27. Hotlines, Castle-Bravo, Three Point Average Winds

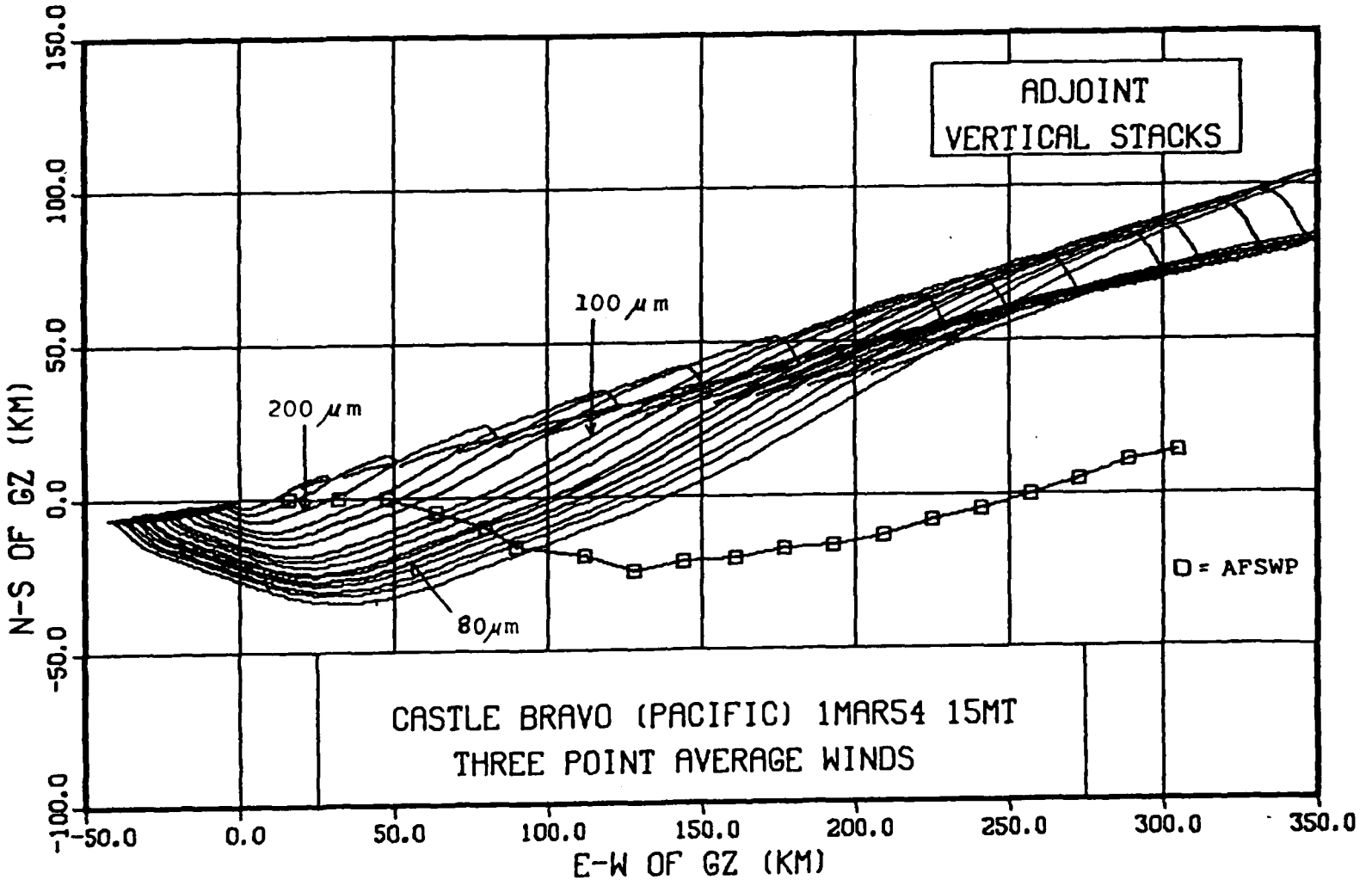

Figure 28. Ground Traces of Single-Size-Particle Stacks, Three Point Average Winds

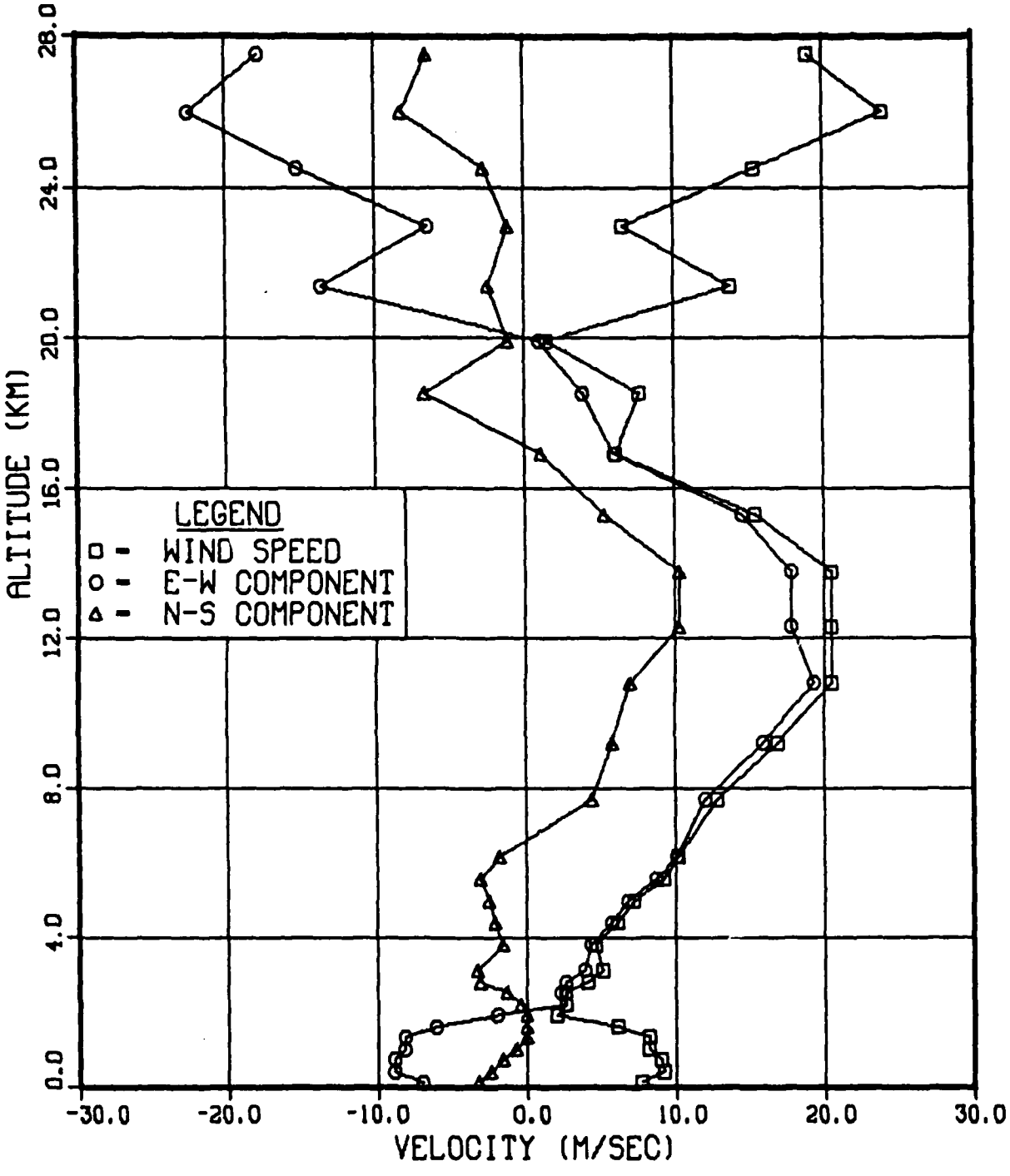

Figure 29. Wind Profile, Castle-Bravo, Three Point Average Winds

Results of the Castle-Bravo case study are summarized as follows:

1. The hotline locator model agreed with the DELFIC prediction; neither predicted the hotline curvature.
2. A vertical stack technique was developed to back calculate particle starting heights in the stabilized cloud to approximate the actual hotline.
3. The back calculated starting heights provided a new interpretation of the stabilized cloud that included a stem and a mixing region beneath the cloud.
4. Hotline location is extremely sensitive to the assumed winds and spatial/temporal variations.

VII. Linear Temporal Interpolation for Wind Updates

As suggested in previous sections, the use of a single wind profile may be inadequate for predicting fallout locations at distances greater than the synoptic weather scale. Wind updating can be achieved with a pseudo-Lagrangian scheme of following the fallout particles. In the hotline locator model, a particle resides in a layer for a finite time. During that time, the winds in layers beneath the particle may change. If the changed wind profile is known at a later time, then the winds in any layer can be estimated by linearly interpolating (in time) the vector component magnitudes.

Specifically, for two wind profiles, the temporally interpolated wind speed in a model layer is computed as follows:

$$U_{LTI} = U_o\left(\frac{t-T}{t}\right) + U_t\left(\frac{T}{t}\right)$$

U_{LTI} = linear temporal interpolated wind speed

U_o = wind speed at time zero

U_t = wind speed at time $t > 0$

t = time when U_t is applicable (if $t = 0$, there is only one wind profile and the equation does not apply)

T = elapsed time of particle fall from starting height to layer where interpolated winds are computed

when $T = 0$, $U_{LTI} = U_o$

and $T = t$, $U_{LTI} = U_t$

The technique was tested with the T = 0 and T + 1 hr Castle-Bravo (Dean and Olmstead) winds (Figure 30) in the hotline locator model. In Section VI, the later winds were shown to explain Bravo hotline trend beyond 280 km from ground zero. This exercise was an attempt to check the linear temporal interpolation (LTI) method and to explain the 3rd segment of the AFSWP hotline. Stack traces are shown in Figure 31. The effect of linear interpolation to the T + 1 hr wind profile is that particles starting from high altitudes land to the north.

The hotlines from pancake clouds and distributed initial clouds are shown in Figure 32. "LTI-P" and "LTI-wfrs" refer to LTI winds beneath pancake and wafer-distributed clouds, respectively. The "LTI-wfrs" hotline agrees with the AFSWP hotline beyond 280 km, implying that particles falling from the high cloud (not stem) were more affected by the T + 1 hr winds than by the T + 0 winds. However, T + 1 hr winds may not be recent enough, since arrival times at x > 280 km are much longer than 1 hour.

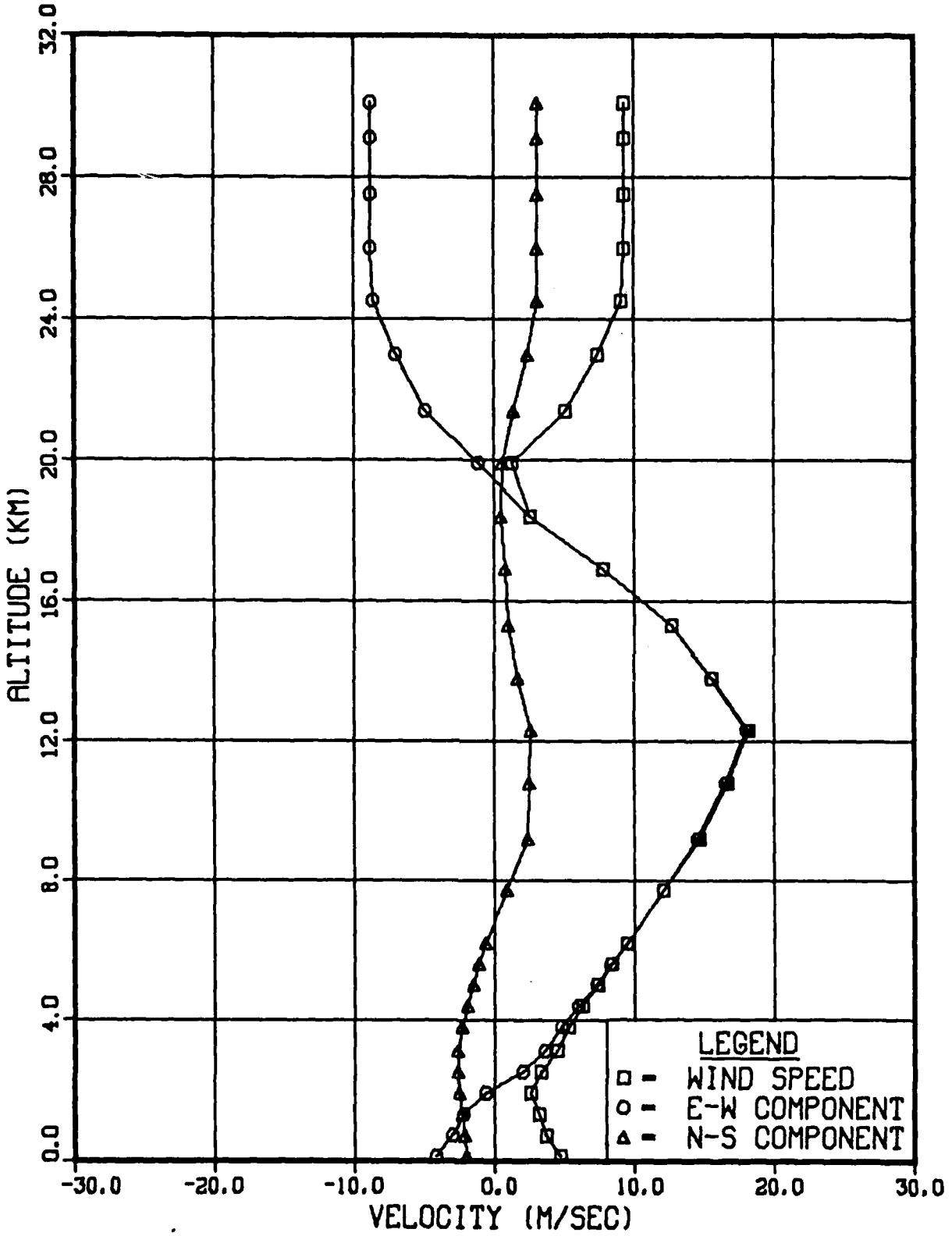

Figure 30. Wind Profile, Castle-Bravo, T+1Hr Dean and Olmstead Winds

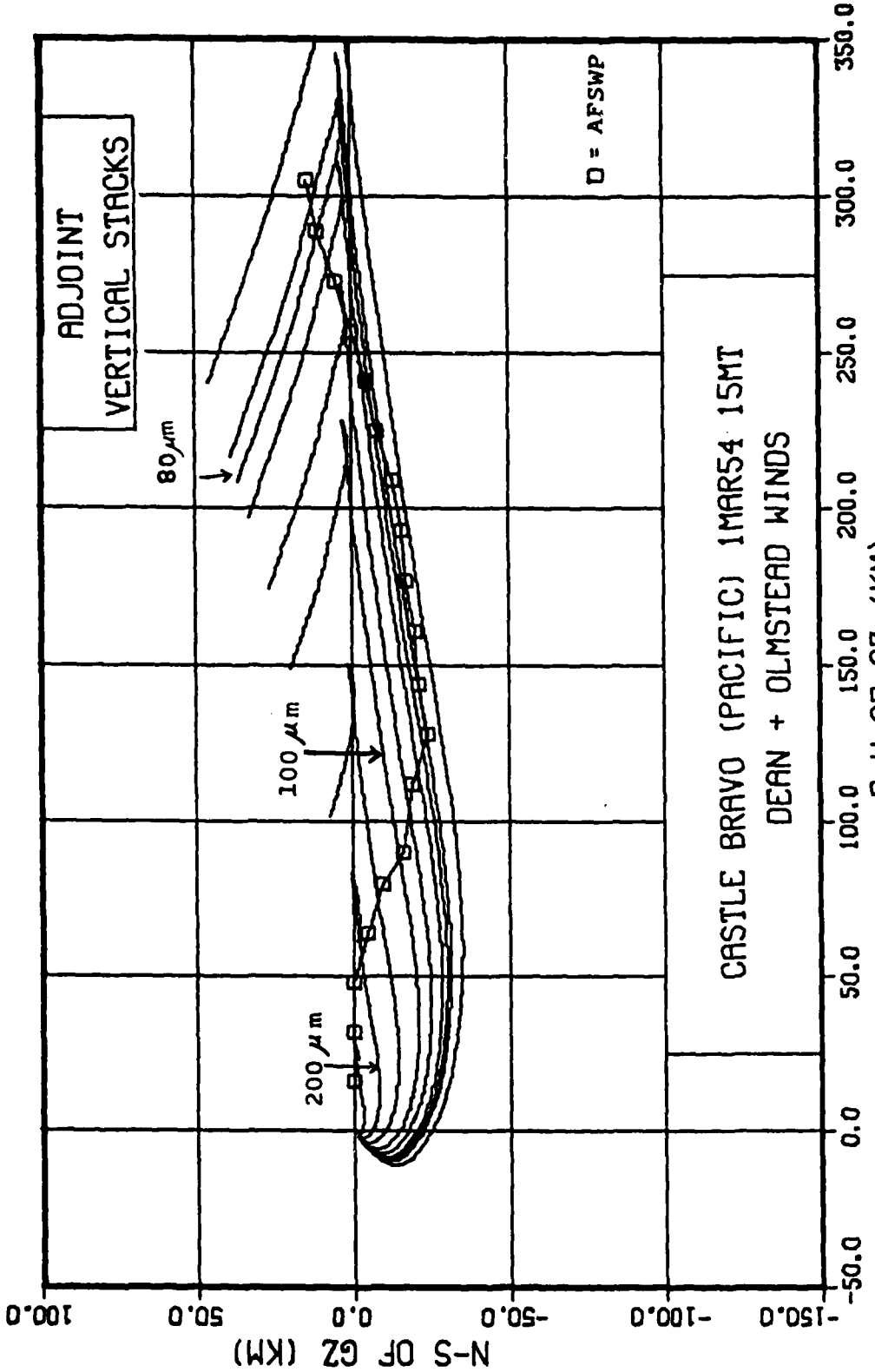

Figure 31. Ground Traces of Single-Size-Particle Stacks, Dean and Olmstead T+1Hr Winds

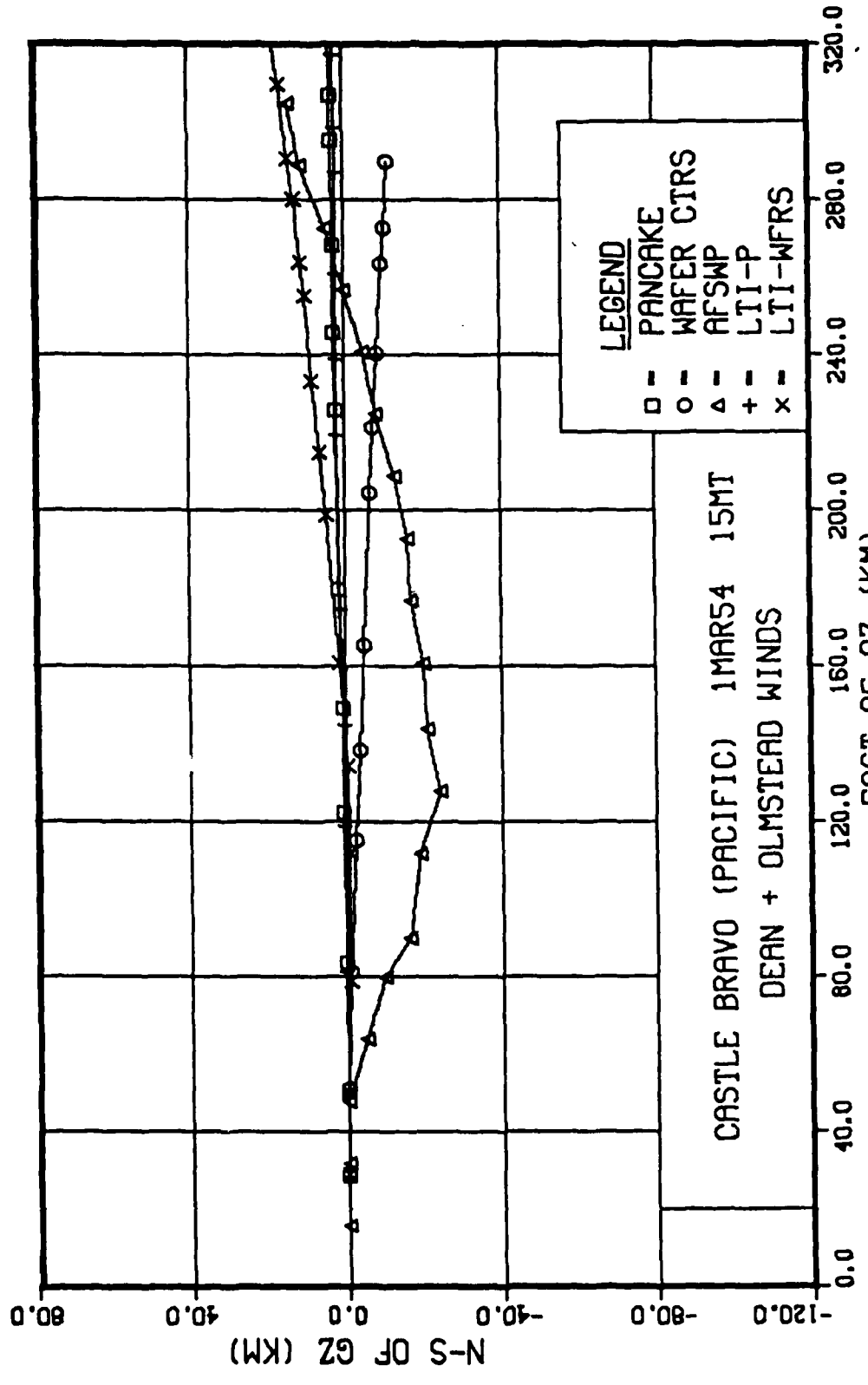

Figure 32. Hotlines, Castle-Bravo, Linear Temporal Interpolation and Fixed Profile Traces

The back calculated hotline was computed by combining the linear-temporal interpolation technique with wafer starting heights shown in Table IV. Figure 33 depicts the hotline predicted with the the locator model using starting heights estimated from stack trace intersections and linearly interpolated T + 0 and T + 1 hr Dean and Olmstead winds. The calculation properly replicated the southward extent of the hotline observed in the AFSWP data. The wind interpolation produced nearly identical hotlines beyond 280 km from ground zero. In fact, beyond 280 km, particle starting heights were predicted with the correlations derived from DELFIC data (Section III). The pancake cloud was found to best represent the hotline between 100 and 120 km east of the burst point. Closer than 100 km, the stack trace method indicated that the stabilized cloud did not contain gravity-sorted activity peaks. In fact, analysis of the stack trace calculations showed that some large particles started from higher altitudes than smaller particles. The low altitudes in which this occurred correspond to the stem region hypothesized in Section VI.

All references which discussed the Castle-Bravo test emphasized the large uncertainties in the fallout trace data; most of the fallout was deposited over the ocean and the measurement netowrk was modest. However, the southward curvature was verified by data from inhabited atolls (Rongerik and Rongelap) downwind of the detonation. At close range

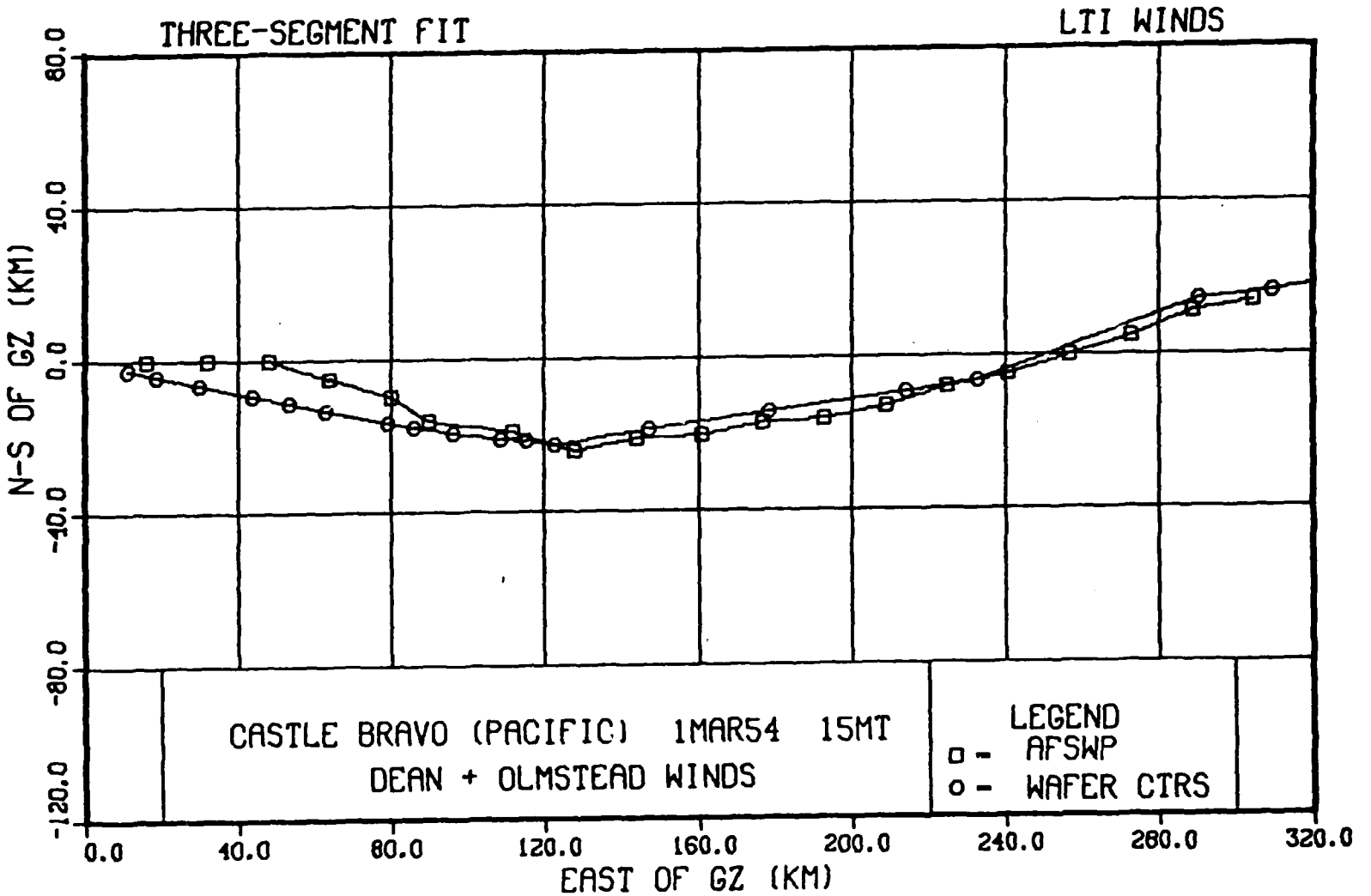

Figure 33. Hotlines, Castle-Bravo, Three-Segment Fit

(< 80 km), it is interesting to note that the stack traces show that low altitude debris would first move to the southwest, then turn to the east-northeast. This implies that the hotline inferred from the AFSWP contours (which starts going due east from the burst point) may be incorrectly located and should actually be curving southward.

VIII. Solution of Dose Rate Integral for a Curved Hotline

This section presents the second step to modeling variable winds in fallout smearing codes. An analytic expression is developed for the activity distribution on the ground away from the curved hotline.

The fundamental equation for ground dose rate from a smearing code was given as Eq (II-1).

$$\dot{D}(x,y) = KY_K \int_0^\infty f(x,y,t')g(t')dt' \qquad \text{(II-1)}$$

The spatial distribution function $f(x,y,t')$ was given by Eq (II-2):

$$f(x,y,t') = \frac{1}{\sqrt{2\pi}\ \sigma_x(t')} \text{ EXP } \left[-\tfrac{1}{2}\left(\frac{x-v_x t'}{\sigma_x}\right)\right]^2$$

$$\cdot \frac{1}{\sqrt{2\pi}\ \sigma_y(t')} \text{ EXP } \left[-\tfrac{1}{2}\left(\frac{y-v_y t'}{\sigma_y}\right)\right]^2 \qquad \text{(II-2)}$$

$f(x,y,t')$ can be generalized to variable winds by replacing the terms $v_x t'$ and $v_y t'$:

$$v_x t' \rightarrow \int_0^{t'} v_x dt'$$

$$v_y t' \rightarrow \int_0^{t'} v_y dt'$$

where v_x and v_y are now the variable wind components experienced by the falling particles during their residence times in discrete model layers.

Therefore, for a curved hotline ($v_y \neq 0$), the spatial distribution function has the form:

$$f(x,y,t) = \frac{1}{\sqrt{2\pi}\,\sigma_x} \text{ EXP } -\tfrac{1}{2}\left[\left(\frac{x-\int_0^{t'} v_x dt}{\sigma_x}\right)^2\right]$$

$$\frac{1}{\sqrt{2\pi}\,\sigma_y} \text{ EXP } -\tfrac{1}{2}\left[\left(\frac{y-\int_0^{t'} v_y dt}{\sigma_y}\right)^2\right] \qquad \text{(VIII-1)}$$

Reference 1 showed that $g(t)$ can be approximated with the first two terms of a Taylor series expanded about t_a, the arrival time of cloud center at hotline location (X,Y) :

$$g(t-t_a) = g(t_a) + \left(\frac{dg}{dt}\right)_{t_a} (t-t_a) + \ldots$$

Then,

$$\dot{D} \simeq KY_K \int_0^{\infty} f(x-\int_0^{t'} v_x dt'')\, f(y-\int_0^{t'} v_y dt'')\, g(t_a)\, dt$$

$$+ \int_0^{\infty} f(x-\int_0^{t'} v_x dt'')\, f(y-\int_0^{t'} v_y dt'')\left(\frac{dg}{dt}\right)_{t_a} (t-t_a)\, dt \qquad \text{(VIII-2)}$$

The second term on the right-hand side of (VIII-2) is zero if the limits of integration are changed from $\int_0^\infty$ to $\int_{-\infty}^\infty$. The limit change is valid if the contribution to the integral from the $\int_{-\infty}^\infty$ portion is small. The contribution will be small if the integral is evaluated at (x,y) distant from the origin, i.e., late times after burst. The second integral takes the form:

$$\int_{-\infty}^{\infty} (\text{gaussian})(\text{gaussian})(\text{constant})(\text{odd function})dt \quad ,$$

which is the integral of an odd function about the origin, equal to zero.

Only the first integral on the right-hand side of (VIII-2) remains to contribute to the dose rate calculation.

$$\dot{D} = KY_K g(t_a) \int_0^\infty \frac{1}{\sqrt{2\pi}\,\sigma_x} \text{EXP}\left[-\tfrac{1}{2}\left(\frac{x-\int_0^{t'} v_x dt''}{\sigma_x}\right)^2\right]$$

$$\cdot \frac{1}{\sqrt{2\pi}\,\sigma_y} \text{EXP}\left[-\tfrac{1}{2}\left(\frac{y-\int_0^{t'} v_y dt''}{\sigma_y}\right)^2\right] dt \qquad \text{(VIII-3)}$$

Since the distribution is gaussian centered on the hotline, the displacements $\int_0^{t'} v_x dt$ and $\int_0^{t'} v_y dt$ are coordinates of the hotline at arrival time, $t' = t_a$. These coordinates

were determined from the hotline locator model (Section IV). Therefore,

$$\int_0^{t_a} v_x dt = X = V_x t_a$$

$$\int_0^{t_a} v_y dt = Y = V_y t_a$$

where V_x and V_y are particle residence time weighted averages of wind components.

$$V_x = \frac{dX}{dt}$$

Exponential and differential terms of the integrand become:

$$\text{EXP}\left[-\tfrac{1}{2}\left(\frac{x-X}{\sigma_x}\right)^2\right] \text{EXP}\left[-\tfrac{1}{2}\left(\frac{y-Y}{\sigma_y}\right)^2\right] dt$$

$$= \text{EXP}\left[-\tfrac{1}{2}\left(\frac{x-X}{\sigma_x}\right)^2\right] \text{EXP}\left[-\tfrac{1}{2}\left(\frac{y-\frac{V_y}{V_x}X}{\sigma_y}\right)^2\right] \frac{dX}{V_x}$$

Expanding the exponents in the integrand:

$$\text{EXP}\left[-\tfrac{1}{2}\left(\frac{x^2-2xX+X^2}{\sigma_x^2}+\frac{y^2-2y\left(\frac{V_y}{V_x}\right)X+\left(\frac{V_y}{V_x}\right)X^2}{\sigma_y^2}\right)\right]$$

$$=\text{EXP}\left[-\tfrac{1}{2}\left(\left\{\frac{x^2}{\sigma_x^2}+\frac{y^2}{\sigma_y^2}\right\}-2X\left\{\frac{x}{\sigma_x^2}+\frac{y\left(\frac{V_y}{V_x}\right)}{\sigma_y^2}\right\}+X^2\left\{\frac{1}{\sigma_x^2}+\frac{\left(\frac{V_y}{V_x}\right)^2}{\sigma_x^2}\right\}\right)\right]$$

$$=\text{EXP}\left[-\tfrac{1}{2}\left(\frac{x^2}{\sigma_x^2}+\frac{y^2}{\sigma_y^2}\right)\right]\text{EXP}\left[X\left(\frac{x}{\sigma_x^2}+\frac{y\left(\frac{V_y}{V_x}\right)}{\sigma_y^2}\right)-\frac{X^2}{2}\left(\frac{1}{\sigma_x^2}+\frac{\left(\frac{V_y}{V_x}\right)^2}{\sigma_y^2}\right)\right]$$

$$=\text{EXP}\left[-\tfrac{1}{2}\left(\frac{\sigma_y^2x^2+\sigma_x^2y^2}{\sigma_x^2\sigma_y^2}\right)\right]\text{EXP}\left[X\left(\frac{\sigma_y^2x+\sigma_x^2y\left(\frac{V_y}{V_x}\right)}{\sigma_x^2\sigma_y^2}\right)-\frac{X^2}{2}\left(\frac{\sigma_y^2+\left(\frac{V_y}{V_x}\right)^2\sigma^2}{\sigma_x^2\sigma_y^2}\right)\right]$$

The right exponential has the form: $\text{EXP}(-XB-X^2A)$. If the contribution from $\int_{-\infty}^{\infty}$ is negligible (as assumed earlier, and in (1)), the integral can be evaluated as one of the form:

$$J_n = \int_{-\infty}^{\infty} x^n \,\text{EXP}[-XB-X^2A]dX$$

with $n = 0$.

The solution is shown in Reference 16 as

$$J_o = \sqrt{\frac{\pi}{A}}\ \mathrm{EXP}[B^2/4A]$$

In this case:

$$A = \frac{\sigma_y^2 + (\frac{V_y}{V_x})^2 \sigma_x^2}{2\sigma_x^2\sigma_y^2}$$

$$B = \frac{\sigma_y^2 + \sigma_x^2 y(\frac{V_y}{V_x})}{-\sigma_x^2\sigma_y^2}$$

$$J_o = \left[\frac{\pi}{\frac{\sigma_y^2+(\frac{V_y}{V_x})^2\sigma_x^2}{2\sigma_x^2\sigma_y^2}}\right]^{\frac{1}{2}} \mathrm{EXP}\left[\left(\frac{\sigma_y^2 x+\sigma_x^2 y(\frac{V_y}{V_x})}{-\sigma_x^2\sigma_y^2}\right)^2 \Big/ 4\left(\frac{\sigma_y^2+(\frac{V_y}{V_x})^2\sigma_x^2}{2\sigma_x^2\sigma_y^2}\right)\right]$$

$$= \left[\frac{2\pi\sigma_x^2\sigma_y^2}{\sigma_y^2 + (\frac{V_y}{V_x})^2\sigma_x^2}\right]^{\frac{1}{2}} \mathrm{EXP}\left[\frac{[\sigma_y^2 x+\sigma_x^2 y(\frac{V_y}{V_x})]^2}{\sigma_x^2\sigma_y^2)^2} \cdot \frac{2\sigma_x^2\sigma_y^2}{4(\sigma_y^2+(\frac{V_y}{V_x})^2\sigma_x^2)}\right]$$

$$= \left[\sigma_x^2\sigma_y^2 \quad \frac{2\pi}{\sigma_y^2+(\frac{V_y}{V_x})^2\sigma_x^2}\right]^{\frac{1}{2}} \mathrm{EXP}\left[\frac{[\sigma_y^2 x+\sigma_x^2 y(\frac{V_y}{V_x})]^2}{2(\sigma_x^2\sigma_y^2)(\sigma_y^2+(\frac{V_y}{V_x})\sigma_x^2)}\right]$$

Simplifying the exponential term:

$$\frac{[\sigma_y^2 x+\sigma_x^2 y(\frac{V_y}{V_x})]^2}{2(\sigma_y^2+(\frac{V_y}{V_x})^2\sigma_x^2)(\sigma_x^2\sigma_y^2)}$$

$$= \frac{(\sigma_y^2 x)^2+2\sigma_x^2 y(\frac{V_y}{V_x})\sigma_y^2 x+(\sigma_x^2 y(\frac{V_y}{V_x}))^2}{2(\sigma_y^2+(\frac{V_y}{V_x})^2\sigma_x^2)(\sigma_x^2\sigma_y^2)}$$

$$= \frac{\frac{\sigma_y^2}{\sigma_x^2}x^2+2yx(\frac{V_y}{V_x})+\frac{\sigma_x^2}{\sigma_y^2}y^2(\frac{V_y}{V_x})^2}{2(\sigma_y^2+(\frac{V_y}{V_x})^2\sigma_x^2)}$$

$$= \frac{[(\frac{\sigma_y}{\sigma_x}x)+(\frac{\sigma_x}{\sigma_y}y(\frac{V_y}{V_x}))]^2}{2(\sigma_y^2+(\frac{V_y}{V_x})^2\sigma_x^2)}$$

$$J_o = \sigma_x\sigma_y\left[\frac{2\pi}{\sigma_y^2+(\frac{V_y}{V_x})^2\sigma_x^2}\right]^{\frac{1}{2}} EXP\left[\frac{1}{2}\left\{\frac{(\frac{\sigma_y}{\sigma_x}x+(\frac{\sigma_x}{\sigma_y})(\frac{V_y}{V_x})y)^2}{\sigma_y^2+(\frac{V_y}{V_x})^2\sigma_x^2}\right\}\right]$$

The integral for $\dot{D}$ becomes:

$$\dot{D} = \overbrace{\frac{KY_K g(t_a)}{V_x 2\pi\sigma_x\sigma_y}\left[\frac{2\pi\sigma_x^2\sigma_y^2}{\sigma_y^2+\left(\frac{V_y}{V_x}\right)^2\sigma_x^2}\right]^{\frac{1}{2}}}^{I} \cdot \underbrace{EXP\left\{-\tfrac{1}{2}\left[\frac{\sigma_y^2x^2+\sigma_x^2y^2}{\sigma_x^2\sigma_y^2}\right]\right\} EXP\left\{\tfrac{1}{2}\left[\frac{\left(\frac{\sigma_y}{\sigma_x}+\left(\frac{\sigma_x}{\sigma_y}\frac{V_y}{V_x}y\right)\right)^2}{\sigma_y^2+\left(\frac{V_y}{V_x}\right)^2\sigma_x^2}\right]\right\}}_{II} \qquad \text{(VIII-4)}$$

Simplifying part I of (VIII-4):

$$\frac{KY_K g(t_a)}{V_x}\ \frac{1}{2\pi\sigma_x\sigma_y\sigma_x\sigma_y}\left[\frac{2}{\sigma_y^2+\left(\frac{V_y}{V_x}\right)^2\sigma_x^2}\right]^{\frac{1}{2}}$$

$$= \frac{KY_K g(t_a)}{\sqrt{2\pi}}\left[\frac{1}{\sigma_y^2V_x^2+\sigma_x^2V_y^2}\right]^{\frac{1}{2}} = \frac{Kg(t_a)}{\sqrt{2\pi}}\left(\sigma_y^2V_x^2+\sigma_x^2V_y^2\right)^{-\frac{1}{2}} \qquad \text{(VIII-5)}$$

Combining the exponential terms of part II of the integral:

$$-\tfrac{1}{2}\left[\frac{\sigma_y^2x^2+\sigma_x^2y^2}{\sigma_x^2\sigma_y^2}\right] + \tfrac{1}{2}\frac{\left[\frac{\sigma_y}{\sigma_x}x+\frac{\sigma_x}{\sigma_y}\frac{V_y}{V_x}y\right]^2}{\sigma_y^2+\left(\frac{V_y}{V_x}\right)^2\sigma_x^2}$$

$$= -\tfrac{1}{2}\left[\frac{x^2}{\sigma_x^2} + \frac{y^2}{\sigma_y^2}\right] + \tfrac{1}{2}\,\frac{\left[\left(\frac{\sigma_y}{\sigma_x}\right)^2 x^2 + 2xy\left(\frac{V_y}{V_x}\right) + \left(\frac{\sigma_y}{\sigma_x}\right)^2\left(\frac{V_y}{V_x}\right)^2 y^2\right]}{\sigma_y^2 + \left(\frac{V_y}{V_x}\right)^2 \sigma_x^2}$$

$$= \frac{-\tfrac{1}{2}\left[x^2\frac{\sigma_y^2}{\sigma_x^2} + x^2\left(\frac{V_y}{V_x}\right)^2 + y^2 + y^2\frac{\sigma_x^2}{\sigma_y^2}\left(\frac{V_y}{V_x}\right)^2 - \left(\frac{\sigma_y}{\sigma_x}\right)^2 x^2 - 2xy\left(\frac{V_y}{V_x}\right) - \left(\frac{\sigma_x}{\sigma_y}\right)^2\left(\frac{V_y}{V_x}\right)^2 y^2\right]}{\sigma y^2 + \left(\frac{V_y}{V_x}\right)^2 \sigma_x^2}$$

$$= -\tfrac{1}{2}\left[\frac{x^2\left(\frac{V_y}{V_x}\right)^2 - 2xy\left(\frac{V_y}{V_x}\right) + y^2}{\sigma_y^2 + \left(\frac{V_y}{V_x}\right)^2 \sigma_x^2}\right]$$

The numerator is a perfect square, therefore:

$$= -\tfrac{1}{2}\left[\frac{\left(x\left(\frac{V_y}{V_x}\right) - y\right)^2}{\sigma_y^2 + \left(\frac{V_y}{V_x}\right)^2 \sigma_x^2}\right]$$

$$= -\tfrac{1}{2}\left[\frac{(xV_y - yV_x)^2}{\sigma_y^2 V_x^2 + \sigma_x^2 V_y^2}\right]$$

Combining the constant and the exponential terms for $\dot{D}$:

$$\dot{D} = \frac{KY_k g(t_a)}{\sqrt{2\pi}} (\sigma_y^2 V_x^2 + \sigma_x^2 V_y^2)^{-\frac{1}{2}} \text{EXP} \left\{ -\frac{1}{2} \left[\frac{(xV_y - yV_x)^2}{\sigma_y^2 V_x^2 + \sigma_x^2 V_y^2} \right] \right\} \quad \text{(VIII-6)}$$

Equation (VIII-6) reduces to the equation described in Reference 1 for a constant, unidirectional wind when $V_y = 0$:

$$\dot{D} = \frac{KY\ g(t_a)}{\sqrt{2\pi}\ \sigma_y V_x} \text{EXP} \left\{ -\frac{1}{2} \left(\frac{y}{\sigma_y} \right)^2 \right\}$$

Reference 21 demonstrated that (VIII-6) is a gaussian function centered at the hotline coordinate (x,y) and perpendicular to a straight line between the origin (ground zero) and (x,y).

$$\dot{D} = \frac{KY_K\ g(t_a)}{\sqrt{2\pi}} \left[\frac{\sigma_y^2 X^2}{t_a^2} + \frac{\sigma_x^2 Y^2}{t_a^2} \right]^{-\frac{1}{2}} \text{EXP} \left\{ -\frac{1}{2} \left[\frac{(xY - yX)^2}{\sigma_y^2 X^2 + \sigma_x^2 Y^2} \right] \right\} \quad \text{(VIII-7)}$$

Either (VIII-6) or (VIII-7) can be used in the smearing codes with the hotline locator model to compute dose rates at the ground resulting from variable winds.

IX. Summary

A method was developed to enable smearing codes to predict fallout footprints in variable winds. Two steps are required: predict the curved hotline and compute the off-axis dose rates.

A hotline locator model was developed to predict curved hotlines.

a. The hotline locator model uses real wind profiles and the McDonald-Davies method to predict particles' terminal velocities and translations through atmospheric model layers to the ground. Polynomial fits to DELFIC data are used to compute yield-dependent slopes and intercepts of a linear particle size vs height description of the stabilized fallout cloud. The assumption that particle heights are locations of constant-size activity distribution peaks is verified by results which agree with DELFIC output (Washington DC, 100 kt).

b. A vertical stack technique was devised to perform adjoint calculations of the Castle-Bravo hotline. Calculations show that the Bravo hotline can be explained by the presence of a stem and a mixing region beneath the classical fallout cloud.

c. A pseudo-Lagrangian technique was developed to update atmospheric winds in model layers beneath the

falling particles. The technique was tested with T = 0 and T + 1 hr Bravo winds and the resulting hotline agreed with the late-time AFSWP hotline asymptote.

The two-dimensional dose-rate integral has been solved analytically, enabling smearing codes to compute off-axis levels near curved hotlines.

X. Conclusions

On the basis of the research and calculations performed for this study, it is evident that:

a. A pancake cloud falling through an altitude-varying wind field produces a slightly curved hotline. Curvature is minimal and does not improve the single, effective wind results of smearing codes.

b. Realistic hotline curvature can be obtained by computing the motions of fallout particle arrays which start from altitudes that are the geometric centers of the DELFIC population of wafers in stabilized clouds. Starting heights can be predicted from polynomial and least-squares fits to DELFIC data.

c. Particle starting heights represent altitudes of peaks in constant-size activity distribution. Therefore, the ground trace of the activity peaks describes the fallout hotline.

d. Hotline location does not depend on particle size distribution. The hotline locator model prescribes an array of trace particles only to define the hotline coordinates.

AD-A115 514 AIR FORCE INST OF TECH WRIGHT-PATTERSON AFB OH SCHOO--ETC F/G 18/3
A TWO STEP METHOD TO TREAT VARIABLE WINDS IN FALLOUT SMEARING C--ETC(U)
MAR 82 A T HOPKINS

UNCLASSIFIED AFIT/GNE/PH/82M-10 NL

2 OF 2
AD A115 514

END
DATE FILMED
7-82
DTIC

e. Analysis of the Castle-Bravo fallout data and reconstruction of particle trajectorires inferred that the hotline was generated from (at least) three distinct particle size-altitude functions: stem, mixing region, and stabilized cloud.

f. Fallout from high yield shots remains aloft so long that use of a single wind profile (much less a single wind vector) may introduce significant errors into fallout predictions. A linear temporal interpolation technique has been developed to update winds beneath particles, as the particles fall and translate.

g. The two-dimensional dose rate integral was solved analytically to produce a form which reduces to the one-dimensional form when a constant wind vector is assumed.

h. The two-step method will enable smearing codes to predict realistically curved hotlines with real wind data and to compute dose rates on and near the hotline.

Bibliography

1. Bridgman, Charles J. and Winfield S. Bigelow. A New Fallout Prediction Model for Use in Operational Type Studies, Unpublished Article, Wright-Patterson AFB OH: Air Force Institute of Technology, January 1981.

2. Pugh, George E. and Robert J. Galiano. An Analytical Model of Close-In Deposition of Fallout for Use in Operational Type Studies. WSEG Research Memorandum No. 10, Washington DC: Weapon Systems Evaluation Group, The Pentagon, 15 October 1959. (AD 261752)

3. Nier, Alfred O.C., et al. Long-Term Worldwide Effects of Multiple Nuclear Weapons Detonations. Washington DC: National Academy of Sciences, 1975.

4. Norment, Hillyer G. Evaluation of Three Fallout Models: DELFIC, SEER and WSEG-10. Bedford MA: Atmospheric Science Associates. Draft of 28 April 1978 for Defense Nuclear Agency, Washington DC.

5. Bigelow, W.S. DELFIC Calculations for Hypothetical Nuclear Detonations at Washington DC. Unpublished Microfiche and Computer Output, December 1979 and June 1981.

6. McDonald, James E. "An Aid to Computation of Terminal Fall Velocities of Spheres," Journal of Meteorology, 17: 463-465, August 1960.

7. Davies, C.N. "Definitive Equations for the Fluid Resistance of Spheres," The Proceedings of the Physical Society, London, 57: 259-270, July 1945.

8. Hedman, Fritz A. and Ralph C. Simmons. Wind-Weighting Factors for Fallout Calculations. NMCSSC TR 10-66. Washington DC: Defense Communications Agency, December 1966.

9. National Oceanic and Atmospheric Administration, U.S. Standard Atmosphere, 1976. Washington DC: National Aeronautics and Space Administration and the United States Air Force, October 1976.

10. The Times Atlas of the World, Vol. I. Mid-Century Edition. Boston MA: Houghton-Mifflin Co., 1958.

11. Valley, Shea L. (Editor). Handbook of Geophysics and Space Environments. Bedford MA: Air Force Cambridge Research Laboratories and Office of Aero-Space Research, United States Air Force, 1965.

12. ASD Computer Center Subprogram Library Guide, CDC 6600 FORTRAN Subroutine: Polynomial Least Squares Curve Fit. Wright-Patterson AFB OH: Aeronautical Systems Division, January 1978.

13. Eisenbud, Merril. Environmental Radioactivity, Second Edition. New York: Academic Press, 1973.

14. Glasstone, Samuel and Philip J. Dolan. The Effects of Nuclear Weapons, Third Edition. Washington DC: U.S. Government Printing Office, 20402, 1977.

15. Holton, James R. An Introduction to Dynamic Meterology. New York: Academic Press, 1972.

16. Saxon, David S. Elementary Quantum Mechanics. UCLA, San Francisco CA: Holden-Day, Inc., 1968.

17. Polan, M. An Analysis of the Fallout Prediction Models Presented at the USNRDC-DASA Fallout Symposium of September 1962. Vol. II: Analyses, Comparison, and Evaluation of Model Predictions. NRDL TRC-68-59. San Francisco CA: Naval Radiological Defense Laboratory, 28 August 1968.

18. Riehl, Herbert. Tropical Meteorology. New York: McGraw-Hill, 1954.

19. Bridgman, Charles J. Personal Communication. Air Force Institute of Technology, Wright-Patterson AFB OH, August 1981.

20. Hawthorne, Howard A. Fallout Hazard Prediction Inconsistencies. DASIAC SR 174. General Electric Company - TEMPO, Santa Barbara CA. For Defense Nuclear Agency, Washington DC, 1 October 1979.

21. Bridgman, Charles J. Unpublished Working Paper, Air Force Institute of Technology, Wright-Patterson AFB OH, December 1981.

Appendix A

Atmospheric Models

Atmospheric state parameters are used to compute terminal velocities of fallout particles at appropriate heights in the atmosphere. In this study, the computational equations from Reference 9 were used to generate altitude-dependent density and kinematic viscosity values needed to calculate particle fall speeds. Following is a description of the process used to compute atmospheric terms in the U.S. Standard and a tropical atmosphere.

U.S. Standard Atmosphere

Altitude-dependence of the atmospheric state variables is motivated by the assumed temperature profile. The standard atmosphere uses the temperature profile shown in Figure 34; temperature decreases linearly from the earth's surface to a geopotential height of 11 kilometers, at which point the temperature profile is isothermal up to 20 kilometers. The computational sequence is as follows:

1. Geopotential Height

$$HGEO = \frac{\Gamma \cdot Re \cdot ZMSL}{(Re+ZMSL)} \qquad (A-1)$$

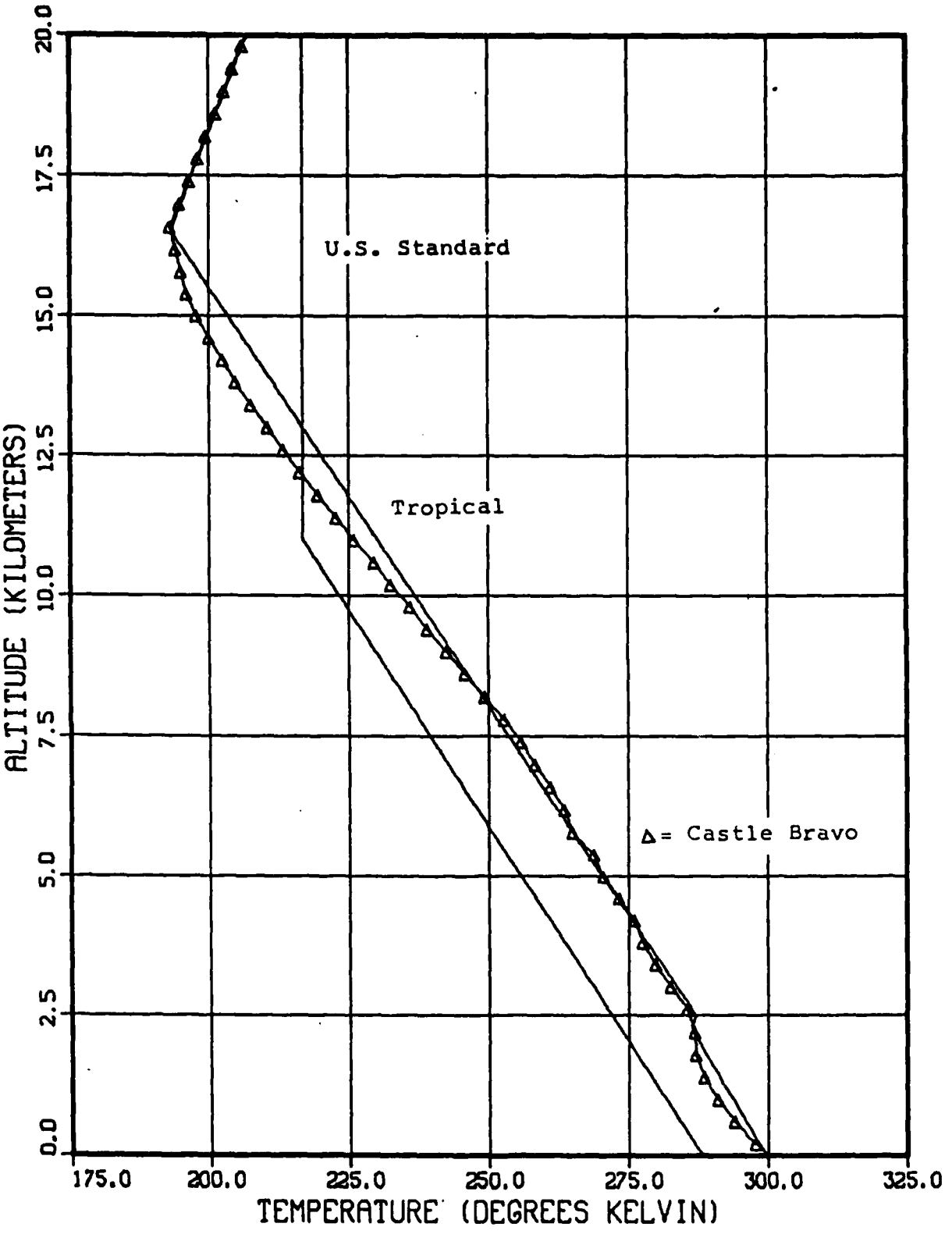

Figure 34. Temperature vs Altitude

HGEO = geopotential height (m)

$$= \frac{\text{acceleration of gravity in geopotential meters}}{\text{acceleration of gravity in meters}}$$

$$\Gamma = \frac{g_o'}{g_o} = 1$$

Re = effective earth radius = 6356766 meters

ZMSL = height of calculation (meters above mean sea level)

2. Temperature

$$TZ = T_{m,b} + L_{m,b} (HGEO-HB) \qquad (A-2)$$

TZ = temperature at ZMSL (0^oK)

$T_{m,b}$ = temperature at base of profile segment

= 288.15 (^oK) for HGEO $\leq$ 11 km

= temperature at 11 km for 11 km < HGEO $\leq$ 20 km

$L_{m,b}$ = lapse rate in profile segment $(\frac{^oK}{meter})$

= $-.0065 \frac{^oK}{m}$ for HGEO < 11 km

= 0 for 11 < HGEO $\leq$ 20 km

HB = geopotential height of temperature profile segment base

= 0 meters for HGEO $\leq$ 11 km

= 11000 meters for 11 km < HGEO $\leq$ 20 km

3. Pressure

(a) If $L_{m,b} \neq 0$,

$$PR = PB \cdot \left[\frac{T_{m,b}}{T_{m,b}+L_{m,b}(HGEO-HB)}\right]^{\left[\frac{g_o' M_o}{R-L_{m,b}}\right]} \qquad (A-3)$$

PR = pressure at AMSL (Newtons/m^2 ≡ Pascals)

PB = pressure at base of temperature profile segment (Pascals)

g_o' = 9.80665 $(\frac{\text{geopotential meters}}{\text{second}^2})$

M_o = molecular weight of air at sea level
= 28.9644 $\frac{kg}{Kmole}$

R* = gas constant = 8.31432x10 $(\frac{N \cdot m}{Kmole^oK})$

(b) If $L_{m,b} = 0$,

$$PR = PB \cdot EXP\left(\frac{-g_o' M_o (GHEO-HB)}{R^* T_{m,b}}\right) \qquad (A-4)$$

4. Density

$$DENS = \frac{PR \cdot M_o}{R^* TZ} \qquad (A-5)$$

DENS = Mass density $(\frac{kg}{m^3})$

5. Kinematic Viscosity

$$VISK = \frac{(B(TZ)^{1.5}}{(TZ+S)} \Big/ DENS \qquad (A\text{-}6)$$

VISK = Kinematic viscosity $(\frac{m^2}{sec})$

B = constant = 1.458×10^{-6} $(kg/(sec \cdot m \cdot {}^{o}K^{\frac{1}{2}}))$

S = Sutherland constant = 110^{o} K

Tropical Atmosphere

Most of the high-yield atmospheric test data was obtained from nuclear weapon tests in the Bikini Atoll. Bikini is located at 11.35^{o} north latitude and 165.20^{o} east longitude (Ref 10). To compute particle motions in realistic atmospheric parameters, a tropical atmosphere was computed using the equations from Reference 9. However, a tropical temperature lapse rate was used to motivate the altitude-dependence of the state variables. Specifically, TZ is obtained from the segmented temperature profile given in Reference 11 and shown in Table A-I. Figure 34 shows the tropical lapse rate compared to the U.S. Standard profile. The lapse rate reported for the Castle-Bravo Pacific test is also plotted on Figure 34 to show the close agreement between computed and actual values.

Figures 35, 36, and 37 plot pressure, density and kinematic viscosity computed for both atmospheres. Figure 35 includes the pressure profile reported for the Castle-Brave weapon test.

Table A-I

Temperature vs Altitude: Tropical Atmosphere

Altitude (km)	Temperature (^{o}C)
0	+26.5
2.256	+13.0
2.507	+13.8
16.582	-80.0
22.128	-58.0
47.463	- 3.0

A vertical temperature profile is generated by linear interpolation.

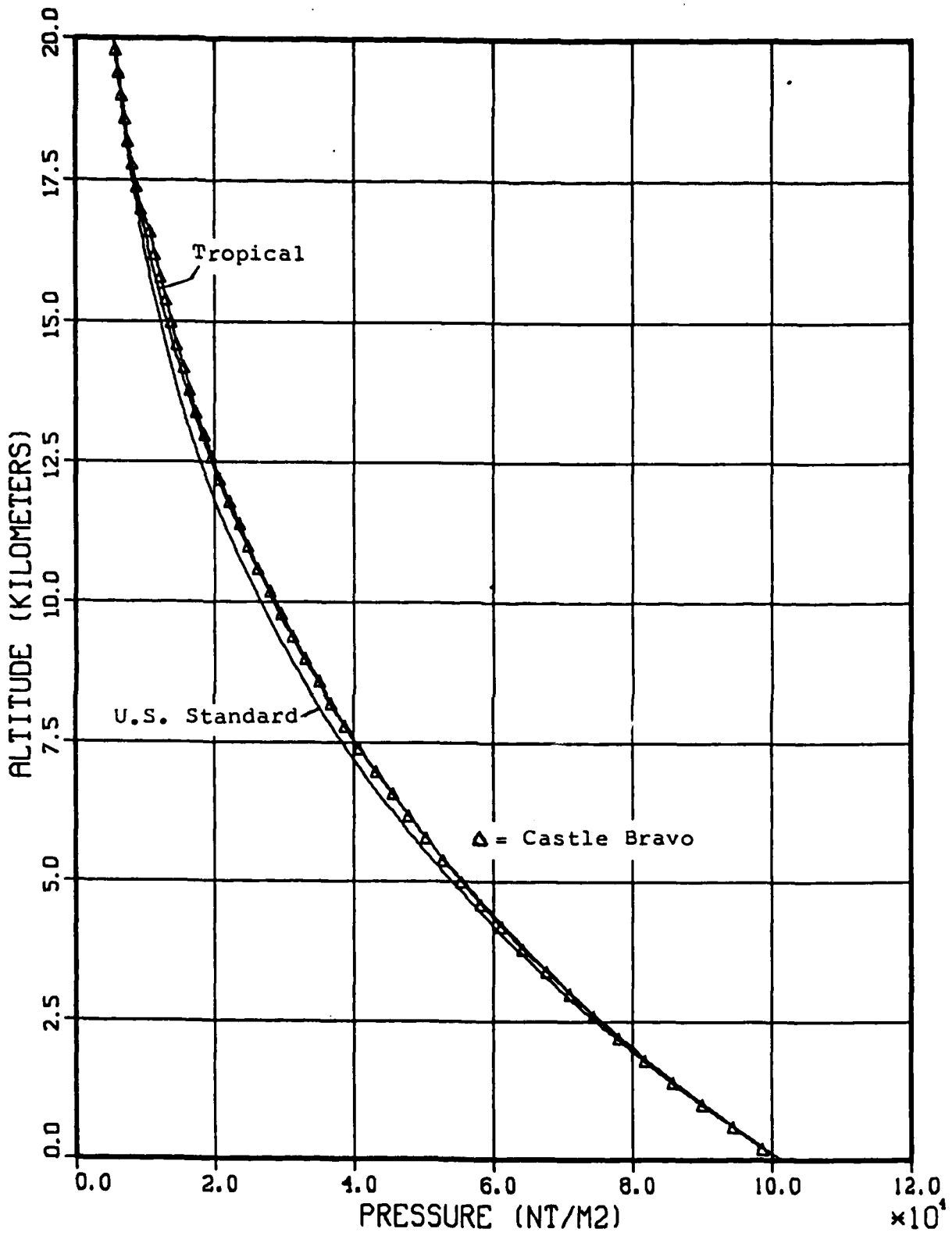

Figure 35. Pressure vs Altitude

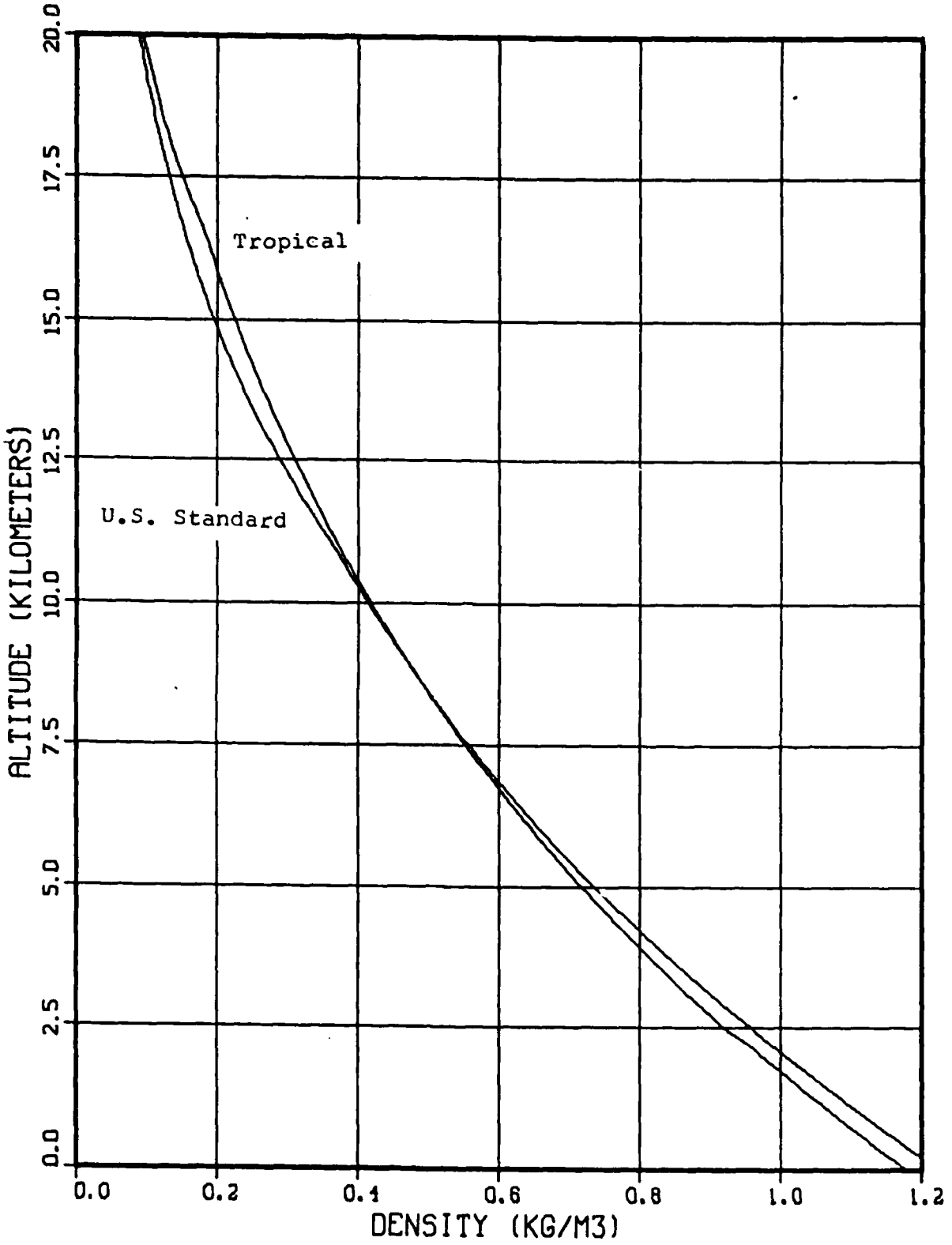

Figure 36. Density vs Altitude

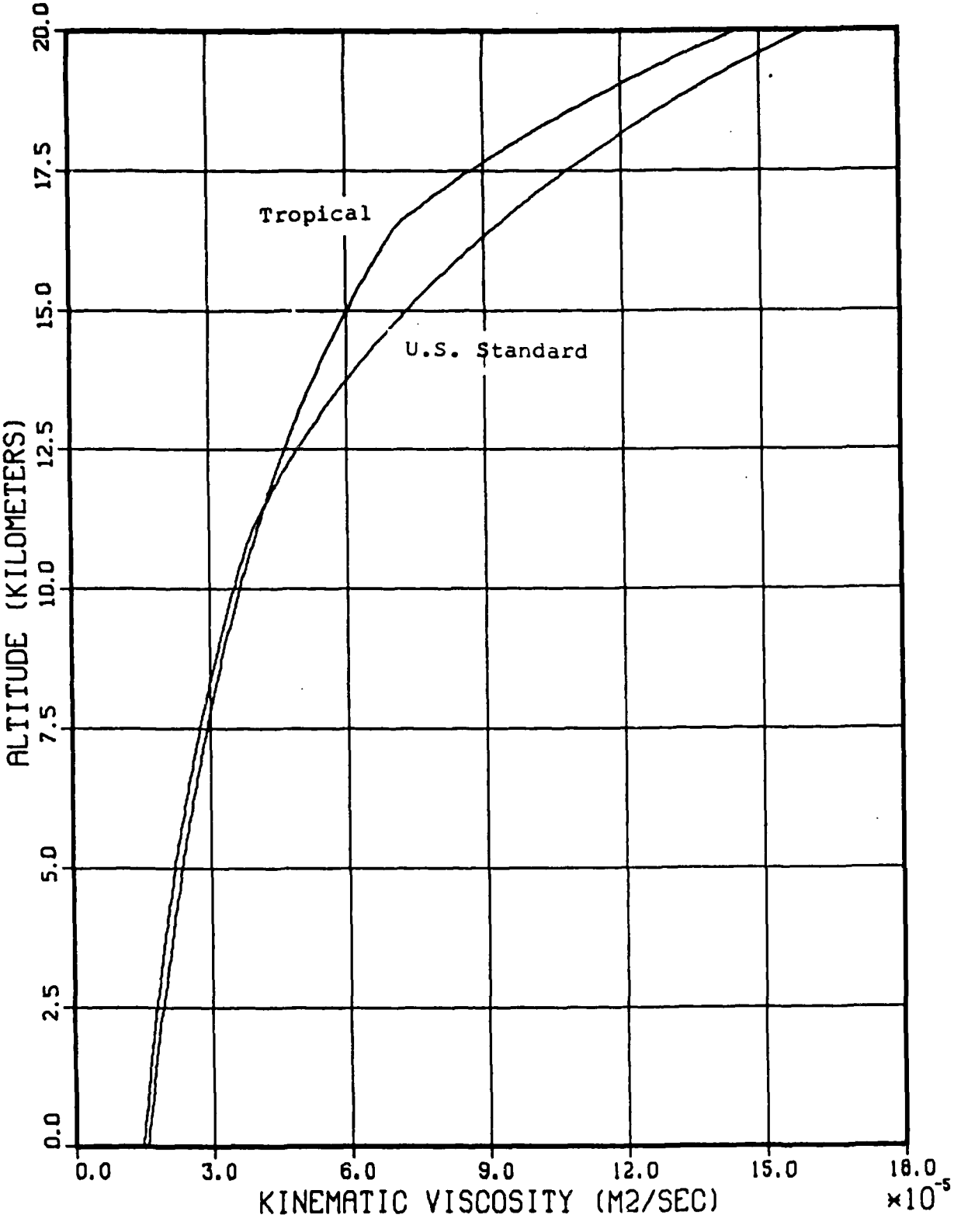

Figure 37. Kinematic Viscosity vs Altitude

Appendix B

Hotline Locator Model Program

The hotline locator model was written in FORTRAN V and executed from the AFIT computer facility using the ASD CDC 6600 computer. Ambient wind data is read into the code by defining the reported wind speed and direction at integer levels of the model (0 to 30 km in 100 meter increments). See lines 140 through 196. This listing contains the Dean and Olmstead wind data developed for the Castle-Bravo nuclear test (Ref 4). This appendix contains:

I. The computational algorithm
II. A list of code variables with definitions
III. A listing of the main program.

I. The Computational Algorithm

The hotline locator model uses real wind data, a twenty particle size array and the McDonald-Davies method to calculate ground traces of particles which start from specific altitudes in a stabilized nuclear cloud. As contained in Part III, the model computes according to the following algorithm:

1. Read Inputs
   a. Particle density (g/cm^3)
   b. Twenty particle diameters (cm)
   c. Actual hotline coordinates (x,y in kilometers east and north of ground zero)
   d. Pancake cloud levels (three model layer numbers $\leq$ 300; high/low/increment; hotline from a single pancake cloud will be computed when low + increment > high)
   e. Twenty particle starting levels for adjoint calculation (model layer numbers specify the altitudes from which each particle starts to fall)
   f. Weapon yield (kilotons)

2. Compute atmospheric density and kinematic viscosity from equations described in Section III.

3. Read actual wind velocities (m/sec) and directions (degrees clockwise from north) at reported atmospheric heights. Velocities and directions are entered at appropriate model levels, where levels are separated by 100 m and numbered from 1 to 301.

4. Compute x and y components of the wind vector. Since standard meteorological practice is to report wind direction in "ϕ degrees clockwise from north-upwind," the vector components of wind are:

$$V_x = V\ (-\sin\ \phi)$$

$$V_y = V\ (-\cos\ \phi)$$

5. Linearly interpolate the component magnitudes between reported levels and assign two components to each model level. Compute the interpolated wind angles at each level to compare with actual profiles.

6. Use Davies-McDonald to compute terminal velocities of each particle size at each model level.

7. Compute residence time of each particle in each layer.

8. Compute the two-dimensional translation of each particle in each layer.

9. Compute residence-time weighted wind vectors for comparison with the method described in References 2 and 8. The effective wind vector, for uni-directional smearing code calculations, is obtained by "weighting" the altitude-distributed winds by the time that particles reside in the corresponding altitudes. Since particles fall faster at higher altitudes, high altitude winds contribute less to the effective wind vector than low altitude winds. The effective wind is a mean value defined as:

$$\bar{W} = \frac{\sum_{i=1}^{n} \tau_i W_i}{\sum_{i=1}^{n} \tau_i}$$

$\bar{W}$ = mean effective wind speed (m/sec)

τ_i = residence time of a particle in i^{th} layer (second)

W_i = wind speed in i^{th} layer

10. Initialize Plot #1 by calling plot library subroutines.

11. Compute and plot hotline coordinates for particles dropped from pancake cloud level through a real wind distribution. Hotline coordinates are obtained by

summing the x and y translations in all model layers beneath the specified pancake cloud level.

12. Compute slope and intercept of particle-height lines from polynomial fits with specified yield.

13. Use slope and intercept to compute 20 starting altitudes of 20 particle sizes in stabilized clouds.

14. Compute and plot hotline coordinates for particles which fall from heights computed in Step 13.

15. Plot the real hotline coordinates provided as input.

16. Initialize Plot #2.

17. Plot the real hotline coordinates provided as input.

18. Compute ground traces for each of 20 particles dropped through each of the 300 model layers.

19. Plot the ground traces of vertical stacks of particles which extend from the surface to adjoint heights (input #1.e). Vertical stacks produce ground contours which help to define the altitudes from which particles would have to fall in order to land on the real hotline.

The model is designed as a diagnostic program to compute and plot hotline coordinates and stack traces after printing

intermediate results, such as wind profiles, particle velocities and atmospheric state variables.

II. Code Variables and Definitions

1. A = The number of atmosphere layers in a vertical stack (back calculations)
2. ADXT = Two dimensional array of ground coordinates (x-direction) for each particle size and model level at starting height
3. ADYT = Two dimensional array of ground coordinates (y-direction) for each particle size and model level at starting height
4. AFX = x-coordinate array of the actual fallout hotline
5. AFY = y-coordinate array of the actual fallout hotline
6. AP = Array of model levels that specify adjoint stack heights
7. BETA = Constant used to compute kinematic viscosity of air
8. DENS = Array of atmospheric density values at each of 301 model levels
9. DVX = Incremental velocity in x-direction computed between published wind levels and used for linear interpolation fallout wind profiles
10. DVY = Incremental velocity in y-direction computed between published wind levels and used for linear interpolation fallout wind profiles
11. DX = Two dimensional array of x-distances traveled by each particle in each model layer
12. DXT = Array of ground coordinates (x-direction) obtained by summing DX from the ground upward
13. DY = Two dimensional array of y-distances traveled by each particle in each model layer
14. DYT = Array of ground coordinates (y-direction) obtained by summing DY from the ground upward
15. GAMMA = Ratio of gravitational constants: meters to geopotential meters

16. GOP = Graviational constant in geopotential meters per second squared

17. HB = Bottom height of an atmospheric temperature profile segment

18. HGEO = Geopotential height in atmosphere

19. I = Dummy index for manipulating subscripted variables

20. IL = Natural logarithm of intercept obtained from polynomial least squares correlation with natural logarithm of weapon yield

21. INTCPT = Height of zero diameter particle in a stabilized cloud: EXP(IL)

22. IPAK = Array of characters used by DISSPLA to store information for plot legends

23. J = Dummy index for manipulating subscripted variables

24. L = Dummy index for manipulating subscripted variables

25. LMB = Slope of an atmospheric temperature profile in ^{O}K/meter

26. MO = Mean molecular weight of air

27. N = Dummy index for manipulating subscripted variables

28. PB = Atmospheric pressure (Newtons/m^2) at the base of each linear temperature profile segment

29. PCB = Input height (model level) of a pancake cloud: the lowest level desired for calculation of hotline coordinates

30. PCS = Input incremental height (model levels) between pancake clouds, if multiple calculations are computed

31. PCT = Input height (model level) of a pancake cloud: the highest level desired for calculation of hotline coordinates. Note: If PCS > (PCT-PCB), the code will compute the hotline coordinates from a single pancake cloud (PCB).

32. PDEN = Fallout particle density (grams/cm^3)

33. PDIA = Array of 20 fallout particle diameters (cm)

34. PDXT = Array of hotline x-coordinates used for plot subroutine

35. PDYT = Array of hotline y-coordinates used for plot subroutine

36. PHI = Array of wind directions in degrees clockwise from north: upwind

37. PR = Array atmospheric pressure values (Nt/m^2) at each model level

38. Q = Product of particle drag coefficient and the square of Reynold's number used for terminal velocity calculation with Davies' method

39. R = Array of Reynold's numbers computed with Davies' correlations with Q

40. RERTH = Earth radius (6356766 meters)

41. RL = Array of ($\log_{10}R$) computed with Davies' correlations with $\log_{10}Q$

42. RSTAR = Universal gas constant (8314.32(N+ M)/(KMole$\cdot^{o}$K)

43. RTD = Array of radial distances from burst ground zero to ground impact coordinates of each particle size

44. RX = X-coordinate array of the actual fallout hotline

45. RY = Y-coordinate array of the actual fallout hotline

46. S = Sutherland's constant (110^{o} K) used to compute kinematic viscosity of air

47. SL = Natural logarithm of slope obtained from polynomial least squares correlation with natural logarithm of weapon yield

48. SLOPE = Height variation of particle sizes in a stabilized cloud: EXP(SL)

49. SVX = Array of x-components of wind summed to compute a mean wind (used for reference only)

50. SVY = Array of y-components of wind summed to compute a mean wind (used for reference only)

51. TAU = Two-dimensional array of residence times of particles between each pair of model levels (sec)

52. TB = Temperature at the base of atmospheric temperature profile segment (^{o}K)

53. TZ = Array of atmospheric temperature values at each model level

54. VISK = Array of kinematic viscosity values (sec^2/meter) at each model level

55. VT = Two-dimensional array of terminal velocities (cm/sec) of each particle size at each model level

56. VTA = Array of average terminal velocity in a model layer (cm/sec)

57. VX = Array of wind velocity x-components (m/sec)

58. VXEFF = Two-dimensional array of effective Vx values obtained by averaging the residence-time-weighted VX values from each model layer (used for reference only)

59. VXM = Array of mean wind x-components beneath each model level (used for reference only)

60. VY = Array of wind velocity y-components (m/sec)

61. VYEFF = Two-dimensional array of effective VY values obtained by averaging the residence-time-weighted VX values for each model layer

62. VYM = Array of mean wind x-components beneath each model level (used for reference only)

63. VZ = Array of terminal velocities of each particle size obtained from definition of Reynold's number in Davies' method (cm/sec)

64. WIND = Array of wind speeds: magnitudes of wind vectors at each model level

65. WT = Array of particle weights (g cm/sec^2)

66. WVEFF = Two-dimensional array of effective wind speeds obtained by averaging the residence-time-weighted VX values for each model layer

67. WVM = Array of mean wind speeds beneath each model level (used for reference only)

68. X = Array of hotline x-coordinates used for plotting adjoint stacks (km)

69. Y = Array of hotline y-coordinates used for plotting adjoint stacks (km)

70. YKT = Weapon yield in kilotons

71. YL = Natural logarithm of YKT

72. Z = Height of particle size in a stabilized cloud generated with linear fits to mean wafer center heights and polynomial fits for slope and intercept (m)

73. ZMSL = Array of model level heights above sea level used to generate atmospheric parameters.

III. Program Listing

```
      PROGRAM BRAV03
      DIMENSION WIND(301),PHI(301),VX(301),VY(301)
      DIMENSION ZMSL(301),HGEO(301),TZ(301),PR(301),DENS(301),VISK(301)
      DIMENSION WT(20),Q(20),R(20),RL(20),VZ(20),PDIA(20)
      DIMENSION VT(20,301),TAU(20,301),DX(20,301),DY(20,301),VTA(20,301)
      DIMENSION DXT(20),DYT(20),RTD(20)
      DIMENSION VXM(301),VYM(301),WVM(301),SVX(301),SVY(301)
      DIMENSION VXEFF(20,301),VYEFF(20,301),WVEFF(20,301)
      DIMENSION PDXT(20),PDYT(20)
      DIMENSION ADXT(20,301),ADYT(20,301)
      DIMENSION AFX(19),AFY(19),RX(19),RY(19)
      DIMENSION IPAK(100)
      DIMENSION X(300),Y(300)
      DIMENSION AF(20)
      REAL INTCPT,IL,LMB,MO
      INTEGER PCB,PCT,PCS
      INTEGER A
C
C  INPUTS
C
      READ*,PDEN
      READ(*,*) PDIA
      READ*,AFX
      READ*,AFY
      READ*,PCB,PCT,PCS
      READ*,AF
      READ*,YKT
      DO 422 I=1,19
      RX(I)=AFX(I)
      RY(I)=AFY(I)
  422 CONTINUE
C
C  TROPICAL ATMOSPHERE **********
C
C
```

```
36=C  301 LEVELS FOR 300 MODEL LAYERS
37=C
38=       DO 11 I=1,301
39=       ZMSL(I)=100.*I-100.
40=   11  CONTINUE
41=C
42=C  GEOPOTENTIAL HEIGHT
43=C
44=       RERTH=6356766.
45=       GAMMA=1.
46=       DO 12 I=1,301
47=       HGEO(I)=GAMMA*((RERTH*ZMSL(I))/(RERTH+ZMSL(I)))
48=   12  CONTINUE
49=C
50=       GOP=9.80665
51=       MO=28.9644
52=       RSTAR=8314.32
53=C
54=C  TEMPERATURE, PRESSURE, AND DENSITY
55=C
56=       DO 3 I=1,301
57=       IF(HGEO(I).LE.2250.)THEN
58=       TB=299.65
59=       LMB=-.006
60=       HB=0.
61=       PB=101325.
62=       ELSEIF(HGEO(I).GE.2251..AND.HGEO(I).LE.2500.)THEN
63=       TB=286.15
64=       LMB=.0032
65=       HB=2250.
66=       PB=77933.2
67=       ELSEIF(HGEO(I).GE.2501..AND.HGEO(I).LE.16500.)THEN
68=       TB=286.95
69=       LMB=-.0067
70=       HB=2500.
```

```
      PB=75644.6
      ELSEIF (HGEO(I).GE.16501..AND.HGEO(I).LE.22000.) THEN
      TB=193.15
      LMB=.004
      HB=16500.
      PB=10050.6
      ELSEIF(HGEO(I).GE.22001.) THEN
      TB=215.15
      LMB=.0022
      HB=22000.
      PB=4094.13
      ENDIF
      TZ(I)=TB+LMB*(HGEO(I)-HB)
      PR(I)=PB*((TB/TZ(I))**(GOP*MO/(RSTAR*LMB)))
      DENS(I)=(PR(I)*MO)/(RSTAR*TZ(I))
3     CONTINUE
C
C  KINEMATIC VISCOSITY
C
      BETA=1.458E-6
      S=110.4
      DO 4 I=1,301
      VISK(I)=BETA*(TZ(I)**1.5)/(TZ(I)+S)/DENS(I)
4     CONTINUE
      PRINT 5
5     FORMAT('1',' TROPICAL ATMOSPHERE')
      PRINT*,' COMPUTATIONAL EQUATIONS FROM NOAA-S/T 76-1562'
      PRINT*,' LAYER        ZMSL                HGEO                TZ
     C                PR                  DENS                VISK'
      DO 6 I=1,301
      PRINT 7,I,ZMSL(I),HGEO(I),TZ(I),PR(I),DENS(I),VISK(I)
7     FORMAT(I5,6E20.6)
6     CONTINUE
C
C  ******************************
```

```
106=C
107=       DO 10 J=1,301
108=       DENS(J)=DENS(J)*(.001)
109=       VISK(J)=VISK(J)*(10000.)
110=  10   CONTINUE
111=       DO 30 I=1,301
112=       WIND(I)=0.
113=       PHI(I)=0.
114=       VX(I)=0.
115=       VY(I)=0.
116=       VXM(I)=0.
117=       VYM(I)=0.
118=       WVM(I)=0.
119=       SVX(I)=0.
120=       SVY(I)=0.
121=  30   CONTINUE
122=       DO 200 I=1,20
123=       DO 210 N=1,301
124=       VT(I,N)=0.
125=       VTA(I,N)=0.
126=       TAU(I,N)=0.
127=       DX(I,N)=0.
128=       DY(I,N)=0.
129=       DXT(I)=0.
130=       DYT(I)=0.
131=       PDXT(I)=0.
132=       PDYT(I)=0.
133=       VXEFF(I,N)=0.
134=       VYEFF(I,N)=0.
135=       WVEFF(I,N)=0.
136=       ADXT(I,N)=0.
137=       ADYT(I,N)=0.
138=  210  CONTINUE
139=  200  CONTINUE
140=C
```

```
141=C   DEAN & OLMSTEAD WIND DATA
142=C
143=        WIND(1)=4.0
144=        WIND(7)=3.6
145=        WIND(13)=2.7
146=        WIND(19)=2.8
147=        WIND(25)=3.5
148=        WIND(31)=4.8
149=        WIND(38)=5.7
150=        WIND(44)=6.6
151=        WIND(50)=7.5
152=        WIND(56)=8.5
153=        WIND(62)=9.4
154=        WIND(77)=12.2
155=        WIND(92)=14.7
156=        WIND(108)=16.7
157=        WIND(123)=18.2
158=        WIND(138)=15.8
159=        WIND(153)=12.8
160=        WIND(169)=7.8
161=        WIND(184)=2.7
162=        WIND(199)=1.9
163=        WIND(214)=6.1
164=        WIND(230)=6.1
165=        WIND(245)=7.7
166=        WIND(260)=9.4
167=        WIND(275)=9.4
168=        WIND(291)=9.4
169=        WIND(301)=9.4
170=        PHI(1)=53.3
171=        PHI(7)=45.0
172=        PHI(13)=14.6
173=        PHI(19)=338.2
174=        PHI(25)=316.8
175=        PHI(31)=302.7
```

```
176=       PHI(38)=295.2
177=       PHI(44)=286.9
178=       PHI(50)=281.2
179=       PHI(56)=277.0
180=       PHI(62)=273.1
181=       PHI(77)=264.7
182=       PHI(92)=259.9
183=       PHI(108)=261.1
184=       PHI(123)=262.4
185=       PHI(138)=263.1
186=       PHI(153)=264.2
187=       PHI(169)=262.4
188=       PHI(184)=255.4
189=       PHI(199)=73.0
190=       PHI(214)=71.9
191=       PHI(230)=71.3
192=       PHI(245)=71.1
193=       PHI(260)=71.4
194=       PHI(275)=71.4
195=       PHI(291)=71.7
196=       PHI(301)=71.7
197=C
198=C  VECTOR COMPONENTS: X=W-E  Y=S-N
199=C
200=       DO 40 N=1,301
201=       PHI(N)=PHI(N)*6.2832/360.
202=       VX(N)= WIND(N) * (-SIN(PHI(N)))
203=       VY(N)= WIND(N) * (-COS(PHI(N)))
204=   40  CONTINUE
205=       L=1.
206=C
207=C  LINEAR INTERPOLATION OF WIND VELOCITY COMPONENTS AND VECTOR DIRECTION
208=C
209=       DO 60 N=2,301
210=       IF (WIND(N).EQ.0) GO TO 60
```

```
      DVX= (VX(N)-VX(L))/(N-L)
      DVY= (VY(N)-VY(L))/(N-L)
80    VX(L+1)= VX(L)+ DVX
      VY(L+1)= VY(L)+DVY
      PHI(L+1)= ATAN (VY(L+1)/VX(L+1))
      IF (PHI(L+1).GE.0) GO TO 31
      IF (VY(L+1).LT.0) GO TO 33
      PHI(L+1)= 90.- ((PHI(L+1))*360./6.2832)
      GO TO 70
31    IF(VX(L+1).LT.0) GO TO 32
      PHI(L+1)= 270.-((PHI(L+1))*360./6.2832 )
      GO TO 70
32    PHI(L+1)= 90.- ((PHI(L+1))*360./6.2832)
      GO TO 70
33    PHI(L+1)= 270.-((PHI(L+1))*360./6.2832 )
70    L=L+1.
      IF (L.EQ.N) GO TO 60
      GO TO 80
60    CONTINUE
C
C  MEAN WIND FROM OMSL TO LEVEL N
C
      SVX(1)=VX(1)
      SVY(1)=VY(1)
      DO 61 N=2,301
      SVX(N)=VX(N)+SVX(N-1)
      SVY(N)=VY(N)+SVY(N-1)
      VXM(N)=SVX(N)/N
      VYM(N)=SVY(N)/N
      WVM(N)=SQRT((VXM(N)**2.)+(VYM(N)**2.))
61    CONTINUE
C
C  INTERPOLATED WIND SPEED COMPONENTS
C
      PRINT 95
```

```
 95  FORMAT ('1',' WIND PROFILE')
     PRINT*,'          VX          VY          WIND          PHI          VXM
    C   VYM          WVM'
     DO 50 N=1,301
     WIND(N)= SQRT((VX(N)**2.)+ (VY(N)**2.))
     WRITE(*,45)N,VX(N),VY(N),WIND(N),PHI(N),VXM(N),VYM(N),WVM(N)
 45  FORMAT(I5,7F10.3)
 50  CONTINUE
C
C
C  DAVIES-MCDONALD METHOD TO COMPUTE TERMINAL VELOCITIES
C  WT--CDR**2--R--VZ
C
     PRINT 155
 155 FORMAT('1',' PARTICLE DIAMETER AND WEIGHT')
     PRINT*,'       PDIA                WT'
     DO 100 N=1,20
     WT(N)=(4./3.)*3.1416*((PDIA(N)/2.)**3.)*PDEN*980.
     WRITE(*,110) PDIA(N),WT(N)
 110 FORMAT (F12.4,F20.10)
 100 CONTINUE
     DO 120 N=1,301
     DO 130 I=1,20
     Q(I)=8.*WT(I)/(3.1416*DENS(N)*(VISK(N)**2.))
     IF(Q(I).GE.140.) GO TO 150
     R(I)=Q(I)/24.-(2.3363*(10.**(-4.))*(Q(I)**2.))+(2.0154*(10.**(-6.
    C))*(Q(I)**3.))-(6.9105*(10.**(-9.))*(Q(I)**4.))
     GO TO 170
 150 RL(I)=-1.29536+.986*(LOG10(Q(I)))-.046677*((LOG10(Q(I))**2.))+
    C.0011235*((LOG10(Q(I))**3.))
     R(I)=(10.)**RL(I)
C
C  TERMINAL VELOCITY  CM/SEC
C
 170 VZ(I)=R(I)*VISK(N)/PDIA(I)
```

```
281=       VT(I,N)=VZ(I)
282=       IF(N.EQ.1) GO TO 130
283=       VTA(I,N)=(VT(I,N-1)+VT(I,N))/2.
284=C
285=C  PARTICLE RESIDENCE TIME IN LAYER AND VECTOR TRANSLATION
286=C
287=       TAU(I,N)=10000./VTA(I,N)
288=       DX(I,N)=((VX(N-1)+VX(N))/2.)*TAU(I,N)
289=       DY(I,N)=((VY(N-1)+VY(N))/2.)*TAU(I,N)
290=   130 CONTINUE
291=   120 CONTINUE
292=C
293=C  PARTICLE TRANSLATION HISTORY
294=C
295=       DO 260 I=1,20
296=       IF(I.EQ.1) GO TO 283
297=       IF(I.EQ.20) GO TO 283
298=       GO TO 284
299=   283 PRINT 271
300=   271 FORMAT ('1','  N         PDIA                    DXT
301=      CDYT                  RTD                     TAU')
302=   284 DO 250 N=2,301
303=       TAU(I,N)=TAU(I,N)+ TAU(I,N-1)
304=       DXT(I)=DXT(I)+DX(I,N)
305=       DYT(I)=DYT(I)+DY(I,N)
306=       ADXT(I,N)=DXT(I)
307=       ADYT(I,N)=DYT(I)
308=       RTD(I)=SQRT(((DXT(I))**2.)+((DYT(I))**2.))
309=       IF(I.EQ.1) GO TO 281
310=       IF(I.EQ.20) GO TO 281
311=       GO TO 282
312=   281 WRITE(*,270) N,PDIA(I),DXT(I),DYT(I),RTD(I),TAU(I,N)
313=   270 FORMAT (I5,F12.4,4F20.1)
314=C
315=C  EFFECTIVE FALLOUT WIND USING WWF METHOD
```

```
316=C
317=  282 IF(TAU(I,N).EQ.0.) GO TO 250
318=      VXEFF(I,N)= DXT(I)/TAU(I,N)
319=      VYEFF(I,N)= DYT(I)/TAU(I,N)
320=      WVEFF(I,N)= SQRT((VXEFF(I,N))**2.+(VYEFF(I,N))**2.)
321=  250 CONTINUE
322=  260 CONTINUE
323=C
324=C  PRINT THE EFFECTIVE WIND VECTORS FOR THE SMALLEST AND LARGEST
325=C   PARTICLE SIZES
326=C
327=      DO 310 I=1,20,19
328=      PRINT 312
329=  312 FORMAT (/,'  N       PDIA        VXEFF        VYEFF        WVEFF')
330=      DO 311 N=2,301
331=      WRITE(*,313)N,PDIA(I),VXEFF(I,N),VYEFF(I,N),WVEFF(I,N)
332=  313 FORMAT (I5,F12.4,3F10.3)
333=  311 CONTINUE
334=  310 CONTINUE
335=C
336=C  PANCAKE CLOUD LEVELS (BOTTOM,TOP,SIGMA)
337=C
338=      PRINT*,'  PCB= ',PCB,'  PCT= ',PCT,'  PCS= ',PCS
339=      DO 401 N=PCB,PCT,PCS
340=      PRINT*,'  N          PDIA                  PDXT                  PDYT'
341=      DO 400 I=1,20
342=      PDXT(I)=ADXT(I,N)/1000.
343=      PDYT(I)=ADYT(I,N)/1000.
344=      PRINT 403,N,PDIA(I),PDXT(I),PDYT(I)
345=  403 FORMAT (I5,F12.4,2F20.1)
346=  400 CONTINUE
347=      IF (N.EQ.PCB) GO TO 404
348=      GO TO 402
349=  404 CONTINUE
350=C
```

```
C  PLOT ROUTINE FOR HOTLINES
C
      CALL COMPRS
      CALLBGNPL(1)
      CALL TITLE ('HOTLINES$',-100,'EAST OF GZ (KM)$',100,
     C'N-S OF GZ (KM)$',100,8.,6.)
      CALL FRAME
      CALL GRAPH (0.,40.,-120.,40.)
      CALL RLMESS ('CASTLE BRAVO (PACIFIC)  1MAR54  15MT$',100,
     C38.,-100.)
      CALL RLMESS ('DEAN + OLMSTEAD WINDS$',100,75.,-112.)
      CALL LINES (' PANCAKE $',IPAK,1)
      CALL LINES (' WAFER CTRS$',IPAK,2)
      CALL LINES (' AFSWP$',IPAK,3)
      CALL BLNK1(5.5,7.5,0.0,1.0,1)
      CALL BLNK2(0.5,5.5,0.0,1.0,1)
      CALL GRID(1,1)
  402 CALL CURVE (PDXT,PDYT,14,1)
  401 CONTINUE
C
C  WAFER CENTER HEIGHT CORRELATION WITH PDIA FOR CURVED HOTLINE
C
      YL=LOG(YKT)
      SL=1.574-.01197*YL+.03636*YL**2.-.0041*YL**3.+.0001965*YL**4.
      SLOPE=EXP(SL)
      IL=7.889+.34*YL+.001226*YL**2.-.005227*YL**3.+.000417*YL**4.
      INTCPT=EXP(IL)
      PRINT*,'  YIELD (KT) = ',YKT
      PRINT*,'  SLOPE = ',SLOPE,' INTERCEPT = ',INTCPT
      PRINT*,'  ALTITUDE DISTRIBUTED HO'
      PRINT*,'  N          PDIA                  PDXT                PDYT'
      DO 410 I=1,20
      PDIA(I)=PDIA(I)*10000.
C
C  Z VS PDIA AT STABILISATION FOR CURVED HOTLINE
```

```
      Z=-SLOPE*PDIA(I)+INTCPT
C
      IF(Z.LT.0.)THEN
      PRINT*,Z,PDIA(I),'LOW'
      Z=0.
      ENDIF
      IF(Z.GT.30000.) THEN
      PRINT*,Z,PDIA(I),'HIGH'
      Z=30000.
      ENDIF
      Z=1.+Z/100.
      N=Z
      IF((Z-N).GE.0.51) N=N+1
      IF(I.LE.16) N=AP(I)
      PDXT(I)=ADXT(I,N)/1000.
      PDYT(I)=ADYT(I,N)/1000.
      PRINT 411, N,PDIA(I),PDXT(I),PDYT(I)
411   FORMAT (I5,F12.4,2F20.1)
410   CONTINUE
      PRINT*,'  I      AFX      AFY   :  AFSWP HOTLINE (KM)'
      DO 1 I=1,19
      PRINT 2,I,AFX(I),AFY(I)
2     FORMAT (I5,2F10.1)
1     CONTINUE
      CALL CURVE(PDXT,PDYT,14,1)
C
C  HOTLINE ESTIMATES FROM AFSWC DATA CONTOURS
C
      CALL CURVE (AFX,AFY,19,1)
      CALL RESET('BLNK1')
      CALL LEGEND(IPAK,3,5.6,0.1)
      CALL ENDPL(1)
C
C
C
```

```
C  ADJOINT CALCULATION SPECIFIES STARTING LEVEL FOR EACH PDIA
C    TO APPROXIMATE AFSWP HOTLINE  (LEVELS ARE INPUT ARRAY AP(20) )
C
C
      DO 423 I=1,20
      PRINT*,'  ADJOINT LEVEL = ',AP(I),'  PDIA = ',PDIA(I)
  423 CONTINUE
C
C  GENERATE ARRAYS TO PLOT PARTICLE TRAJECTORIES
C
      CALL BGNPL(2)
      CALL TITLE ('GROUND TRACES OF SINGLE-SIZE-PARTICLE STACKS$',-100,
     C'E-W OF GZ (KM)$',100,'N-S OF GZ (KM)$',100,8.,6.)
      CALL FRAME
      CALL GRAPH (-50.,50.,-150.,50.)
      CALL RLMESS ('CASTLE BRAVO (PACIFIC) 1MAR54 15MT$',100,
     C50.,-125.)
      CALL RLMESS ('DEAN + OLMSTEAD WINDS$',100,100.,-140.)
      CALL RLMESS ('ADJOINT$',100,255.,127.)
      CALL RLMESS ('VERTICAL STACKS$',100,230.,112.)
      CALL BLNK1 (1.5,6.5,0.0,1.0,1)
      CALL BLNK2 (5.5,7.5,5.2,5.8,1)
      CALL GRID(1,1)
      CALL CURVE (RX,RY,19,1)
      PRINT*,'  ADJOINT HOTLINE COORDINATES'
      PRINT*,'          PDIA                X                   Y'
      DO 420 I=1,20
      DO 421 J=2,301
      X(J-1)=ADXT(I,J)/1000.
      Y(J-1)=ADYT(I,J)/1000.
  421 CONTINUE
      A=AP(I)
C
C  A SPECIFIES THE NUMBER OF LAYERS IN AN ADJOINT COLUMN
C
```

```
      PRINT 424,PDIA(I),X(A),Y(A)
  424 FORMAT (3F20.6)
      CALL CURVE (X,Y,A,0)
  420 CONTINUE
      CALL ENDPL(2)
C
      CALL DONEPL
      END
```

Vita

Arthur Thomas Hopkins was born 8 January 1949 in Lewiston, Maine. He graduated from Lewiston High School and attended the Catholic University of America, Washington, DC, where he earned Bachelor and Master of Science in Engineering degrees in Aerospace and Atmospheric Sciences. He entered the U.S. Air Force in July 1973 as a reentry physics project officer at the Space and Missile Systems Organization, Los Angeles, California. In 1977, he was assigned to the Defense Nuclear Agency, Washington, DC, as a nuclear research officer. He entered the Air Force Institute of Technology Nuclear Engineering program in August 1980. He is a member of Tau Beta Pi and the American Nuclear Society.

Permanent Address: 12 Whipple Street
Lewiston, Maine 04240

UNCLASSIFIED

SECURITY CLASSIFICATION OF THIS PAGE (When Data Entered)

REPORT DOCUMENTATION PAGE	READ INSTRUCTIONS BEFORE COMPLETING FORM
1. REPORT NUMBER: AFIT/GNE/PH/82M-10 — 2. GOVT ACCESSION NO.: AD-A115 514	3. RECIPIENT'S CATALOG NUMBER
4. TITLE (and Subtitle): A TWO-STEP METHOD TO TREAT VARIABLE WINDS IN FALLOUT SMEARING CODES	5. TYPE OF REPORT & PERIOD COVERED: MS Thesis
	6. PERFORMING ORG. REPORT NUMBER
7. AUTHOR(s): Arthur T. Hopkins, Capt USAF	8. CONTRACT OR GRANT NUMBER(s)
9. PERFORMING ORGANIZATION NAME AND ADDRESS: Air Force Institute of Technology (AFIT-EN), Wright-Patterson AFB OH 45433	10. PROGRAM ELEMENT, PROJECT, TASK AREA & WORK UNIT NUMBERS
11. CONTROLLING OFFICE NAME AND ADDRESS	12. REPORT DATE: March 1982
	13. NUMBER OF PAGES: 134
14. MONITORING AGENCY NAME & ADDRESS (if different from Controlling Office)	15. SECURITY CLASS. (of this report): UNCLASSIFIED
	15a. DECLASSIFICATION/DOWNGRADING SCHEDULE

16. DISTRIBUTION STATEMENT (of this Report)

Approved for Public Release; Distribution Unlimited

17. DISTRIBUTION STATEMENT (of the abstract entered in Block 20, if different from Report)

15 APR 1982

18. SUPPLEMENTARY NOTES

APPROVED FOR PUBLIC RELEASE AFR 190-17.

Lynn E. Wolaver

Dean for Research and Professional Development
Air Force Institute of Technology (ATC)
Wright-Patterson AFB, OH 45433

19. KEY WORDS (Continue on reverse side if necessary and identify by block number)

Fallout — Castle-Bravo

Wind Models — Dose Rate

20. ABSTRACT (Continue on reverse side if necessary and identify by block number)

A method was developed to treat non-constant winds in fallout smearing codes. The method consists of two steps: (1) location of the curved hotline, and (2) determination of the off-hotline activity. To locate the curved hotline, the method begins with an initial cloud of 20 discretely sized pancake clouds, located at altitudes determined by weapon yield. Next, the particles are tracked through a 300 layer atmosphere, translating with different winds in each layer. The connection of the 20 particles' impact points is the

(Continued on Reverse)

DD FORM 1 JAN 73 1473 EDITION OF 1 NOV 65 IS OBSOLETE

UNCLASSIFIED

SECURITY CLASSIFICATION OF THIS PAGE (When Data Entered)

BLOCK 20: ABSTRACT (Continued)

fallout hotline. The hotline location was found to be independent of the assumed particle size distribution in the stabilized cloud. The off-hotline activity distribution is represented as a two-dimensional gaussian function, centered on the curved hotline. Hotline locator model results were compared to numerical calculations of a hypothetical 100 kt burst and to the actual hotline produced by the Castle-Bravo 15 Mt nuclear test.